Simulation of the Performance of Vapor Absorption Air Conditioner for a Mid Bus Passenger Car Powered by Engine Exhaust Heat and Photo Voltaic Cell (PVC)

M.Sc. Thesis

By

Million Matewose Mada

GSR/0161/09

Thermal and Aerospace Engineering Program

School of Mechanical, Chemical and Materials Engineering

Adama Science and Technology University

Adama, Ethiopia
December, 2018

Simulation of the Performance of Vapor Absorption Air Conditioner for a Mid Bus Passenger Car Powered by Engine Exhaust Heat and Photo Voltaic Cell (PVC)

M.Sc. Thesis

By

Million Matewose Mada

A Thesis Submitted to Thermal and Aerospace Engineering Program of School of Mechanical, Chemical and Materials Engineering, Adama Science and Technology University in partial fulfillment of the requirement of the degree of Master of Science in Thermal Engineering.

Advisor: Dr. Gezahegn Habtamu

Adama, Ethiopia

December, 2018

APPROVAL BY BOARD OF EXAMINERS

We, the undersigned, members of the Board of Examiners of the final open defense by Million Matewose have read and evaluated his thesis entitled "Simulation of the Performance of Vapor Absorption Air Conditioner for a Mid Bus Passenger Car Powered by Engine Exhaust Heat and Photo Voltaic Cell (PVC)" and examined the candidate. This is, therefore, to certify that the thesis has been accepted in partial fulfillment of the requirement of the Degree of masters of Science in Thermal Engineering.

Dr. Addisu Bekele		04/02/2019
Chairperson	Signature	Date
Dr. Dawit Gudeta		2/2/19.
Internal Examiner	Signature	Date
Dr. Getachew Shunki		02/02/2019
External Examiner	Signature	Date

Declaration

I hereby declare that this M.Sc. Thesis entitled "Simulation of the Performance of Vapor Absorption Air Conditioner for a Mid Bus Passenger Car Powered by Engine Exhaust Heat and Photo Voltaic Cell (PVC)" in partial fulfillment of the requirement of the degree of Master of Science in Thermal Engineering is an authentic record of my own work carried out from September 2017 to December 2018 under supervision of Dr. Gezahegn Habtamu, Thermal Engineering department, Adama Science and Technology University.

The matter embedded in this thesis has not been submitted for the award of a degree or diploma in any other university. All relevant resource information used in this paper has been duly acknowledged.

Million Matewose ....

Student Signature:

This is to certify that the above statement made by the candidate is correct to the best of our knowledge and belief. This has been submitted for examination with our approval.

Dr. Gezahegn Habtamu ....

Advisor Signature:

DEDICATION

I dedicate this work to my father
Matewose Mada, my mother Mame W/Michael,
My lovely sister Firehiwot and my little brother Bereket

upon whose advice and loving support I drew
courage strength and patience.

ACKNOWLEDGMENT

Prior from all the acknowledgments followed, I would like to thank God for giving health and patience to accomplish this thesis work successfully and giving me strength on difficult times.

I would like to appreciate the school of Mechanical, Chemical and Materials Engineering for giving me this scholarship opportunity to develop my engineering portfolio and engineering science knowledge.

With sincerity I express my gratitude to my advisor Dr. Gezahegn Habtamu, whose encouragement, guidance, motivation, intelligence, and expectations are crucial to my achievements and will serve as a continuous encouragement for my future duty which started in the anchor of the work.

My gratitude extends to the Mechanical Engineering Departmental staff, in particular to Dr. Addisu Bekele, Mr. Samuel G/Mariam, Mr. Mebratu Yishak and Mr. Sentayehu. I admire all of them, who gave me technical expertise counseling about the Mid Bus passenger car and car air conditioner and who has effortlessly provided their support at an instant's call.

I wish to thank the staff of Bishoftu vehicle manufacturing company in particular Commander Habtom for providing me all the necessary standards of Mid Bus passenger car.

But above all I owe life-long thanks to my family and friends whose support and understanding made all this possible.

Abstract

This thesis focuses on simulating the performance of a vapor absorption refrigeration system of 16.3 kW cooling capacity that is powered by heat energy recovered from exhaust gas of a Mid Bus and by dissipating electrical energy collected by direct solar PV cell. The major components of the AC system are evaporator, condenser, absorber, generator, pump and expansion valves. The AC system uses ammonia as refrigerant obtained by distillation of ammonia -water (NH_3-H_2O) solution in the generator. The cooling load was calculated for 23 passengers of the Mid Bus using heat balance method (HBM). For this load the vapor absorption air conditioner was simulated and modeled by EES software at 5°C evaporator temperature, 50°C condenser temperature, 10°C absorber temperature and 105°C generator temperature. The COP obtained is 0.656 which is good performance for vapor absorption system. For sizing each component of the AC system computer codes were developed in EES. The power source for the AC system was heat from the Mid Bus engine exhaust and heat obtained by dissipating electricity collected by photovoltaic cell (PVC) under Adama weather conditions. That is, solar PV will supply some power to support the exhaust energy to drive the air conditioning system. The size of the solar PV cell was 5.39 m x 2.455 m. From experimental test at 2300 RPM the exhaust temperature of flue gas was 422.66℃ . The average generator heat was 44.35 kW from engine exhaust and 10.33 kW by dissipating electric energy generated by solar PV cell. The energy consumption of the pump in driving the NH_3-H_2O solution was 1.06 W which is small. The performance of the system is also analyzed in EES for various working conditions.

Key words: - Vapor absorption refrigeration system, COP, Cooling load, Solar PV, Exhaust heat

TABLE OF CONTENTS

List of figures

List of tables

List of abbreviations

A/C	Air conditioning
A/F	Air fuel ratio
ARS	Absorption refrigeration system
CC	Cubic centimeter
CFC	Chlorofluorocarbon
COP	Coefficient of performance
CRS	Compression refrigeration system
DC	Direct current
EES	Engineering equation solver
G	Gram
Gr	Grashof's number
H_2O	Water
HBM	Heat balance method
IC	Internal combustion
Kg	Kilogram
LiBr	Lithium bromide
LMTD	Log mean temperature difference
M	Meter
NH_3	Ammonia
Pr	Prandtl number
PV	Photovoltaic
TR	Tone of refrigeration
VAC	Vapor absorption cycle
VAS	Vapor absorption system

Nomenclature

ε	Heat exchanger effectiveness
$\dot{Q}$	Rate of heat flow, kJ/s
c_p	Specific heat per unit mass
A	Area, m^2

C	Air heat factor, $W/(LK/s)$ and specific heat capacity, kJ/kgK
G	Local acceleration of gravity, kg/m^2
H	Enthalpy, kJ/kg
I	Current, A
K	Conductivity
L	Latitude,°
M	Mass, kg
$\dot{m}$	Mass flow, kg/s
N	Number of, dimensionless
P	Pressure, pa
Q	Heat energy, kJ
R	Ideal gas constant
S	Entropy, kJ/(kg·K)
T	Temperature, °C
U	Over all heat transfer coefficient, kW/m^2K
V	Velocity of fluid, m/s
W	Specific humidity, g/kg and mechanical work, J
$\dot{W}$	Rate of work, power
X	Mass fraction of ammonia
Z	Compressibility factor
f	Circulation ratio, dimensionless
v,v	Specific volume, m^3/kg
ab	Beam air mass exponents, dimensionless
ad	Diffuse air mass exponents, dimensionless
E	Irradiance, W/m^2
H	Heat transfer coefficient, kW/m^2K
IAC	Indoor solar attenuation coefficient, dimensionless
SHGC	Solar heat gain coefficient, dimensionless
Σ	Slope of the surface, °

θ	Incident angle, °
β	Solar altitude angle, °
δ	Declaration, °

Subscripts

Abs	Absorber
B	Beam
C	Convection, Cold
Cg	Condenser to generator
Cond	Condenser or cooling mode
D	Direct beam
dif	Diffuse
eng	Engine
Evap	Evaporator
Ex	Extraterrestrial
F	Fenestration
Fa	Fresh air
gal	Galvanized sheet
Gen	Desorber (generator)
Gh	High temperature generator
Gs	Glass surface
H	Hot
I	Inside
inf	Infiltration
L	Latent
O	Outside
Oc	Occupant
P	Pump
ply	Plywood
pol	Polystyrene foam

R	Refrigerant
R	Radiation
Rhx	Refrigerant heat exchanger
S	Sensible
S	Strong solution
Shx	Solution heat exchanger
Sit	Sitting
solar	Solar radiation
Sw	Sidewall
T	Transmission
W	Week solution

Acronyms

ε	Emissivity, dimensionless
Α	Absorptivity
Δ	Difference
Τ	Transmitivity
ϒ	Specific heat ratio
η	Efficiency, dimensionless
μ	Dynamic viscosity, Ns/m^2
ρ	Density, kg/m^3
σ	Steffen Boltzmann constant, 5.67*10^{-8} W/m^2K^4
τ	Optical depth, dimensionless
ϑ	Kinematic viscosity coefficient, Pa s

CHAPTER ONE

1. INTRODUCTION

1.1. Brief history

For prehistoric people, open fires were the primary means of warming their dwellings; shade and cool water were probably their only relief from heat. No significant improvements in human kind‘s condition were made for millions of years. There were a few exceptions to this lack of progress. The ancient Romans had remarkably good radiant heating in some buildings, which were achieved by warming air and then circulating it in hollow floors or walls. In Europe, Leonardo daVinci designed a large evaporative cooler.

The development of effective heating ventilation, and air conditioning, however, was begun scarcely 100 years ago. Central heating systems were developed in the nineteenth century, and summer air conditioning using mechanical refrigeration has grown into major industries only in last 60 years (David, 2003). The first air conditioning system was used for industrial as well as comfort air conditioning. Eastman Kodak installed the first air conditioning system in1891 in Rochester, New York for the storage of photographic films. An air conditioning system was installed in a printing press in 1902 and in a telephone exchange in Hamburg in 1904.

Due to the pioneering efforts of carrier and also due to simultaneous development of different components and controls, air conditioning quickly became very popular, especially after 1923 (Charles, 2003). At present air conditioning is widely used in residences, offices, commercial buildings, hospitals and in mobile applications such as rail coaches, automobiles, aircrafts etc.

1.2. General air conditioning

Air conditioning is a fuller automatic controlling of the atmospheric environment either for comfort of human beings or animals or for the proper performance of some industrial process, manufacturing plants and scientific process. The adjective "full" demands purity, movement, temperature and the relative humidity of the air be controlled within the limits imposed by the design specification. It is possible for certain applications; the pressure of the air in the environment may also have to be controlled. Air conditioning is often misused as a term and is loosely and wrongly adopted to describe a system of simple ventilation. It is really correct to talk of air conditioning only when a cooling and dehumidification function is intended, in addition to other aims. This means that air conditioning is always associated with refrigeration and it accounts for the comparatively high cost of air conditioning. Refrigeration plant is precision -built machinery and is the major item of cost in an air conditioning installation, thus the expense of air conditioning in a building is four times greater than that of only heating it. Full control over relative humidity is not always exercised, hence for this reason a good deal of partial air conditioning is carried out; it is still referred to as air conditioning because it does contain refrigeration plant and is therefore capable of cooling and dehumidifying air.

The essential feature of comfort conditioning is that it aims to produce an environment which is comfortable to the majority of the occupants. The ultimate comfort can never be achieved, but the use of individual automatic control for individual rooms helps considerably in satisfying most people comfort condition.

1.3. Common automotive air conditioning

With the invention of the R-12 in 1928 by General Motors researchers, the dawn of the automotive air-conditioning started. The first prototype self-contained system was installed in a 1939 Cadillac. Packard Motor Company in 1939 was the first company to offer complete auto air-conditioning system for cooling in summer and heating in winter using R12 refrigerant. The first bus A/C proto developed in 1934 by a joint venture between Houde Engineering Corporation of Buffalo, NY and Career Engineering Corporation of New York, NJ and others followed. Initial air-conditioners had a number of problems as well as Second World War hampered the production/progress. In the 1953 model year, many of the problems had been resolved and General Motors and Chrysler came back with improved air conditioning and that luxury became the necessity now for a common car owner forever! Until then most of the A/C parts were placed in the trunk and took up whole space of trunk. In 1953, Harrison Radiator Division of General Motors came up with a revolutionary air conditioner that was totally spaced in the under hood and dashboard (eliminating it from the trunk). Harrison Radiator analyzed nine refrigerants and by 1976 arrived at R134a as the replacement of R12 eliminating chlorine. However, there was no commercial availability of R134a then

Allied Chemicals, the major company conducting research on R134a then, would supply about 1 lb. of refrigerant per week and the need was about 1000 lb. per week for A/C system development work at Harrison in those days. Although the viability of R134a was proven by Harrison through wind tunnel tests on 1978 Chevrolet, the development of A/C system with R134a was discontinued due to the lack of availability of R134a till the Montreal Protocol was adopted by United Nations in September 1987 (Ghodbane et al., 2003). The first major revolution in the A/C system thus came starting 1990s by replacement of R-12 to R-134a to eliminate the ozone depletion in stratosphere by introducing a refrigerant having chlorine replaced by fluorine in its composition. The commercial production of R134a started with DuPont and ICI in 1990.Conversion from R12 to R134a in the USA, Europe and Japan took place during 1991-1994. The rest of the world has changed to R134a as the refrigerant for the A/C system during late 1990s and early 2000s.

1.3.1. Compression refrigeration cycle

Refrigeration is a process of removing heat from an object, mainly in a confined space, and rejecting the unwanted heat into a specific preferable environment. In other words, the refrigeration process is a method of lowering the temperature of an object. There are two common refrigeration systems which are widely used. These are Absorption Refrigeration System (ARS) and Compression Refrigeration System (CRS).

A compression refrigeration system utilizes a mechanical compressor, i.e. electric motor, to mechanically drive the heat from a low temperature to a high temperature (Figure 1.1). Conversely, in an absorption refrigeration system (Figure 1.2), the mechanical compressor in the compression cycle is replaced by two heat exchanger unites, a generator/desorber and an absorber, which creates a heat transfer from a low temperature to a high temperature.

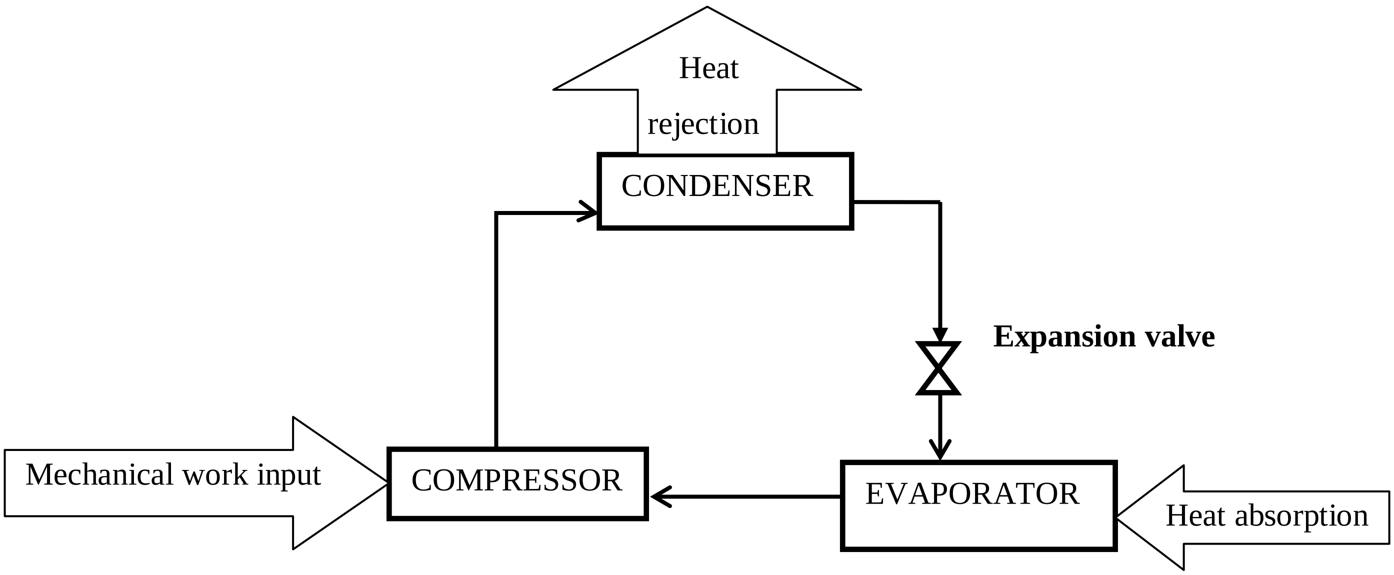

Figure 1.1 A simple compression refrigeration system.

1.3.2. Vapor absorption refrigeration cycle

Absorption cycles produce cooling and/or heating with thermal input and minimal electric input, by using heat and mass exchangers, pumps and valves. The absorption cycle is based on the principle that absorbing ammonia in water causes the vapor pressure to decrease (Mittal et al., 2015). The basic operation of an ammonia-water absorption cycle is as follows. Heat is applied to the generator, which contains a solution of ammonia water, rich in ammonia. The heat causes high pressure ammonia vapor to desorb the solution. Heat can either be from combustion of a fuel such as clean-burning natural gas, or waste heat from engine exhaust, other industrial processes, solar heat, or any other heat source. The high pressure ammonia vapor flows to a condenser, typically cooled by outdoor air. The ammonia vapor condenses into a high pressure liquid, releasing heat which can be used for as heat source for space heating. The high pressure ammonia liquid goes through a flow restriction to the low pressure side of the cycle. This liquid, at low pressures, boils or evaporates in the evaporator. This provides the cooling or refrigeration effect. The low pressure vapor flows to the absorber, which contains a water-rich solution obtained from the generator. This solution absorbs the ammonia while releasing the heat of absorption. This heat can be used as product heat or for internal heat recovery in other parts of the cycle, thus unloading the burner and increasing cycle efficiency. The solution in the absorber which becomes rich in ammonia again is pumped to the generator where it is ready to repeat the cycle (Mittal et al., 2015).

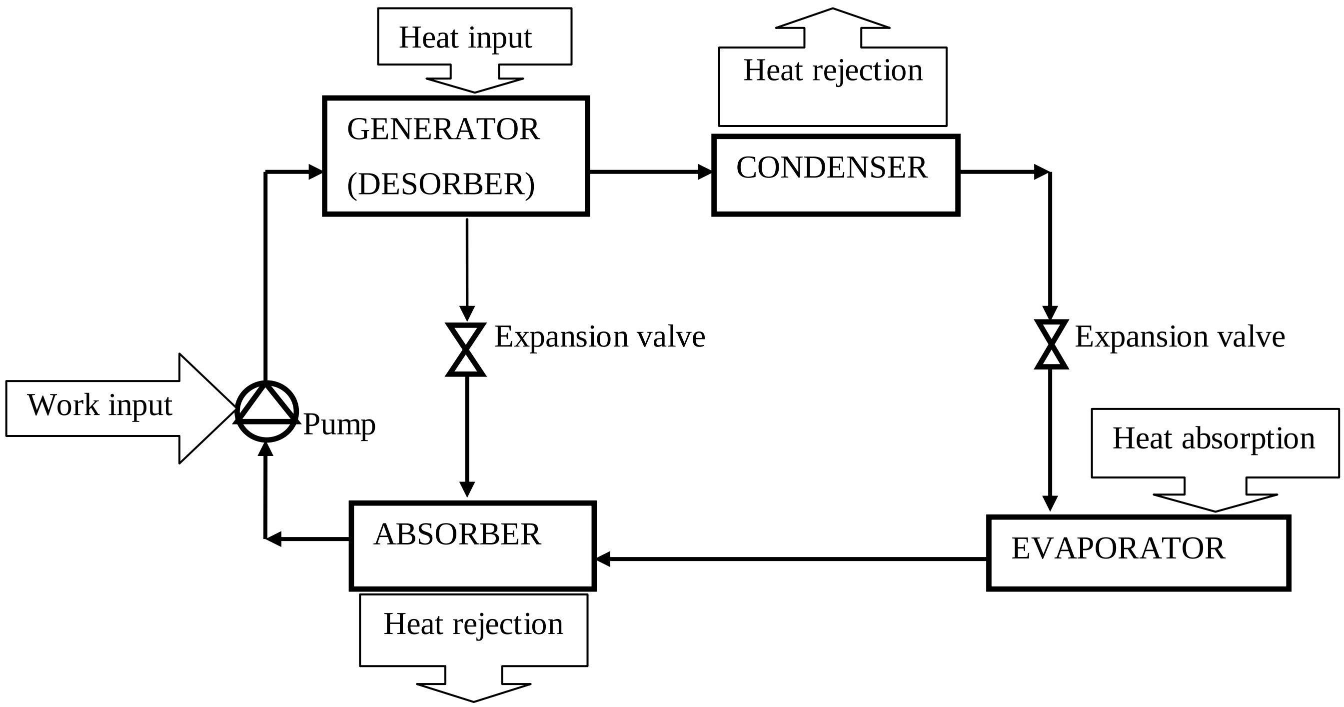

Figure 1.2 A simple absorption refrigeration system.

1.4. Working fluid for vapor absorption refrigeration systems

Performance of an absorption refrigeration system is critically dependent on the chemical and thermodynamic properties of the working fluid. A fundamental requirement of absorbent/refrigerant combination is that, in liquid phase, they must have a margin of miscibility within the operating temperature range of the cycle. The mixture should also be chemically stable, non-toxic, and non-explosive. In addition to these requirements, the following are desirable.

1. The elevation of boiling (the difference in boiling point between the pure refrigerant and the mixture at the same pressure) should be as large as possible.
2. Refrigerant should have high heat of vaporization and high concentration within the absorbent in order to maintain low circulation rate between the generator and the absorber per unit of cooling capacity.
3. Transport properties that influence heat and mass transfer, e.g., viscosity, thermal conductivity, and diffusion coefficient should be favorable.

4. Both refrigerant and absorbent should be non-corrosive, environmental friendly, and low-cost.

Many working fluids are suggested in literature. A survey of absorption fluids provided that the most common working fluids are Water-NH_3 and LiBr-water. The reasons why aqua-ammonia was chosen will be given in the following discussion.

The use of LiBr/water for absorption refrigeration systems began around 1930. Usually, this combination serves large scale water-chilling units for central plant air-conditioning systems (capacity from 100 kW to 3500 kW). The system is normally more complex and requires additional auxiliary components. Another problem is the crystallizing of lithium bromide in aqueous solutions. Two outstanding features of LiBr/water are non-volatility absorbent of LiBr (the need of a rectifier is eliminated) and extremely high heat of vaporization of water (refrigerant). However, using water as a refrigerant limits the low temperature application to that above 0°C. As water is the refrigerant, the system must be operated under vacuum conditions. At high concentrations, the solution is prone to crystallization. It is also corrosive to some metal and expensive. The choice of lithium bromide refrigerant combination for our application would not be acceptable, because the heat energy in the exhaust gas varies with the engine's rotation and the cooling effect at the evaporator changes with the vehicle's speed creating conditions which would encourage crystallization.

Aqua-ammonia is one of the oldest and most widely used combinations for absorption refrigeration systems. The solubility of ammonia under absorber conditions is typically around four times the Raoult value. Ammonia has a high latent heat of vaporization and a small specific volume of liquid refrigerant, which is necessary for efficient performance of the system. Since both NH_3 and water are volatility, the cycle requires a rectifier to strip away water that normally evaporates with NH_3. Without a rectifier, the water would accumulate in the evaporator and offset the system performance. There are other disadvantages such as its high pressure, toxicity, and corrosive action to copper and copper alloy. However, water/NH_3 is environmental friendly and low cost. For Ammonia-Water combination possesses most of the desirable qualities are listed below (Mittal et al., 2015):

- 1 m^3 of water absorbs 800 m^3 of ammonia (NH_3).
- Latent heat of ammonia at-15^oC = 1314 kJ/kg.
- Critical temperature of ammonia = 132.6^oC.
- Boiling point of ammonia at atmospheric pressure = -33.3^oC.

1.5. General introduction on vapor absorption refrigeration cycle for automotive air conditioning

The vapor absorption refrigeration is a heat operated system. This is older than the vapor compression system. In the early 1900's, refrigeration with this system using kerosene burner was popular. When CFC's were introduced and electric power was cheap, compression system having better COP got popular. With increase in the electricity charges and the phase out of the CFC's, the absorption system is again becoming popular in large capacities. In the generator the absorbent is heated to release the refrigerant vapor as a high pressure vapor, to be condensed in the condenser (Pavoodath, 2012).

A rough energy balance of the available energy in the combustion of fuel in a motor car engine shows that one part is changed into shaft work to drive the car, one part is lost at the radiator and another one is wasted at the exhaust system**.** Even for a small motor car engine, energy of the order of 10 kW is wasted in the exhaust gas. This heat is enough to power an absorption refrigeration system.

In a motor car air-conditioner using the absorption refrigeration cycle, the waste heat energy is utilized and about 10 percent of shaft power normally used to run the compressor of a conventional system could be saved.

In order to study the performance of running a passenger car air-conditioner using the absorption refrigeration cycle, a Mid Bus was employed.

1.6. The Mid Bus passenger car existing AC system

Figure 1.3 Mid Bus [Changzhou Huanghai Automotive Co., Ltd.]

As we can see in figure 1.3 the Mid Bus is assembled in Bishoftu Automotive Industry. It has size of $8.54\,m \times 2.455\,m \times 3.35\,m$ (with air conditioner) and sits for 32 passengers plus driver.

The actual air-conditioning system of Mid Bus car is a vapor compression system which is non-independent type, and the compressor is driven by mechanical energy taken from the engine. The air-conditioning unit can operate normally only when the engine is running, electricity supplying by the power generator. The condenser placed on the top of Mid Bus and also the evaporator assembly behind the condenser in to control volume of refrigeration. The operation panel of the air conditioner is as indicated as per the following drawing:

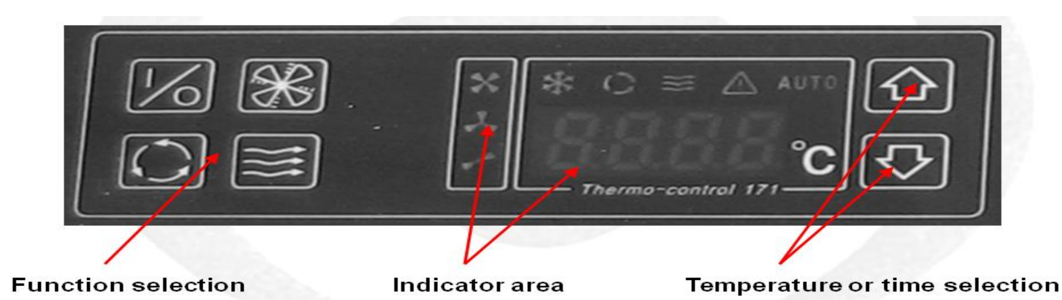

Figure 1.4 A compression refrigeration system of Mid Bus electrical control panel [Changzhou Huanghai Automotive Co., Ltd.].

Exhaust gas energy is being invested in many forms. In this study it is required to extract information on the present Mid Bus air conditioning structure so that its replacement with vapor absorption AC system may be successful. The heat required to drive the vapor absorption AC system for Mid Bus passenger car are engine exhaust heat and heat obtained by dissipating electricity harnessed by photo voltaic cell. Table 1.1 indicates the specification of the existing vapor compression air conditioner installed on the Mid Bus.

Table 1.1 Air conditioner of Mid Bus specification [Changzhou Huanghai Automotive Co., Ltd.].

<table>
<tr><td rowspan="6">Air-conditioning system of WP5.180E3</td><td>Air-conditioning system</td></tr>
<tr><td>Type: KT20D5-2C-type non-independent overhead air conditioner</td></tr>
<tr><td>Refrigerating capacity: 20000 kcal/h</td></tr>
<tr><td>Defrost system</td></tr>
<tr><td>Model: CS-7</td></tr>
<tr><td>Heating capacity: 7 kW</td></tr>
</table>

1.7. Motivations for this work

In the vapor absorption refrigeration system, a physicochemical process replaces the mechanical process of the vapor compression refrigeration system by using energy in the form of heat rather than work. The vapor absorption systems have many more favorable characteristics. Typically a much smaller electrical input is required to drive the solution pump, also it is having fewer moving parts means lower level of noise. In this system the compressor is replaced by an absorber, a pump and generator. These installed components performed the same work as that of compressor used in vapor compression system. The efficiency of an IC engine is 35–40% which is mounted on a vehicle, meaning that only about one-third of the energy in the fuel used is converted to useful work like running the vehicle. Automotive air-conditioning system has played an important role in human comfort and to some extent safety during vehicle driving in varied atmospheric conditions. It has become an essential part of the vehicles of all categories worldwide. In automobile air conditioning normally vapor compression refrigeration cycle is used. The cycle run by engine power and consumes around 10% of the total power produced by the engine (Rahul et al., 2015) and engine power reduction of the vehicle will be observed. Because of this reason most automobile owners turned them off to save the extra fuel. Therefore these ways of air conditioning use in a car has economic consideration failures, only one-third of the energy in the fuel is converted into useful work and the remaining one is wasted to the environment. One of the losses is in the form of exhaust gases. Hence to utilize the exhaust gases and waste heat from an engine the vapor absorption refrigerant system can be put into practice. Due to this reason, replacing the present vapor compression refrigeration system which uses the engine power with another vapor absorption refrigeration air conditioning system that works with engine waste heat recovery and green energy would be a better alternative to be considered. In addition, the top part of most vehicles of Mid Bus size can accommodate a grid of size $2.455\ m \times 8.54\ m$ which would be good consideration to use this space for solar energy harnessing. The idea of renewable energy is not new but the need for it now is greater than ever before. Introducing solar powered air conditioner vehicle to assist conventional IC engine exhaust gas utilizing car has two-fold advantages, First, solar power is renewable and abundant and second, a photo voltaic cell powered vehicle body will increase space utilization and energy production by solar would have zero emission.

Now a day's Ethiopian Automotive Industry located in Debrezeyt manufacture different kinds of buses with vapor compression air conditioning system mounted on it. This paper tries to simulate the performance of a vapor absorption air conditioning system for the Mid Bus by using the exhaust heat from its engine and a solar PV cell mounted on its roof top area of $2.455\ m \times\ 8.54\ m$ for harnessing solar electricity that would later converted into heat by dissipating for heating the ammonia-water solution in the generator.

1.8. Objective

1.8.1. General objective

It is possible to power AC systems of passenger cars using the engine exhaust and also heat obtained by dissipating electricity by solar photo voltaic cell to save fuel by replacing the vapor compression system with heat based air conditioners like vapor absorption systems. The general objective of this study is to simulate the performance of a vapor absorption air conditioner for a Mid Bus passenger car using heat from engine exhaust and solar PV cell.

1.8.2. Specific objective

The specific objectives of the study are:

- Estimating total cooling load of a passenger Mid Bus.
- Studying the engine exhaust gases temperature and mass flow rate experimentally.
- Simulating the performance of a vapor absorption refrigeration cycle for the passenger car using engine exhaust gas and solar PV cell(s).
- Sizing the major components of the vapor absorption air conditioner operated by engine exhaust and solar PV for the calculated heat load and,
- Optional test on the performance of the developed vapor absorption air conditioner for the Mid Bus.

CHAPTER TWO

2. LITERATURE SURVEY

2.1. Literature about general vehicle air conditioning system

Vicatos et al., (2008), designed and tested absorption refrigeration cycle using energy from exhaust gas of an internal combustion engine on Nissan 1400 truck, theoretical analysis was verified by both laboratory and road tests through the results obtained. The study chooses refrigerant ammonia with water solution. It also considered certain disadvantages of ammonia: ammonia attacks copper and its alloys when it has been hydrated, therefore all components have been made from mild steel or stainless steel. It concludes that in the exhaust gases of motor vehicle, there is enough heat energy that can be utilized to power an air conditioning system. And also the aqua ammonia combination appears to be a good candidate as a working fluid for an absorption car air conditioning system.

Yılmaz, (2015), reported that air-conditioning is crucial for automobile industry. The need is huge especially for intercity buses. It takes $5-10\ kW$ of mechanical energy from the main engine. Because it is very important to lower the use of fuels both for economic and environmental purposes, it is good to save this mechanical energy needed for air-conditioning. Instead, huge waste heat of exhaust gases should be used for air conditioning. In the study the data of a 6-cylinder, 4-stroke turbocharged diesel engine is used. The data used are given by Shu et al., (1998). Exhaust temperatures of diesel engines of vehicles are around $400-700℃$ and waste thermal energy ranges from $20\ kW$ to $400\ kW$.

Manzela et al., (2010), presented an experimental study of an ammonia-water absorption refrigeration system using the exhaust of an internal combustion engine as energy source. Overall, carbon monoxide emission was decreased when the absorption refrigerator was installed in the exhaust gas, while hydrocarbon emissions increased.

Aiqdah, (2011), presented an experimental study of an aqua-ammonia absorption system used for automobile air conditioning system. It is evident that COP strongly depends on working conditions such as generator, absorber, condenser and evaporating temperature.

Daut et al., (2013), focused in the design and construction of a direct current (DC) air conditioning system integrated with photovoltaic (PV) system which consists of PV panels, solar charger, inverter and batteries. The air conditioning system can be operated on solar and can be used in non-electrified areas. As we all known, solar energy is cost effective, renewable and environmentally friendly.

Abeygunasekara et al., (2014), studied a new air conditioning system for the 1500CC four stroke diesel engine vehicles and consider the exhaust smoke at idle speed. Considering the heat range of the exhaust system of an automobiles, identified the maximum possible heat range provided between the exhaust manifold and flexible joint. Hence, the heat exchanger is designed to install in between the exhaust manifold and flexible joint of exhaust system. Theoretical calculation and studies found that it is possible to design alternative automobile air conditioning system based on vapor absorption refrigeration cycle by utilizing exhaust waste heat.

Sowjanya, (2013), in this thesis, energy from the exhaust gas of an internal combustion engine is used to power an absorption refrigeration system to air-condition an ordinary passenger car. All the required parts for the absorption refrigeration system is designed and modeled in 3D modeling software Pro/Engineer. Thermal analysis is done on the two main parts of the refrigeration system (condenser & evaporator) to determine the thermal behavior of the system. Modeling is done in Pro/Engineer and use ANSYS for the analysis. By observing the analysis results, thermal flux is more for aluminum alloy 204 than copper for both condenser and evaporator. So using aluminum alloy 204 is better.

Chandrakar and Saikhedkar, (2016), have done design of vapor absorption refrigeration system. Design calculations have been made for different components of the system like evaporator, generator, absorber, heat exchanger of vapor absorption system. The vapor absorption system is used for air conditioning of four stroke four cylinder passenger car. As per the calculation in their study, the air conditioning system for small car can run at $0.75\ TR$ and needs $4.5\ kW$ heat for evaporating refrigerant from mathematical modeling calculation. Therefore, the generator is designed to have capacity of $4.5\ kW$ with temperature around $97℃$ and pressure of 17.8 bars from previous calculation. A car mostly runs between 1800 rpm to

2800 rpm and therefore generator has been designed for 2500 rpm at 328℃ temperature. It needs $2.73\ kW$ heat rejections for running $0.75\ TR$ air conditioning in car from calculation. Therefore condenser is designed to have capacity $2.73\ kW$. Air conditioning system of car depends on size of the car. For running air conditioning system in small car for sitting comfortably, $0.75\ TR$ is required which is equivalent to $2.625\ kW$. Hence the evaporator is designed to have capacity $2.625\ kW$ heat transfer. An absorber capable of absorbing $3.85\ kW$ has to be designed. From the above result, the feasibility of the exhaust heat to run vapor absorption system has been reasonably proved. The COP value is found 0.57. As power output increase, the heat recovered from exhaust gas also increase difficulty may occur when the vehicles at rest or in very slow moving traffic conditions.

Raghavulu et al., (2015), studies focused towards the design and development of an air cooling system for the cabin of truck using waste heat from exhaust. The designed parts of the system examined by thermodynamic analysis of ammonia vapor absorption refrigeration system. From the result, it can be concluded that for providing cabin cooling for truck using engine exhaust, the vapor absorption systems can be used i.e. ammonia/water vapor absorption cycle. The COP of ammonia/water system varies from 0.3528 to 0.3113.

Goyal et al., (2013), presented the work procedure in designing and fabrication of solar Air Condition system which is meant specially for creating green environment. The study used PV solar cell. This cell can directly change the solar energy into electric energy. The study used the battery helped to store the solar energy. Single phase DC motor and motor is driven by battery power. This motor is transfer the power to compressor to move and start the next process.

Imam et al., (2013), presented the design of air conditioning system for a Volvo Bus; a fully equipped automotive air-conditioning system consists of five main components: a compressor, a condenser, an orifice tube, an evaporator and an accumulator. R-134a is used as refrigerant by considering the various parameters. The main parameters that were considered in bus air-conditioning system design include:

- Occupancy data
- Dimensions and optical properties of glass

- Outside weather conditions
- Dimensions and thermal properties of materials in bus body
- Indoor design conditions

The heating or cooling load in a passenger bus may be estimated by summing the heat flux from the following loads:

- Solid walls (side panels, roof, floor)
- Glass (Slide, front and rear windows)
- Passengers
- Engine and Ventilation
- Evaporator fan motor

With the experimental set-up, some results have been obtained which revealed some unknown aspects of the automotive air conditioning systems. Design of Air conditioning system in auto mobiles is done successfully for Volvo Bus. The parameters of the bus are $3200\, cu.ft.$ Finally the output obtained is $8.25\, TR$.

Mittal et al., (2015), studied the comparison of absorption refrigeration and compression refrigeration system. The result conclude that possible methods to recover the waste heat from internal combustion engine through the study on the performance and emissions of the internal combustion engine are discussed upon and can be designed. Waste heat recovery system is the best way to recover waste heat and saving the fuel.

In the thesis done by **Kumar et al., (2017)**, energy from the exhaust gas of an internal combustion engine is used to power an absorption refrigeration system to air-condition an ordinary passenger car. All the required parts for the absorption refrigeration system is designed and modeled in 3D modeling software CREO parametric software. Thermal analysis is done on the main parts of the refrigeration system to determine the thermal behavior of the system. Analysis is done using ANSYS. Observing the analysis results, total heat flux is more for copper than remaining three materials for both condenser and evaporator. So using copper is better.

A feasibility study was conducted by **Bergeron, (2001)**, to determine if solar power could be used to offset or eliminate the diesel fuel powered refrigeration systems currently used in transport applications. This study focused on the technical feasibility and economic viability of solar for this application. A target application was selected and a moderately detailed mathematical model was constructed to predict the performance of the system based on hourly solar insulation and temperature data in four U.S. cities. An economic analysis is presented comparing the use of solar photovoltaic *vs.* diesel for this application.

In the study of **Reddy and Yadav, (2015)**, the waste heat from C.I. engine is suggested as one of the alternative energy source for refrigeration system. In this study, an overview of utilization of waste heat with a brief literature of the current related research is studied. The review covers the vapor absorption refrigeration system connected to the four stroke diesel engine. From the engine the two main areas through which the heat exhausted into the atmosphere are the cooling water and the exhaust gases. The heat available at exhaust gas is $5.5\ kW$ and heat carried by cooling water is $12.54\ kW$. Vapor absorption refrigeration system is presented as an attractive substance that utilizes the waste heat from C.I. engine. By using waste heat energy the coefficient of performance is increased to 23% and the energy consumption of $220\ kJ$ is saved than the existing system. So it is estimated that recovery of waste heat reduces heat loss, improves performance of the system, saves the fuel, reduces the emission of exhaust gas, and is economically feasible. Also the area from which heat is lost to the surroundings decreases. From the experimental study, the vapor absorption refrigeration system can be obtained using heat that is expelled in to the atmosphere from C.I. engine. Through the study and by analyzing the obtained results it is evident that the waste heat based refrigeration system is economic, echo-friendly with zero CO_2 emissions. Hence, the system selected is technically proven, echo-friendly and economically better.

Aiqdah, (2011), presented an experimental study of an aqua-ammonia absorption system used for automobile air conditioning system that uses the exhaust waste heat of an internal combustion diesel engine as energy source. The energy availability that can be used in the generator and the effect of the system on engine performance, exhaust emissions, auto air conditioning performance and fuel economy are evaluated. The main purpose of this investigation was to explore the feasibility of using waste energy to design the absorber and generation since these components are the most important components of absorption and they are directly influence the performance of the whole system. It has been found that the aqua - ammonia concentration affect the cooling capacity. The estimated cooling load for the automobile found to be within acceptable ranges which are about 1.37 ton refrigeration. The obtained results indicated that the coefficient of performance (COP) values directly proportional with increasing generator and evaporator temperatures but decrease with increasing condenser and absorber temperatures. Measured values for generator, absorber, and evaporator and condenser temperature were recorded and the coefficient of performance of the system varied between 0.85 and 1.04.

Vinofer and Rajakumar, (2016), used the Heat Balance Method (HBM) for estimating the heating and cooling loads which develops inside the vehicle cabin. The Load Calculation of Automobile Air Conditioning System is calculated and presented. An hourly cooling load is calculated in Tirunelveli region with respect to its latitude. A lumped model of a vehicle cabin was considered for thermal load calculation. Several loads act on the vehicle cabin are classified under nine different categories. The summation of all the load types will be the instantaneous cabin overall heat load gain. The mathematical formulation of the model can thus be summarized as:

$$Q_{tot} = Q_{met} + Q_{dir} + Q_{dif} + Q_{ref} + Q_{amb} + Q_{exh} + Q_{eng} + Q_{ven} + Q_{ac} \qquad (1.1)$$

Using heat balance method, the heat occurred in the cabin consists of metabolic, direct, diffuse, reflected, ambient, exhaust, engine, ventilation, and AC loads has been calculated. A cooling load of negative value of $2154.27\ W$ was estimated using the above relation.

Shinde et al., (2017), were studied the performance of Electrolux vapor absorption refrigeration cycle setup installed in SKNCOE, Pune, India. The main motive behind experimentations was to check the feasibility of implementation of VARC in cars for cabin cooling. Since heat recovered from exhaust gases is utilized in VARC, it results into economical air conditioning. Since performance of any thermodynamic system is dependent on temperatures, variation in performance of VARC system with respect to various temperatures is studied. Along with the performance analysis, the paper focuses on the enlightening the practical approach of implementation of above system into automobiles. It was found that energy saving up to 10% could have been achieved based on experimental data of this system.

Karthik et al., (2014), studies were successful in designing and developing an automobile air conditioning system using engine waste heat based on Vapor Absorption Refrigeration System using R-134a and DMF as a refrigerant and absorbent combination. Further the employed system helped for commercial heavy vehicles including those which are involved in the transportation of refrigerated products.

Pan et al., (2017), developed a novel portable, renewable, solar energy-powered cooling system with wireless power transfer (WPT) and super capacitors to cool the vehicle cabin. The proposed system consists of a solar collector mechanism, an energy conduit, and a temperature control and cooling module. First consisting of folding solar photovoltaic (PV) panels the solar collector mechanism making the proposed system portable. Once collected, the solar energy is converted into electricity and stored in the super capacitors through wireless power transfer without breaching the vehicle body. Automatic temperature regulation is achieved with the cooling device via the temperature control and cooling module. The experimental results indicate that a maximum output power of $2.181\ W$ and a maximum WPT efficiency of 60.3% are achieved when the prototype loaded with $3\ \Omega$ and $5\ \Omega$ respectively. Meanwhile, the simulation showed the temperature inside the cabin is reduced by $4.2℃$ in average, demonstrating that the proposed solar energy-powered cooling system is effective and feasible in cooling a hot vehicle cabin.

Mathapati, (2014), performed feasibility study to find out the energy available from exhaust gas of a vehicle. Cooling load for the automobile has been estimated. In the study theoretical evaluation of LiBr-Water based absorption refrigeration system is presented. Mathematical modeling of system using EES software is done the effects on COP of system with change in different parameters has been also studied.

Padhihari, (2016), carried out to develop a system which will allow the customer to use air conditioning even when the car is at rest. The result indicated that the use of thin film metallic nano particles solar cells will help in bringing down the cost of the solar panel and to increase the efficiency.

2.2. Conclusion from the literature survey

Considerable amount of research and application works regarding the absorption refrigeration system. Based on most of the studies reviewed in this work, air conditioning can be described as the science of controlling the temperature, humidity, motion and cleanliness of the air within an enclosure. In a passenger/driver cabin of a vehicle, air conditioning means controlled and comfortable environment in the passenger cabin during summer and winter, i.e., control of temperature (for cooling or heating), control of humidity (decrease or increase), control of air circulation and ventilation (amount of air flow and fresh intake vs. partial or full recirculation), and cleaning of the air from odor, pollutants, dust, pollen, etc. before entering the cabin. While the AC system provides comfort to the passengers in a vehicle, its operation in a vehicle has twofold impact on fuel consumption: (1) burning extra fuel to power compressor for AC operation, and (2) carrying extra AC component load in the vehicle all the time. Reading all this most of the proposed ideas focused on using solar energy to run the Vehicle or using exhaust gas to increase the temperature on some part of the absorption cycle. Therefore, this work focused on modeling a way to make a use of both solar energy and exhaust gases to run the air conditioner of the bus. Most of the studies has made a partial study on both unused energies and were a huge source of information and numerical data for this study. The standards employed during the studies were taken from (ASHRAE, 2009) which was one of reviewed literatures. Most of the complicated mathematical consideration while load calculations were simplified by the methods they proposed to use which are convincing and would be taken to inform the reader that this is the latest methods used on most of the studies. And it was difficult to find a uniform detail study on Mid Bus as a reference so, this study has made a general consideration on Mid Buses of relative size to take some particular data.

CHAPTER THREE

3. COOLING LOAD CALCULATION

Heating and cooling load calculations are carried out to estimate the required capacity of heating and cooling systems, which can maintain the required conditions in the conditioned space. An automobile air conditioning load factors are constantly and rapidly changing as the automobile moves over highways at different speeds and through all kinds of surroundings (Ruth, 1975). As the car moves faster there is greater amount of infiltration into the car and the heat transfer between the outdoor air and the car surface is increased. The physical sizing of the air conditioning system is critical, since space must be used efficiently to hold the design system. The Heat Balance Method (HBM) is used for estimating the heating and cooling loads which develops inside the bus. The net heat gain by the cabin can be classified under nine different categories. The total load as well as each of these loads can either be positive (heating up the bus) or negative (cooling down the bus) and may depend on various driving parameters.

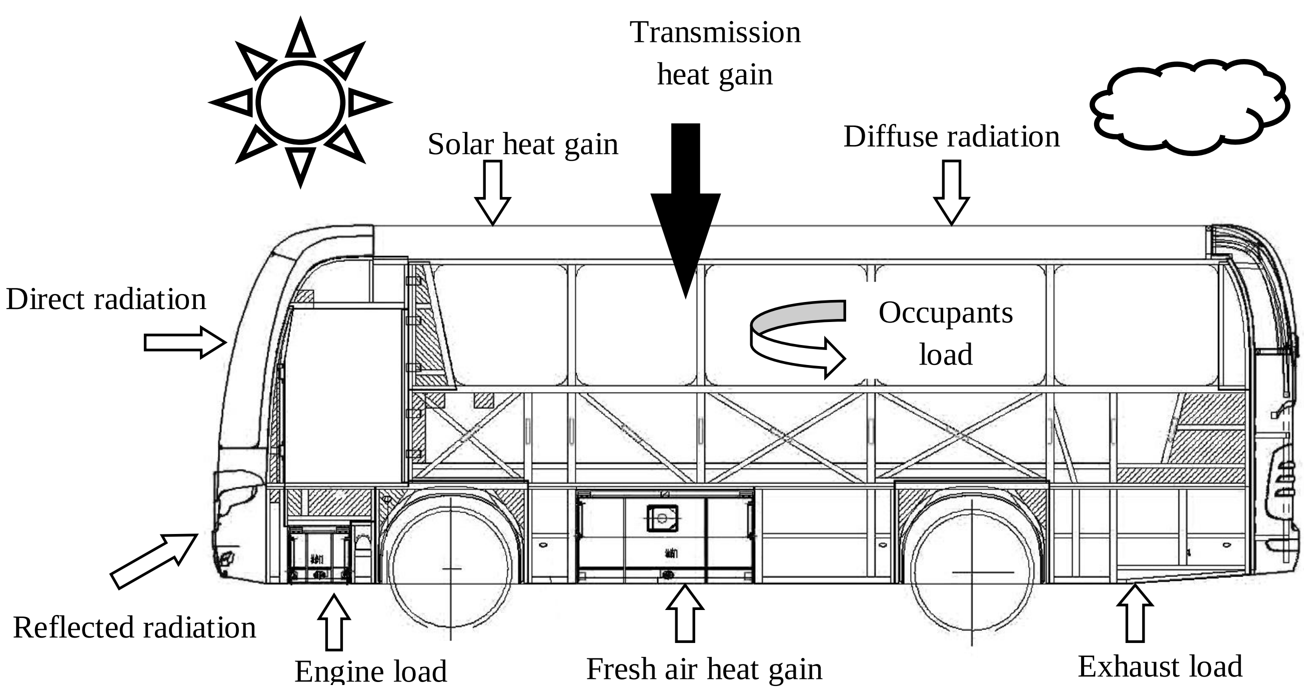

Figure 3.1 Schematic representation of thermal loads in a typical Mid Bus.

The Figure schematically shows the various thermal load categories encountered in a typical Mid Bus. Some of the above loads pass across the vehicle body plates/parts, while others are independent of the surface elements of the cabin.

Relations used in calculating the cooling load of the Mid Bus consists of internal, infiltration, solar, transmission and fresh air heat gains. Parameters affect the cooling load of the bus (heat gains) are gives in the Table 3.1.

Table 3.1 Affecting parameters to calculate the cooling load of Mid Bus.

Parameters	Value	Unit	Parameters	Value	Unit
Speed of the bus	80	km/h	Fresh air rate per passenger	20	m^3/h
Outside temperature	31	℃	Number of passenger	33	-
Outside relative humidity	63	%	Latitude	39	$°N$
Inside temperature	25	℃	Declination	23.086	°
Inside relative humidity	55	%	Total glazed area of both lateral sides	8.232	m^2
				6.552	m^2
Outside absolute humidity	18	g/kg	Glass area at front side	3.49	m^2
Inside absolute humidity	10.9	g/kg	Glass area at rear side	1.093	m^2
Length of the bus	8.54	m			
Height of the bus	3.35	m			
Width of the bus	2.455	m			

The relevant relations used to calculate the cooling load are presented below accordingly with the HBM way of calculating the load.

A. *Internal Heat Gains by Occupants*

Internal heat gain from passengers varies according to the number of passengers and their activity types, and can be calculated by the following relations (ASHRAE, 2009).

$$\dot{Q}_{i,oc} = N_{sit}\left(\dot{Q}_{s,sit} + \dot{Q}_{l,sit}\right) \tag{3. 1}$$

B. *Infiltration Heat Gain*

The cooling load calculation of the bus is made in the spring and summer seasons under the hot ambient conditions. The indoor air temperatures of the bus are generally 5-10℃ lower than the outdoor air temperature (being 6℃ in this study). So, a natural heat movement occurs from outside to inside.

Infiltration occurs due to design failures with time at the external surfaces of the bus (windows, doors, etc.) and the door opening while occupants get on and off the Mid Bus. Infiltration air movement occurs from outside (hotter medium compares with inside), so it handles as a heat gain. It consists of sensible and latent infiltration heat gains based on mass flow rate.

1) *Sensible infiltration heat gain*

Sensible infiltration heat gain corresponds to the change of the dry-bulb temperature of the inside air caused by moving airflow from outside due to infiltration and can be calculated using (ASHRAE, 2009), let as take that flow rate per passenger $20\,m^3/h$

fresh air rate become $33 \times 20\,m^3/h = 660\,m^3/h$

so, infiltration rate is 14.3% of fresh flow rate

$$Q_{inf} = 660\,m^3/h \times 14.3\% \tag{3. 2}$$

$$Q_{inf} = 94.38\,m^3/h \;\; or \;\; 0.0262\,m^3/s$$

The temperature difference between the ambient and inside the bus became $6\ ℃$

$$\dot{Q}_{inf,s} = C_s * Q_{inf} * \Delta T \tag{3. 3}$$

2) Latent infiltration heat gain

Latent infiltration heat gain corresponds to the change of humidity ratio of the inside air caused by air flow movement from outside due to infiltration and can be calculated by (ASHRAE, 2009), the change in relative humidity of ambient and inside the bus is $7.1\ g/kg$.

$$\dot{Q}_{inf,l} = C_l * Q_{inf} * \Delta W \tag{3. 4}$$

C. Solar Heat Gain

The sun is the most powerful and continuously heat source for the world. Also it affects at any moment as a heat gain during the daytime for the conditioned area of the bus. Solar heat gain consists of direct beam, diffuse and conductive components. Their calculation procedure is given below.

1) Direct beam

The first component of the solar heat gain corresponds to pair of solar lights radiated directly from the sun and it can be calculated by the following equations (ASHRAE, 2009).

$$\dot{Q}_{solar,d} = A_{d,f} * E_{t,b} * SHGC_d * IAC_d \tag{3. 5}$$

From meteorological data latitude is $39°N$ and δ for June of Adama 2017 is $23.086°$, and the value $\tau_b\ and\ \tau_d$ takes from (ASHRAE, 2009) so respectively $0.505\ and\ 1.892$.

$$\beta = 90 - |L - \delta| \tag{3. 6}$$

$$\theta = 90 - \beta \tag{3. 7}$$

$$m = {}^{1}/_{[\sin\beta + 0.50572(6.07995 + \beta)^{-1.6364}]} \tag{3. 8}$$

$$ab = 1.219 - 0.043\tau_b - 0.151\tau_d - 0.204\tau_b\tau_d \tag{3. 9}$$

Extraterrestrial normal irradiance E_o is found using equation 3.10,

$$E_o = E_{sc}\left(1 + 0.033\cos\left(360°\left(\frac{n-3}{365}\right)\right)\right) \tag{3. 10}$$

Where n is day of the year so, for June 17 n is 162

$$E_b = E_o exp(-\tau_b m^{ab}) \tag{3. 11}$$

$$E_{t,b} = E_b \cos\theta \tag{3. 12}$$

2) *Diffuse*

The second component of the solar heat gain corresponds to the diffuse component. Calculation of this component is more difficult because it has no isotropic nature. Also, its calculation changes with the surface type affecting on it. This component can be calculated by the flowing equations (ASHRAE, 2009).

$$\dot{Q}_{solar,dif} = A_{dif,f}\left(E_{t,d} + E_{t,r}\right) CHGC_{dif}\ IAC_{dif} \tag{3. 13}$$

$$Y = max(0.45\ or\ 0.55 + 0.437\cos\theta + 0.31\cos^2\theta) \tag{3. 14}$$

$$ad = 0.202 - 0.852\tau_b - 0.007\tau_d - 0.35\tau_b\tau_d \tag{3. 15}$$

$$E_{dif} = E_o\ exp(-\tau_d\, m^{ad}) \tag{3. 16}$$

$$E_{t,d} = E_{dif}\ Y \tag{3. 17}$$

$$E_{t,r} = \left(E_b \sin\beta + E_{dif}\right)\rho_g \frac{1-\cos\Sigma}{2} \tag{3. 18}$$

Transmission Heat Gain

Transmission heat gain occurs at six surfaces of the Mid Bus via temperature difference between outside and inside medium of the bus. In this section, the transmission heat gain is calculated for only lateral surfaces of the bus.

1) Side walls

Transmission heat gain consists of three main heat transfer mechanisms through the side walls, namely (i) the convection heat transfer mechanism at the outside and inside of the bus, (ii) the radiation heat transfer mechanism at the outside of the bus, and (iii) the conduction heat transfer mechanism at each external side of the bus. After calculation of these three parameters, the total heat transfer coefficient is determined, and hence the transmission heat gain from side walls can be obtained.

a) Outside convection heat transfer coefficient

Outside convection heat transfer can be calculated by finding Re_o, Pr_o and $Nu_{L,o}$ values, respectively. Before finding Pr and Nu_L numbers, and the flow type has to be determined (Cengel and Boles, 2007). By interpolation thermodynamic property of air for the given temperatures,

Table 3.2 Extrapolation purpose from the air standard property table (ASHRAE, 2009).

Body interface of air	T(℃)	$\rho(kg/m^3)$	$\mu(J/m^2)$	$K(w/m.k)$	p_r
Outside	31	1.148	186.5×10^{-7}	26.6×10^{-3}	0.706
Inside	25	1.1707	183.6×10^{-7}	26.14×10^{-3}	0.7075

$$Re_o = \frac{\rho_o V_o L}{\mu_o} > 5 \times 10^5 \ \ turbulent\ flow \qquad (3.\ 19)$$

$$Re_o = 11654405.72 > \ 5 \times 10^5$$

So it is turbulent flow now we use the following equation

$$Nu_{L,o} = 0.0337\, Re_d^{0.8} Pr_o^{0.33} \qquad (3.\ 20)$$

$$h_o = Nu_{L,o} * \frac{k_o}{L} \qquad (3.\ 21)$$

b) Inside convection heat transfer coefficient

The most critical parameter is velocity of air at the inside of the bus while calculating the inside convection heat transfer coefficient. Other calculation steps are the same with obtaining h_i . Let us take velocity of the air inside the bus $0.15\, m/s$ from (ASHRAE, 2009).

$$Re_i = \frac{\rho_i V_i L}{\mu_i} \tag{3. 22}$$

$$Re_i = 81489.90196 < 5 \times 10^5$$

So it is laminar flow now we use the following equation:

$$Nu_{L,i} = 0.664\, Re_i^{0.5} Pr_i^{0.33} \tag{3. 23}$$

$$h_i = Nu_{l,i} * \frac{K_i}{L} \tag{3. 24}$$

c) Outside radiation heat transfer coefficient

Outside radiation heat transfer coefficient can be calculated, as given below (ASHRAE, 2009).

$$h_r = \epsilon\sigma(T_{sur} + T_o)(T^2{}_{sur} + T^2{}_o) \tag{3. 25}$$

d) Total heat transfer coefficient

Besides the convection and radiation heat transfer coefficient values, the conduction coefficient for each material has to be calculated. All of them specify resistance to heat transfer and it inverse gives the total heat transfer coefficient (Ozcana et al., 2015).

$$R_{t,sw} = \frac{1}{h_o + h_r} + \left(\frac{L_{gal}}{K_{gal}} + \frac{L_{pol}}{K_{pol}} + \frac{L_{ply}}{K_{ply}}\right) + \frac{1}{h_i} \tag{3. 26}$$

$$U_{t,sw} = \frac{1}{R_{t,sw}} \tag{3. 27}$$

e) Total heat transfer

After calculating the total heat transfer coefficient, the amount of the heat transfer can be easily determined by regarding the heat transfer area and the temperature difference between outside and inside mediums.

$$\dot{Q}_{t,sw} = U_{t,sw} * A_{t,sw} * \Delta T \tag{3. 28}$$

The total side wall area is $32.536\ m^2$.

2) *Transmission heat gains from other surfaces*

In the section, the transmission heat gain from both side walls (lateral surfaces) is calculated. For other four surfaces, the same calculation steps can be followed.

2.1) *Front and back side wall*

Replace the value L by $2.434m$ and total wall areas of front and back side is $8.935\ m^2$.

a) *Outside convection heat transfer coefficient*

$Re_o = 3329469.38 > 5 \times 10^5\ \ turbulent\ flow$

Therefore, h_o is calculated using equation 3.21

b) *Inside convection heat transfer coefficient*

$Re_i = 23280.09641 < 5 \times 10^5$ So it is laminar flow

Therefore, h_i is calculated using equation 3.24

a) *Outside radiation heat transfer coefficient*

Radiation is the same for all side so, we can use h_r of side wall

b) *Total heat transfer coefficient*

To calculate $U_{t,f\&r}$ using equation 3.27 and the values gated on the above

c) *Total heat transfer*

$$\dot{Q}_{t,f\&r} = U_{t,f\&r} * A_{t,f\&r} * \Delta T \tag{3. 29}$$

2.2) *Roof and floor side wall*

The overall heat transfer coefficient is the same as lateral side

$$U_{t,r\&fl} = U_{t,sw} \tag{3. 30}$$

$A_{floor} = A_{roof} = 20.7377m^2$

3) *Conduction heat gain from glass surfaces*

The heat transfer occurs at the glass surfaces not only by direct beam and diffuse radiation, but also by conduction, as calculated below (Ozcana et al., 2015).

$$\dot{Q}_{c,gs} = A_{gs} * U_{gs}(T_o - T_i) \tag{3. 31}$$

Where the total area of the glass is $19.367m^2$,

D. *Fresh Air Heat Gain*

When considering the travel conditions, one of the most important issues is the quality of the air inside the bus. VAC systems are conditioned inside the bus via the targeted specific temperature and the relative humidity values. But with time, the air quality decreases. So, the fresh air from the outside has to be taken to the inside, passing through fresh and return air filters. This requirement leads to the heat gain at the inside of the bus. It consists of sensible and latent components based on mass flow rate of an air.

1) *Sensible fresh air heat gain*

Sensible fresh air heat gain corresponds to the change of the dry-bulb temperature of the indoor air caused by the airflow movement from the outside for increasing the air quality and can be calculated as follows:

$$\dot{Q}_{fa,s} = C_s * Q_{fa} * \Delta T \tag{3. 32}$$

2) <u>Latent fresh air heat gain</u>

Latent fresh air heat gain corresponds to the change of the humidity ratio of the inside air caused by the airflow movement from the outside for increasing the air quality and can be obtained by the flowing equation.

$$\dot{Q}_{fa,l} = C_l * Q_{fa} * \Delta W \tag{3. 33}$$

F) <u>Engine heat gain</u>

From standard books the engine temperature is taken to be T_{eng}, the surface area which contact with the body is taken to be S_{eng} is $0.578m^2$,the overall heat transfer coefficient is the same as floor side wall ,So the heat gain can be calculated using (Ali and Bahrami, 2013),

$$\dot{Q}_{eng} = S_{eng} \times U \times (T_{eng} - T_i) \tag{3. 34}$$

Data used in the analysis are listed in the following Table 3.3.

Table 3.3 Data used in the analysis list (ASHRAE, 2009).

Item	Value	Unit	Remarks
$\dot{Q}_{s,sit}$	70	kW	Seated, very light work (degree of activity) in offices, hotels, apartments
$\dot{Q}_{l,sit}$	45	kW	Seated, very light work (degree of activity) in offices, hotels, apartments
C_s	1.23	$W/\left(\frac{L}{s} \cdot K\right)$	Like as many HVAC applications
C_l	3010	$W/(L/s)$	Like as many HVAC applications
$\dot{Q}_{inf}$	94.38	m^3/h	14.3% of the fresh air rate

ΔT	6	$℃$	Outside air temperature is taken $31℃$ for the city of Adama and inside air temperature is taken $25℃$ for
ΔW	7.1	g/kg	Outside air specific humidity is found under $31℃$ and 63% relative humidity conditions for the city of Adama and inside air specific humidity is obtained under $25℃$ and 55% relative humidity conditions with 1648 m elevation
$A_{d,f}$	8.232	m^2	One lateral side fenestration area of the bus
L	39	$°N$	For the city of Adama
δ	23.086	°	For the city of Adama
E_{sc}	1367	W/m^2	
τ_b	0.505	-	For the city of Adama
τ_d	1.892	-	For the city of Adama
$SHGC_d$	0.8155	-	6 mm thickness, uncoated single glazing
IAC_d	1	-	No inside shading device
ρ_g	0.2	-	Typical mixture of ground surfaces
Σ	90	°	Diffuse solar radiation effects vertical to the external fenestration surfaces of the bus
$SHGC_{dif}$	0.73	-	6 mm thickness, uncoated single glazing
IAC_{dif}	1	-	No inside shading device
μ_o	0.00001865	J/m^2	31℃ air temperature and fully turbulent external flow

ρ_o	1.148	kg/m^3	31°C air temperature and fully turbulent external flow
Pr_o	0.706	-	31°C air temperature and fully turbulent external flow
μ_i	0.00001836	J/m^2	23°C air temperature and combined external flow
ρ_i	1.1707	kg/m^3	23°C air temperature and combined external flow
Pr_i	0.7075	-	23°C air temperature and combined external flow
ε	0.7	-	Isolated rural site
σ	$5.67*10^{-8}$	$W/m^2 \cdot K^4$	
L_{gal}	0.01	m	Galvanized sheet
L_{pol}	0.04	m	Polystyrene
L_{ply}	0.004	m	Plywood
K_{gal}	60	$W/m \cdot K$	Galvanized sheet
K_{pol}	0.032	$W/m \cdot K$	Polystyrene
K_{ply}	0.12	$W/m \cdot K$	Plywood
U_{gs}	5	$W/m^2 \cdot K$	6.4 mm acrylic single glazing

The summation of all the load types will be the instantaneous cabin overall heat load gain. The mathematical formulation of the model can thus be summarized as:

$$\dot{Q}_{tot} = \dot{Q}_{occp} + \dot{Q}_{dir} + \dot{Q}_{dif} + \dot{Q}_{ref} + \dot{Q}_{amb} + \dot{Q}_{exh} + \dot{Q}_{eng} + \dot{Q}_{ven} \tag{3. 35}$$

All of the above $\dot{Q}$ values are thermal energies per unit time. $\dot{Q}_{tot}$ is the net overall thermal load encountered by the cabin. $\dot{Q}_{occp}$ is the occupant load.$\dot{Q}_{dir}$, $\dot{Q}_{dif}$ and $\dot{Q}_{ref}$ are the direct, diffuse, and reflected radiation loads, respectively. $\dot{Q}_{amb}$ is the ambient load. $\dot{Q}_{exh}$ and $\dot{Q}_{eng}$

are the exhaust and engine loads due to the high temperature of the exhaust gases and the engine. Finally, the term $\dot{Q}_{ven}$ is the load generated due to ventilation.

Table 3.4 Heat gain components.

Components parameters		Value
Occupants		$3.79\ kW$
Infiltration heat gain	Sensible	$0.42\ W$
	Latent	$559.45\ W$
Solar heat gain	Direct	$5.09\ kW$
	Diffuse	$2.17\ kW$
Transmission heat gain	Side walls	$60.39\ W$
	Back and front walls	$23\ W$
	Roof and floor walls	$76.98\ W$
	Conduction heat gain from glass surface	$581.01\ W$
Fresh air heat gain	Sensible	$0.0029\ W$
	Latent	$3.91\ kW$
Engine heat gain		$12.51\ W$
Total heat gain		$= 16.28\ kW \sim 16.3\ kW$

CHAPTER FOUR

4. THERMODYNAMIC PERFORMANCE ANALYSIS of VAPOR ABSORPTION CYCLE on MID BUS

4.1. Simulation models for performance prediction

There is one basic approach in solving the absorption refrigeration system. This is, to evaluate the cycle of the refrigerant and the cycle of the solution. If the absorbent is volatile, there is also the cycle of the entrained absorbent which follows the path of the refrigerant.

Performance calculations for the absorption system were done in the past, using state point property data from graphical and tabulated sources which is stated on Appendix C and using EES software.

(Jain and Gable, 1971) were the first to provide a model which computes polynomial equations for the equilibrium property data of aqua-ammonia mixtures for conditions normally encountered in air-conditioning systems. Two sets of equations were developed covering a high pressure range from 1724.14 kPa to 2413.79 kPa and a low pressure range from 344.83 kPa to 551.72 kPa. These pressures correspond approximately to condenser and evaporator temperature ranges from 43°C to 55°C and from -5°C to 7°C respectively. The accuracy becomes questionable, if computations are performed beyond the specified ranges.

(Schulz, 1971) computational model covers all temperatures ranging from -70°C to 180°C and all pressures from 1 kPa to 2500 kPa. It is remarked by (Keizer, 1982) in his Ph.D. thesis that the calculations using Schulz relations show a large deviation from the well-known enthalpy-concentration diagram by Bosnjakovic (1965) especially at concentrations near pure ammonia. This was a surprising conclusion, especially as Schulz used experimental data of many authors to formulate his equations, among which was Bosnjakovic's data too. Despite the availability of the experimental data, Schulz remarked that the data itself was inconsistent.

Keizer also remarked in his thesis that, modeling absorption machines is rather an easy task because the heat and mass balances are very simple. This is true as far as the procedure for the analysis is concerned, and as long as the assumptions made simplify the cycle's operational constraints.

(Vicatos and Gryzagoridis,1994) have presented optimization curves to be used when designing aqua-ammonia absorption systems for a sink temperature range between 5°C and 45°C. As long as the sink temperature and evaporator temperatures are known, an optimum temperature for the generator can be found and the system will operate at an optimum coefficient of performance. In our system, both sink and evaporator temperatures are beyond the ranges presented in (Vicatos and Gryzagoridis, 1994).

4.2. Vapor absorption refrigeration cycle

A schematic diagram for a simple vapor absorption refrigeration cycle used in the present study is shown in Figure 4.1. The system is composed of condenser and evaporator units with an expansion valve similar to an ordinary vapor compression cycle, but the compressor unit is here replaced by an absorber – generator solution circuit, which has a vapor absorber, a gas generator, a heat exchanger, an expansion valve and a solution liquid – pump. The following assumptions have been made in order to develop the mathematical models:

(A) The refrigerant and solution are in steady state and thermodynamic equilibrium conditions at all states.

(B) The solution at the generator and absorber outlets as well as the refrigerant at the condenser and evaporator outlets are all saturated.

(C) Heat losses and gains and pressure losses in various components and piping are neglected.

(D) There are no pressure changes except through the expansion valve and the pump.

(E) Expansion valves are adiabatic.

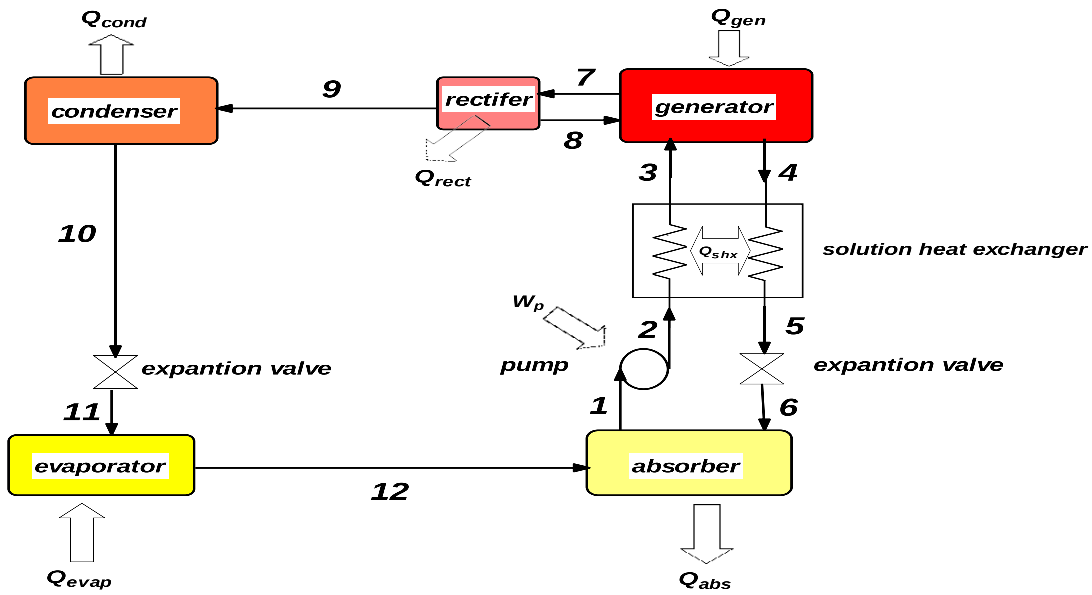

Figure 4.1 Simple absorption refrigeration cycle made by the software EES.

Like vapor compression cycle, it also four steps that completes the thermodynamic cycle, which are as follows:

i) Isothermal heat addition in the evaporator.

ii) Chemical compression in the assembly of generator, absorber and pump.

iii) Isothermal heat rejection of generated refrigerant in the condenser.

iv) Adiabatic expansion of the condensed refrigerant in the expansion valve.

Mathematical modeling

Theoretical cycle performance of the vapor absorption system is calculated in the following way. The overall energy balance gives the following equation (Arora, 2010).

$$Q_{abs} + Q_{cond} + Q_{rect} = Q_{gen} + Q_{evap} + W_p \tag{4. 1}$$

From the material balance in the absorber or generator, we have

$$m_s X_{abs} = (m_s - m_r) X_{gen} \tag{4. 2}$$

Where X gives the mass fraction of absorbent in the solution, and the subscripts abs and gen stand for the generator and absorber solutions, and m_r and m_s are mass flow rates of gaseous refrigerant and the absorber-exit solution (or solution pumping rate), respectively.

Mass flow ratio is an important parameter for determining the system performance, which is calculated from the mass balance for ammonia in the generator-rectifier as follows

$m_9 x_9 + m_4 x_4 = m_3 x_3$ Or $m_r x_9 + m_w x_4 = m_s x_3$

And

$m_r + m_w = m_s$

Therefore,

Mass flow ratio (Arora, 2010), $f = \frac{m_s}{m_r} = \frac{x_9 - x_4}{x_3 - x_4}$ (4. 3)

Now, coming to energy balance around the generator, absorber, condenser and evaporator, we have the following equations (Arora, 2010):

The rate of heat addition in the generator

$$Q_{gen} = m_7 \times h_7 + m_4 \times h_4 - (m_3 \times h_3 + m_8 \times h_8) \quad (4.\ 4)$$

The rate of heat rejection out of the rectifier

$$Q_{rect} = m_7 \times h_7 - (m_8 \times h_8 + m_9 \times h_9) \quad (4.\ 5)$$

The rate of heat rejection out of the condenser

$$Q_{cond} = m_9 \times (h_9 - h_{10}) \quad (4.\ 6)$$

The rate of heat absorption of the evaporator

$$Q_{evap} = m_{12} \times (h_{12} - h_{11}) \quad (4.\ 7)$$

The rate of heat rejection of the absorber

$$Q_{abs} = m_{12} \times h_{12} + m_6 \times h_6 - m_1 \times h_1 \quad (4.\ 8)$$

An energy balance on the hot side of the heat exchanger

$$Q_{shx\_h} = m_4 \times (h_4 - h_5) \quad (4.9)$$

Similarly, an energy balance on the cold side of the heat exchanger

$$Q_{shx\_c} = m_3 \times (h_3 - h_2) \quad (4.10)$$

The overall energy balance on the heat exchanger is satisfied if

$$Q_{shx\_c} = Q_{shx\_h} \times \eta_{ise} \quad (4.11)$$

Where: - η_{ise} is the solution heat exchanger effectiveness

The solution pumping power by small pump

$$swp = V_1 \times (P_2 - P_1) / \eta_{ip} \quad (4.12)$$

$$W_p = m_1 \times swp \quad (4.13)$$

Where: - η_{ip} is isentropic efficiency of the pump

Coefficient of performance (COP)

$$COP = \frac{Q_{evap}}{Q_{gen} + W_p} \quad (4.14)$$

4.3. EES software introduction and the modeling

F-chart software's engineering equation solver (EES) is a powerful tool when the modeling of thermal-fluid systems is concerned. It offers the ability to solve many simultaneous equations by using the Newton-Raphson method, as long as the amount of variables equals the number of equations. Convergence and iteration solution stability are dependent on programmed guess values and limits for variables. As further functionality EES offers several built-in functions for calculating (or estimating) fluid properties, given the required minimum inputs. This allows the determination of the saturated pressure of Ammonia at a Temperature of 5℃ with the following code and pressure function:

$\text{T\_1} = 5[\text{C}]$

$\text{p\_sat} = \text{P\_sat}(\text{Ammonia}, \text{T} = \text{T\_1})$

Here two variables (T_1 and p_sat) can be counted with two equations (one each line). Temperature is the independent property required to obtain a second namely pressure. Solving the above code will result in $p\_sat = 516\ [kPa]$.

The built-in fluid property functions are able to calculate most thermodynamic and transport properties of pure fluids or pre-defined mixtures of compounds such as R134a. A special procedure is included to provide the thermodynamic properties of aqua-ammonia. The *EES NH3H2O Procedure* requires three independent input properties in order to determine any other, as is to be expected when working with a two-component mixture. Properties compatible with this procedure are associated with certain symbols as follows:

1) T = Temperature (K)
2) P = Pressure (kPa)
3) x = Concentration
(mass fraction ammonia)
4) h = Specific enthalpy (kJ/kg)
5) s = Specific entropy (kJ/kgK)
6) u = Specific internal energy (kJ/kg)
7) v = Specific volume (m^3/kg)
8) Q = Quality
(mixture vapor mass fraction)

The numerical code within the procedure call represents the specific input variables according to the list shown above in numerical order. For the example below the code is given by the input properties as: P = 2, x = 3 and Q = 8 thus 238.

The program code for using the procedure in order to obtain the temperature of a $72.18\ \%$ solution aqua-ammonia at a pressure of $2.033\ MPa$ and a quality of 0 is written as:

$\text{Q} = 0\ [\text{dim}]\ (standing\ for\ dimensionless)$

$\text{P} = 2033\ [kPa]$

$\text{x} = 0.7218$

$\text{CALL NH3H2O}(238, \text{P}, \text{x}, \text{Q}: \text{T1}, \text{P1}, \text{x1}, \text{h1}, \text{s1}, \text{u1}, \text{v1}, \text{Q1})$

Solving the above code will cause the function to return values for all eight variables associated with it, including the input variables with their given values. The temperature returned is found to be $337.7\ K\ or\ 64.7℃$, the corresponding boiling temperature of 72.18% aqua-ammonia at $2033\ kPa$.

Giving temperature, enthalpy and quality with their corresponding code as inputs for the procedure to determine the properties of a second point would appear as:

$\mathrm{CALL\ NH3H2O(148, T, h, Q: T2, P2, x2, h2, s2, u2, v2, Q2)}$

This procedure is externally written using the correlations from Ibrahim & Klein (1993:1495) to determine mixture properties.

VALIDATION OF MATHEMATICAL MODELING

After obtaining the final model, the validation of the mathematical model has been performed, for checking the accuracy of model obtained. The work of Chandrakar and Saikhedkar (single effect model of NH_3-H_2O VAS was considered) has been taken to establish a bench mark case. The Table 4.1 shows the inputs for the single effect model with rectifier and heat exchanger of NH_3-H_2O VAS analyzed by Chandrakar and Saikhedkar, (2016). The results of the present system obtained with the mathematical model using EES program (with Chandrakar inputs) in comparison with Results obtained by Chandrakar and Saikhedkar are displayed in Table 4.2.

Table 4.1 Chandrakar's inputs

Refrigeration capacity	0.75 TR or 2.625 kW
evaporator temperature	5℃
Condenser temperature	45℃
Absorber temperature	40℃
Generator temperature	97℃
Solution heat exchanger effectiveness	1

The results obtained for the present model are good comparable with the results of Chandrakar and Saikhedkar.

Table 4.2 Comparison between results of present model and Chandrakar model

Characteristics of VAS	Chandrakar results	Present model results
Heat supplied in evaporator, Q_{evap}	$2.625\ kW$	$2.625\ kW$
Heat rejected in condenser, Q_{cond}	$2.73\ kW$	$2.68\ kW$
Heat rejected in absorber, Q_{abs}	$3.85\ kW$	$3.784\ kW$
Heat supplied in generator, Q_{gen}	$4.5\ kW$	$4.67\ kW$
COP	0.57	0.562

After the successful validation of the present model, it is used to analyze the performance of $16.3\ kW$ VAS. Therefore, EES is used to simulate the performance of exhaust heat and photo-voltaic cell powered aqua ammonia absorption system.

If values are assigned to the evaporator, condenser and absorber temperature respectively, then the generator temperature and the coefficient of performance COP of the reversible cycle can be simulated. The following parameters and assumptions were used in the simulation:

- The working fluid is aqua-ammonia solution
- Temperature of evaporator is 5℃
- Temperature of condenser is 50℃
- Temperature of absorber is 10℃
- And $16.3KW$ refrigeration capacity

The system performance was evaluated for a range of generator temperatures from the minimum generator temperature of 60℃ up to the maximum of 120℃. The input data required for simulating the system consists of the following: generator temperature, absorber temperature, generator and condenser pressure, evaporator and absorber pressure, pump output pressure, mass flow rate entering generator, ammonia solution concentration entering the generator and fixed saturated liquid state from heat exchanger to generator. Figure 6 shows flow-diagram for how simulation works using input data. The output includes the generator heat gain, cooling capacity and COP.

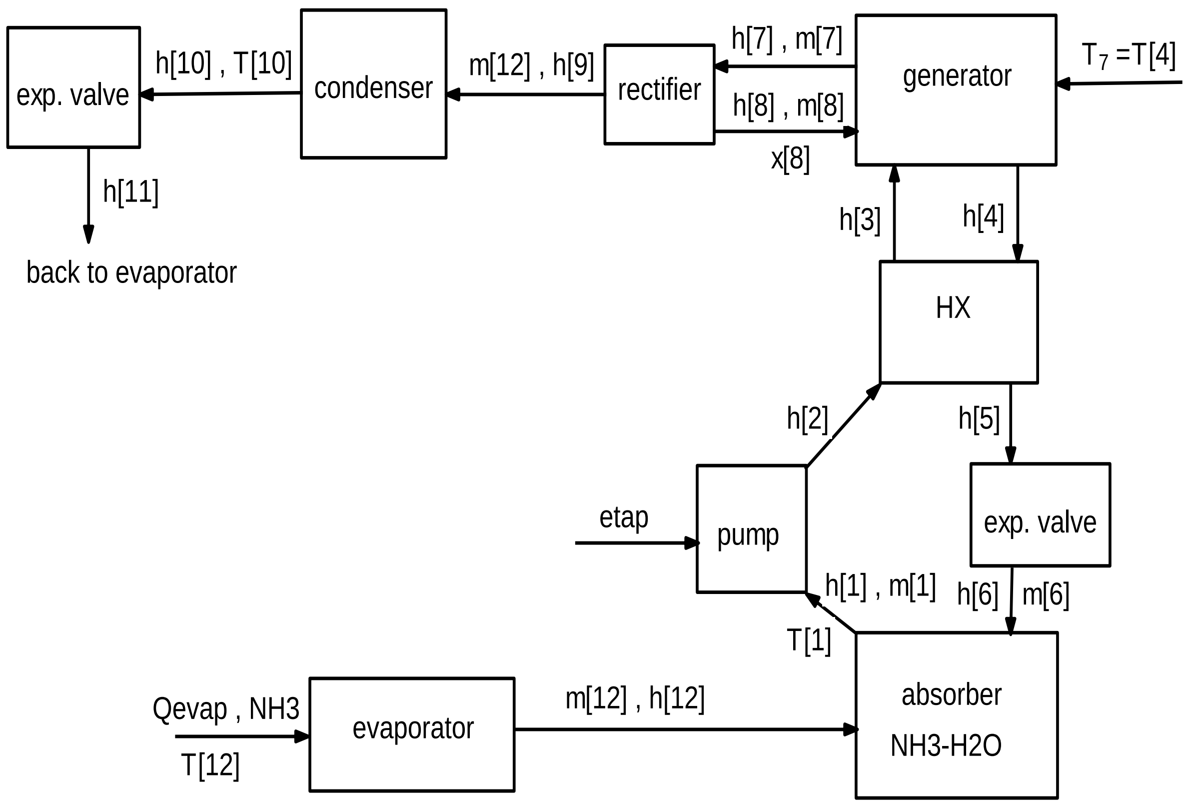

Figure 4.2 Information-flow diagram for exhaust heat and photo-voltaic cell powered absorption cooling system.

The steps followed while developing the hybrid simulation of the energy circulation on the engine and the air conditioning styles that are mostly used, which is single effect vapor absorption cycle. There are so many of them for air conditioning styles but in preference to the simplicity selection go to the single effect from other types. Most of other cycles do not experience that much different increment in COP of the cycle. The literatures reviewed have answered that the COP of most air conditioning cycles does not exceed 0.7 or 70% and not less than 0.5 or 50%. The energy of the generator is of a fixed value but we can see that this energy has got a point of fluctuation as the bus moves and stops and also the energies in the car are in a way of loss while the car is moving and at its stationary point. This has led the results to make a simple simulation on the results to make a good confirmation on the hand calculation. The results require this software because all the other graphical information and chart results require good precision for the analysis to be made in the coming paragraphs.

4.4. Simulation result

The result simulation has required assumptions even for the hand calculation the software also require this assumptions to start the calculations by the software. It is possible to use the standard range of temperature and pressure for the air conditioning components to develop the cycle on the graph by thermodynamic analysis. This is the time to use the cooling load as one part of the assumption to develop a reasonable temperature consideration on each part before the calculations. It was tabulated the values from the calculation (i.e. using the chart values of p-h graph of Ammonia-water solution refer the chart on the appendix C).

This value has given a good reasonable result but it should be confirmed by software including its simulation so that the result would go far up to studying the new sources of energy to support the COP. This project tries to study three soft wares on engineering simulation helper types (i.e. MATHLAB, TRANSYS and EES). From this all it is found EES is easily and adaptable and gain scientifically the thermodynamic properties of Ammonia-water solution was available in.

Effect of various operating parameters on COP

For the performance analysis of the present system for the components of absorption system (i.e. absorber, generator, evaporator and condenser) are selected which broadly affect the performance of the system.

a) **<u>Effect of generator temperature</u>**

To analyze the effect of generator temperature on system performance, varying the generator temperature from 75℃ to 120℃ while keeping all other component constant. This results in COP of the system ranging from 0.8269 to 0.552. Hence, higher generator temperature results in the performance of the absorption system to decrease its performance. The variation of COP versus temperature of generator is displayed in the following graph.

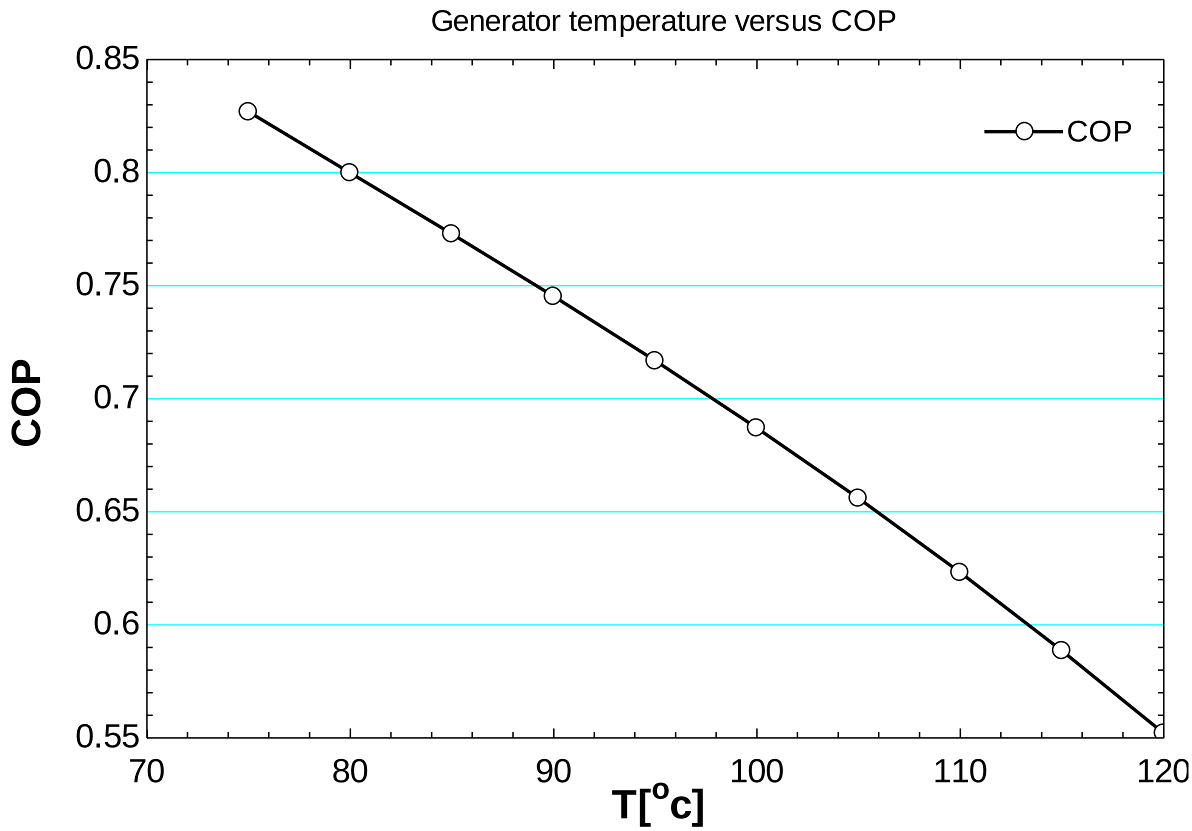

Figure 4.3 Generator temperature versus COP.

b) Effect of absorber temperature

The change in temperature of the absorber from 10℃ to 40℃ causes the overall COP of the system decreased from 0.656 to 0.5366, keeping all other conditions in other components constant. Hence it can be concluded that the higher absorber temperature yield to degrade the performance of the system.

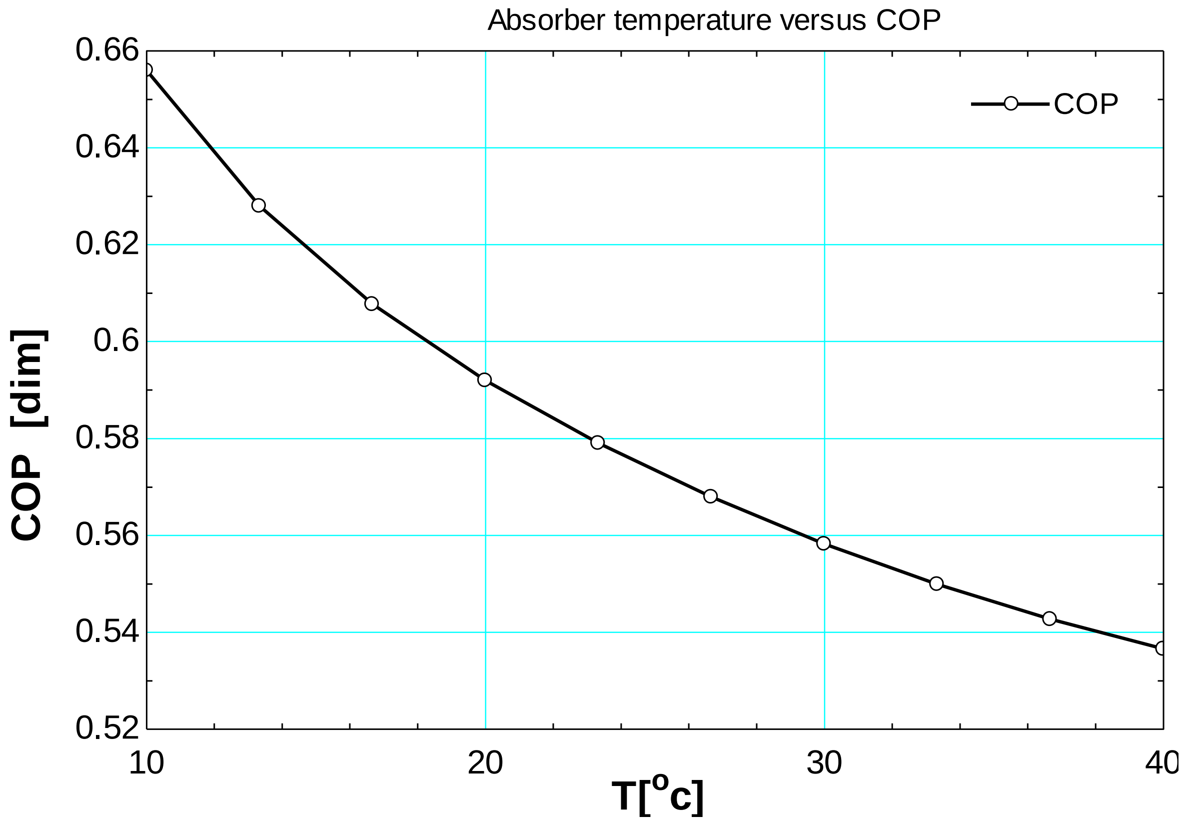

Figure 4.4 Absorber temperature versus COP.

c) **Effect of evaporator temperature**

The change in temperature of evaporator, from 0℃ to 10℃, results increase in COP of the system from 0.5823 to 0.7002 keeping all other conditions in other system constant. Hence, from the point of view of first law analysis, the performance of the whole system upgraded with the increase in evaporator temperature. The variation of COP versus evaporator temperature is shown in the following graph.

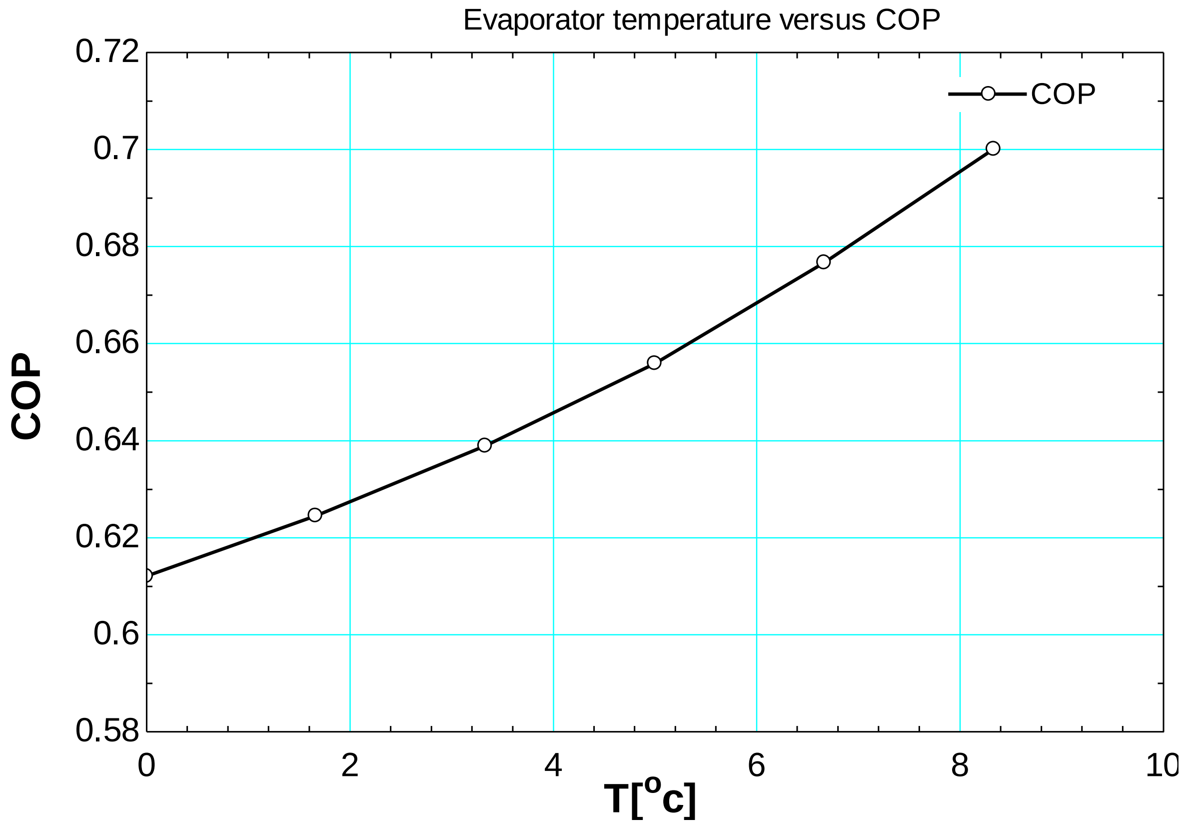

Figure 4.5 Evaporator temperature versus COP.

d) Effect of condenser temperature

For analyzing the effect of condenser on system performance, its temperature varied from 40℃ to 60℃ while keeping all other conditions at the other component constant. This variation of condenser temperature results in increase of the COP of the whole system from 0.6141 to 0.6936. Hence, it can be concluded that the higher condenser temperature yields to improve the overall performance of the system. The plot for the COP versus temperature of condenser is shown in Figure 4.6.

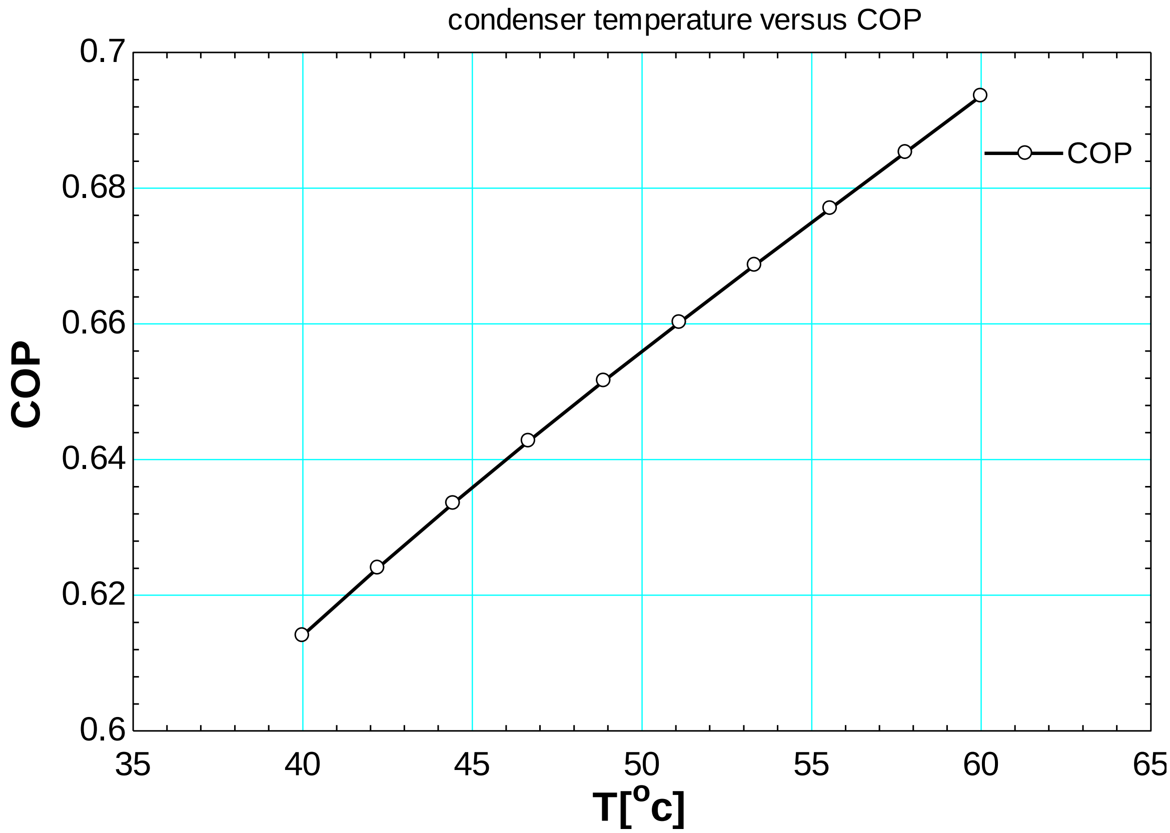

Figure 4.6 Temperature of condenser versus COP.

e) <u>Effect of generator and absorber temperature</u>

The performance of system under operating conditions also has been studied by varying the generator and absorber temperatures. The results indicate that the COP decreases with the increase in generator temperature for given absorber temperature for the system. The COP of the system is very sensitive to change in absorber temperature and decreases rapidly with increase absorber temperature. The COP of the system decreases with increase in generator temperature because evaporator load is constant i.e. 16.3 kW as required for the cabin cooling of bus. And as the generator temperature increases, it increases the heat load of generator. See Figure 4.7 and Figure 4.8:

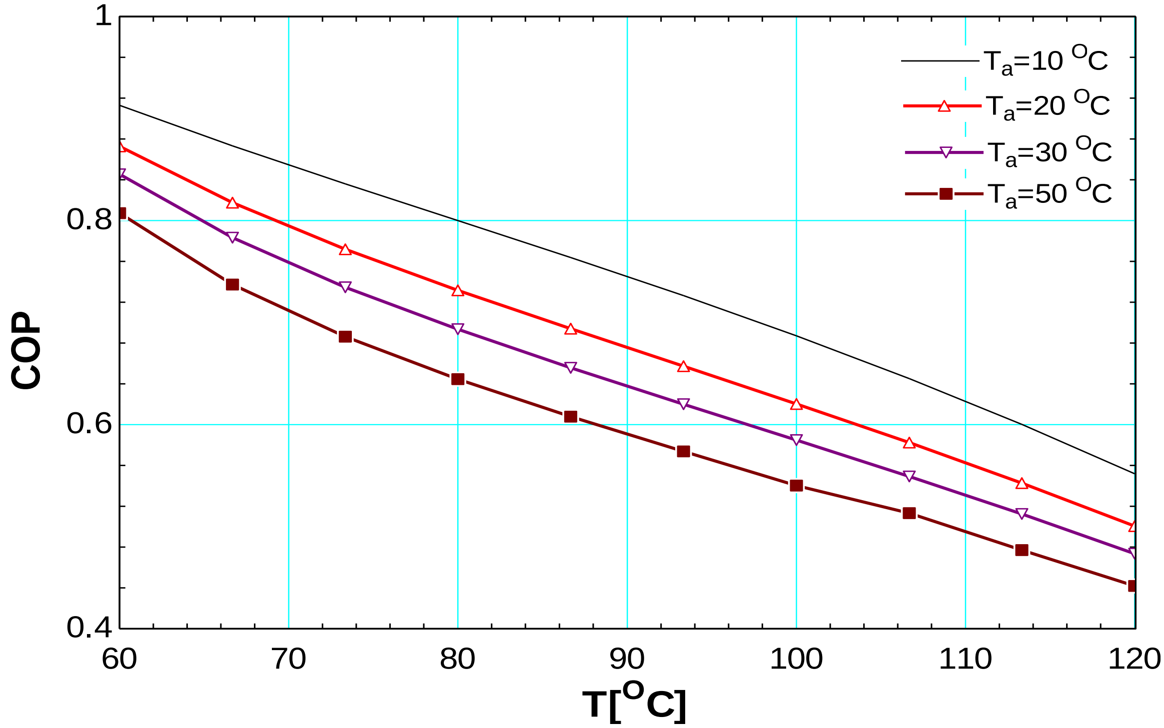

Figure 4.7 COP versus generator temperature for different absorber temperature

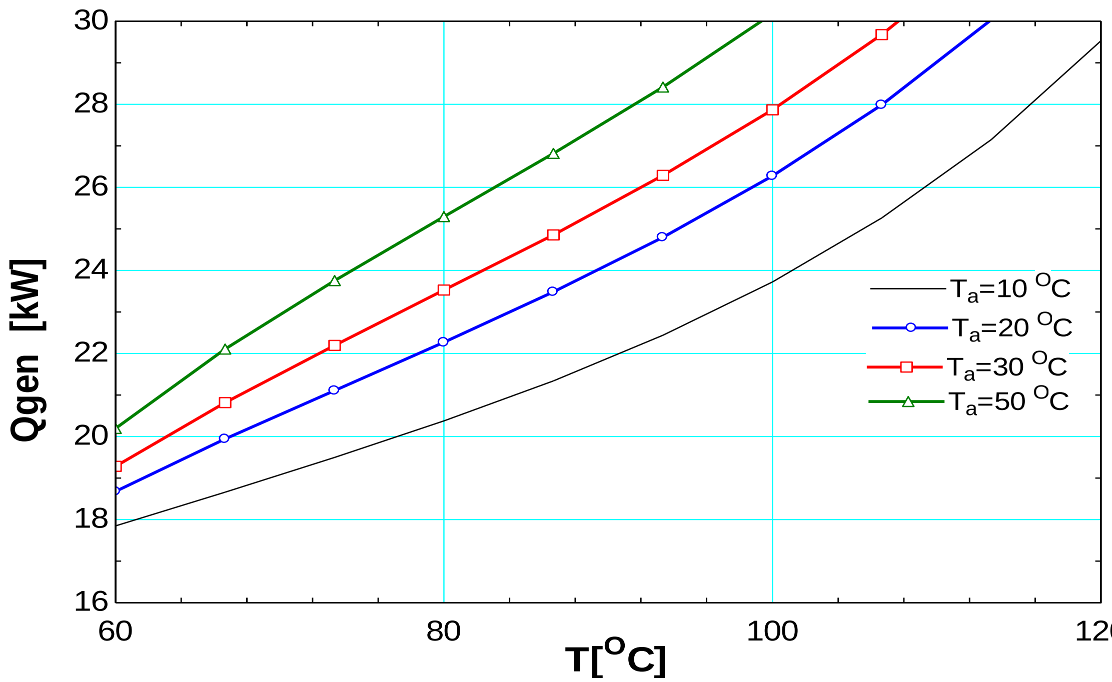

Figure 4.8 Generator heat versus generator temperature for different absorber temperature

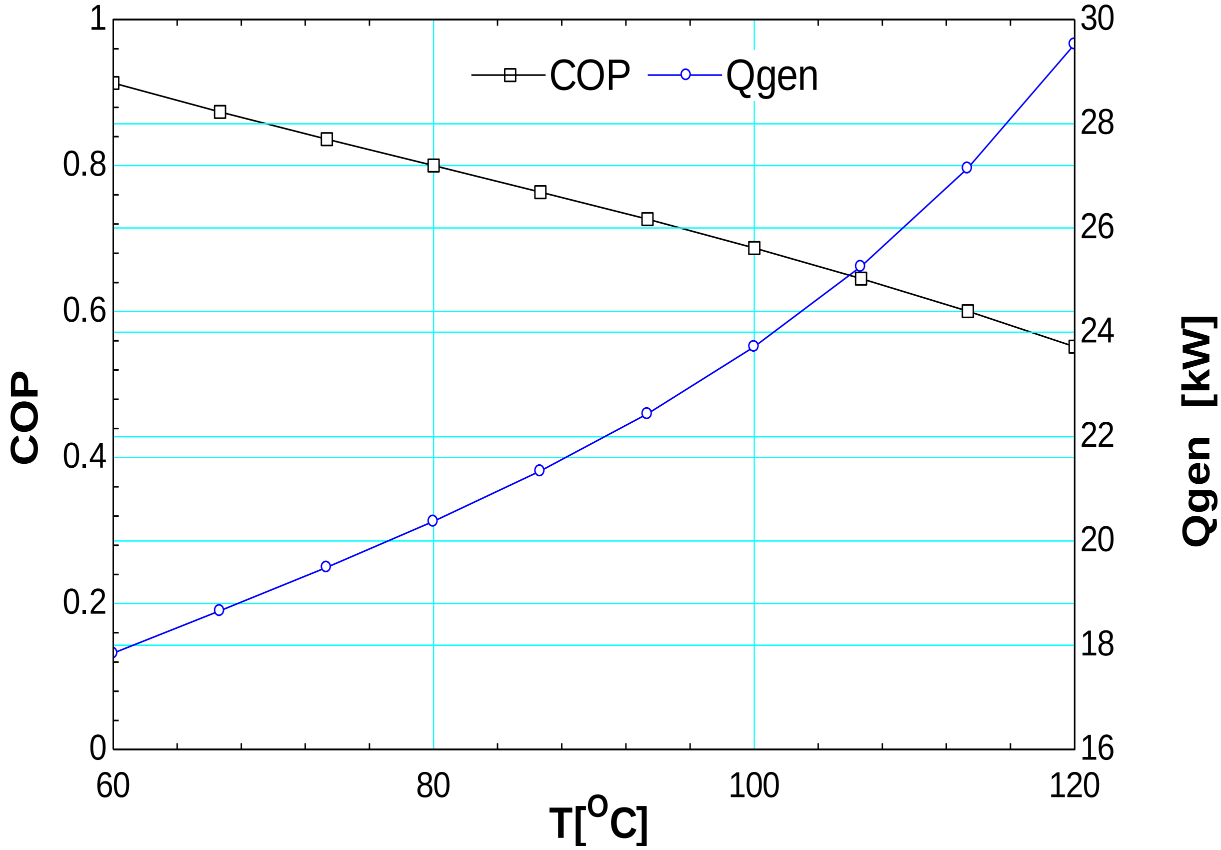

Figure 4.9 COP and Generator heat versus generator temperature for absorber of 10℃

From the Figure plotted between COP and heat load on generator for ammonia/water system, it can be seen that, under the various operating conditions being simulated, for a given evaporator and condenser temperature an optimum temperatures of absorber and generator are selected for thermodynamic analysis of this study.

Thermodynamic analysis:

The cooling capacity of the vapor absorption system is 16.3 kW with the following operating conditions:

Condenser Temperature = 50℃

Evaporator Temperature = 5℃

Absorber Temperature = 10℃

Generator Temperature = 105℃

Pressure values taken from p-h chart of ammonia as refrigerant for condensing temperature 50℃ and evaporating temperature 5℃.

$P_E \ = P_A \ =$ Saturated Vapor pressure at $5^o c \ = \ 516.07 \ kPa$

$P_C \ = \ P_G \ = 2035 \ kPa$

1. **For Evaporator**

Heat load on Evaporator $Q_{evap} = 16.3 \ kW$

By using T_E and P_E can be find from p-h chart of ammonia, $h_{12} \ = \ 1270 \ kJ/kg$.

Using T_C and P_C, $h_{10} = \ 241 \ kJ/kg$

As now h_{10} and h_{11} are equal through expansion valve

Now can find m_{12} from equation 4.7,

$\mathrm{m}_{12} = 0.01584 \ \mathrm{kg/Sec}$

For defined system

$m_{12} = m_{10} \ = \ m_9 = \ 0.01584 \ kg/Sec$

Using T_E and P_E from enthalpy-concentration diagram for ammonia-water solution in APPENDIX C Figure C2 to find concentration of ammonia

$x_{12} = x_{10} = x_9 = 0.9996$

2. **For Absorber**

Mass balancing of weak and strong solution

$$m_1 = m_{12} + m_6 \tag{4. 15}$$

$$x_1 m_1 = x_{12} m_{12} + x_6 m_6 \tag{4. 16}$$

From enthalpy-concentration diagram for ammonia-water solution in Figure C2, ammonia in saturated liquid form using T_A and P_A , $h_1 = \ -80 \ kJ/kg$ and $x_1 = \ 0.84$ and also at T_G and P_G , $h_4 = 240 \ \ kJ/kg$ and $x_4 = 0.44$.

$x_4 = x_5 = x_6 = 0.44$

Therefore,

$m_6 = 0.0063\ kg/sec$

$m_1 = 0.02216\ kg/sec$

For defined system

$x_1 = x_2 = x_3 = 0.84$

Using P_G and x_3 from enthalpy-concentration diagram for ammonia-water solution,

$h_3 = 130\ kJ/kg$

And using equation 4.12,

$$h_2 = h_1 + SWP \tag{4. 17}$$

Where $V_1 = 14.22 \times 10^{-6} m^3$ and $\eta_{ip} = 0.5$

$h_2 = -79.95681\ kJ/kg$

Using Energy balance h_6 can be found

$$m_2(h_3 - h_2) = m_4(h_4 - h_5) \tag{4. 18}$$

$h_6 = h_5 = -498.5\ kJ/kg$

Heat rejected by Absorber is finding using equation 4.8.

Therefore, $Q_{abs} = 18.75\ kW$

3. **For Generator**

Heat input to generator was found using equation 4.4.

For defined system

$x_7 = 0.963$ from enthalpy-concentration diagram for ammonia-water solution using $T_7 = T_G$ and P_G at saturated vapor form.

By using average value of concentration $x_8 = 0.72$ can be found

By mass balance,

$$m_7 = m_9 + m_8 \tag{4. 19}$$

$$x_7 m_7 = x_9 m_9 + x_8 m_8 \tag{4. 20}$$

$m_8 = \ 0.002386 \ kg/Sec$

$m_7 = \ 0.01823 \ kg/Sec$

Using T_G and P_G at saturated vapor from enthalpy-concentration diagram for ammonia-water solution can be find $h_7 = \ 1500 \ kJ/kg$ and also h_8 became $110 \ kJ/kg$ at P_8 and x_8 the solution in saturated liquid.

Therefore, $Q_{gen} = 25.71 \ kW$

4. **For rectifier**

Heat rejection by rectifier is finding using equation 4.5.

Using P_C and x_9 at saturated vapor from enthalpy-concentration diagram for ammonia-water solution can be find $h_9 = \ 1305 \ kJ/kg$

Therefore, $Q_{rect} = 6.411 \ kW$

5. **For condenser**

Heat rejected by condenser was found from equation 4.6,

$Q_{Cond} = 16.85 \ kW$

6. **For solution heat exchanger on hot side**

Using equation 4.9 the value heat exchange from week solution to strong solution is

$Q_{shx-h} = 4.653 \ kW$

7. **For solution heat exchanger on cold side**

Using equation 4.10 the value heat exchange from strong solution to week solution is

$Q_{shx-c} = 4.653\ kW$

8. **Work done by pump**

Using equation 4.13,

$W_p = 0.96 \times 10^{-3}\ kW$

9. **For Mass flow ratio or circulation ratio**

Using equation 4.3 the value of specific rich solution circulation rate became
$f = 1.399\ \ kg/kg$ vapor

Specific poor solution circulation rate
$f - 1 = 1.399 - 1 = 0.399\ \ kg/kg$ vapor

Therefore, $COP = 0.634$

Energy balance of the cycle
Heat rejected

$$Q_{abs} + Q_{cond} + Q_{rect} = 42.011\ kW$$

Heat received

$$Q_{gen} + Q_{evap} + W_p = 42.0109\ kW$$

Thus the energy balance checks very closely.

Table 4.3 Summary thermodynamic state points of the vapor absorption air conditioner for the Mid Bus.

Point	From graph	From EES	From graph	From EES	From graph	From EES	From graph	From EES	From graph	From EES
	P(kPa)		T(℃)		m(kg/sec)		x(-)		h(kJ/kg)	
1	516.1	516	10	10	0.0222	0.024	0.84	0.83	-80	-75.03
2	2035	2033			0.0222	0.024	0.84	0.83	-79.96	-70.71
3	2035	2033			0.0222	0.024	0.84	0.83	130	150.8
4	2035	2033	105	105	0.0063	0.007	0.44	0.44	240	240.1
5	2035	2033			0.0063	0.007	0.44	0.44	-498.5	-486.5
6	516.1	516			0.0063	0.007	0.44	0.44	-498.5	-486.5
7	2035	2033	105	105	0.0182	0.019	0.943	0.97	1500	1498
8	2035	2033			0.0024	0.002	0.72	0.72	110	119.8
9	2035	2033			0.0158	0.017	0.996	1	1305	1292
10	2035	2033	50	50	0.0158	0.017	0.996	1	241	240.6
11	516.1	516			0.0158	0.017	0.996	1	241	240.6
12	516.1	516	5	5	0.0158	0.017	0.996	1	1270	1271

Table 4.4 Comparison of EES software and manual calculations of simulation.

Energy's	From manual simulation	From EES simulation
Q_{evap}	$16.3\ kW$	$16.3\ kW$
Q_{abs}	$18.75\ kW$	$18.34\ kW$
Q_{gen}	$25.71\ kW$	$24.85\ kW$
Q_{cond}	$16.85\ kW$	$16.63\ kW$
Q_{rect}	$6.411\ kW$	$6.173\ kW$
W_p	$0.96 \times 10^{-3}\ kW$	$0.98 \times 10^{-3}\ kW$
COP	0.634	0.656
f	1.399	1.439

CHAPTER FIVE

5. SIMULATIONS OF ENERGY INPUT FROM SOLAR AND EXHAUST HEAT

5.1. Photo voltaic cell on the vapor absorption cycle

There are two major types of renewable technologies that utilize solar energy: solar thermal plants and photovoltaic cells. Solar thermal plants utilize the sun's energy to heat a fluid that drives a turbine to produce electricity. Photovoltaic cells also known as solar cells, which convert light energy directly into electricity. Sunlight carries energy which normally is partly turned into heat when it hits an object. Solar cells are constructed of materials that turn solar energy into electrical current which can be collected for power generation. To increase the voltage of the electricity generated, solar cells can be wired together in series to create larger arrays, known as solar panels. Solar cells accomplish this energy conversion by the use of semiconductor materials.

Temperature of the solar cells plays a large part in the efficiency. As the solar cell heats up, which is inevitable when in direct sunlight, the band gap of the material will shrink. As the band gap shrinks, the efficiency will decrease as well. It is desirable to have a material that has a band gap on the high end of the optimum range, so that as it heats up, the resulting smaller band gap still falls near the maximum efficiency. This energy conversion will be used to help energy interruptions in sunny days in the generator of air conditioning from other sources of the Mid Bus by being wired with a heat resister to keep the temperature of the fluid high to feed for the rectifier.

5.1.1. Introduction on photo voltaic panel

A solar panel is made up of many solar cells wired together. Depending on the energy required for the specific application, many solar panels can be wired together to create a large array. Several components are necessary in a system capable of utilizing the energy generated by the solar panel array as shown in the Figure 5.1.

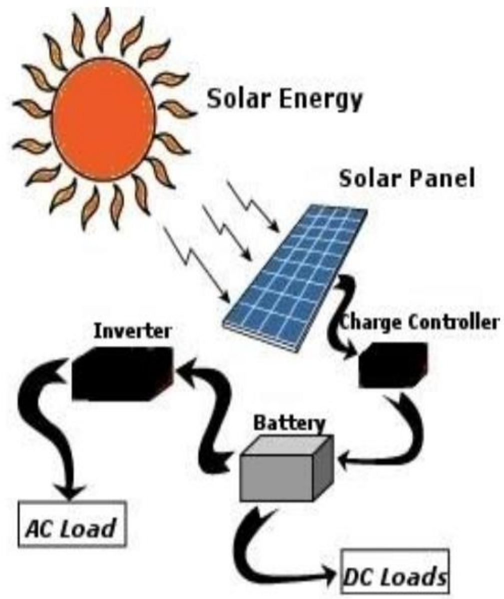

Figure 5.1 Typical solar energy system (Charles, 2012).

The subject components include a battery, or battery chain, charge controller and inverter. Because solar panels are generally not able to generate energy at night, a battery is needed for storage of the energy that is necessary at nighttime or on cloudy days when the production from the panel is lessened or is nonexistent.

The charge controller is also known as a voltage regulator and is included to protect the battery. When the battery is charged to its full capacity, the charge controller prevents the battery from being overcharged, which could decrease its expected lifetime or even cause an explosion.
The last component in this system is the inverter. The inverter takes the charge from the direct current (DC) output and turns it into alternating current (AC), which is the format present in household systems.

Battery System

A battery system was included in the design so that there would be a constant supply of available energy for the air conditioning. The solar panels are not able to directly supply the power required because the air conditioner draw is greater than the solar panels can supply at peak.

Deep cycle batteries are available in many different voltages and capacities. Care needs to be taken to not discharge the batteries below a certain threshold because their expected lifetime can be reduced if they repeatedly dip below this level. Therefore, when sizing the battery, it should be approximately twice the capacity needed.

5.1.2. Energy calculation

Silicon solar cells are manufactured in several different ways; the three to be examined are mono crystalline, polycrystalline, and thin film, also known as amorphous silicon. Mono crystalline solar cells offer the best efficiencies, but are the most expensive because large single crystals are uncommon naturally and are instead grown in a laboratory environment. Mono crystalline silicon has, as the name implies, an unbroken crystal structure, meaning there are no grain boundaries. Grain boundaries introduce discontinuities that hamper the desired electrical characteristics of the material. Polycrystalline silicon consists of many small silicon crystals or grains. It is less expensive than mono crystalline silicon, but offers a lower efficiency. Typically crystalline silicon solar cells have a longer lifetime than amorphous silicon cells. Amorphous silicon solar cells have the lowest efficiency, but are also the least expensive and lightest weight of the three types. Amorphous silicon solar cells are manufactured by laying a thin film of silicon onto another material. Depending upon how the amorphous silicon is manufactured, it can have a band gap between 1.4 and 1.8 electron volt, which is one reason for its decreased efficiency. Another reason is the method in which it is manufactured inherently creates many grain boundaries and incomplete bonds in the silicon. Therefore, the better type which would meet good energy harnessing demand is the mono crystalline silicon bendable panel.

A 12V battery rated for 833 ampere hours (Ah) will supply approximately 10kWh. Therefore, four batteries can be used for this project to achieve the generator energy needed.

5.1.2.1. Solar irradiance

Different areas of the earth receive different amounts of daily sunlight. These variances are due to the angle of incoming sunlight as a result of the curvature of the earth, orientation of its axis and the path around the sun. For instance, the average irradiance in Adama (39° latitude and longitude, 8) is approximately $433\ W/m^2$ for the month of June.

Given a location on earth and time of the year, the irradiance can be defined well. Knowing the irradiance allows the maximum energy that can be generated by a solar panel to be calculated. A comparison of daily irradiance with months is shown for Adama, in Figure 5.2. (Appendix B)

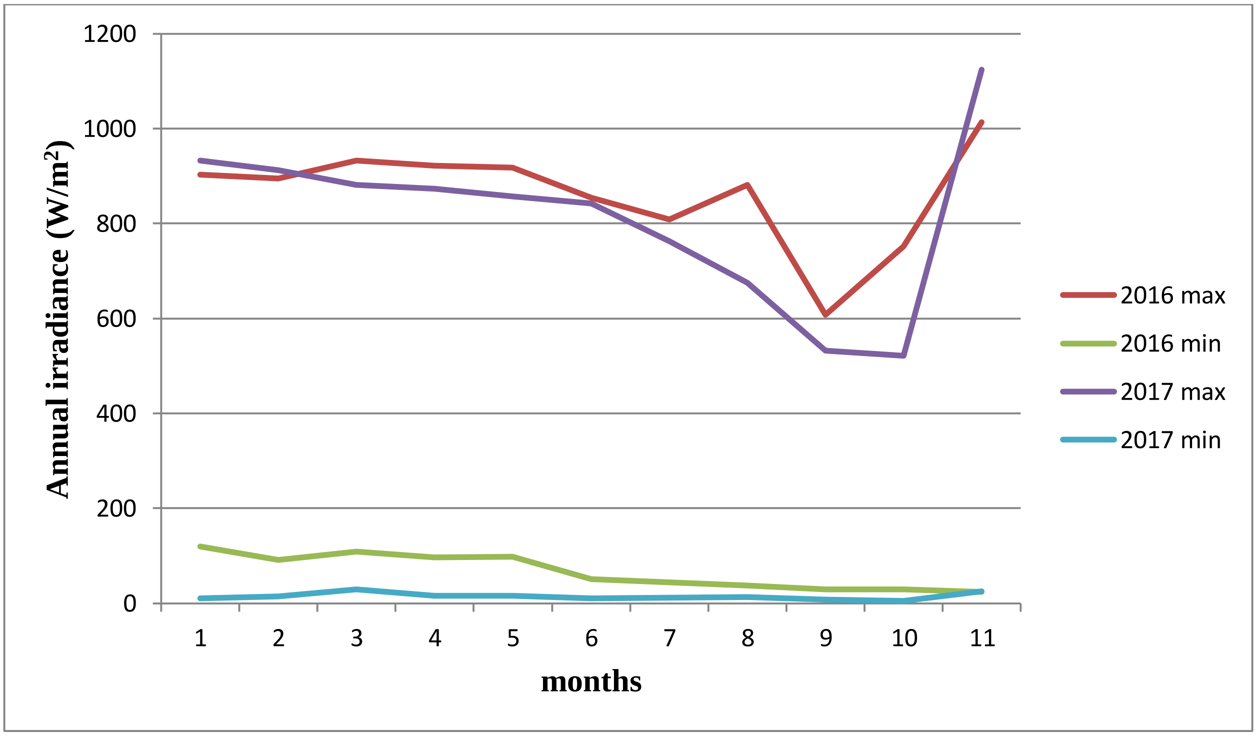

Figure 5.2 Annual irradiance versus months of the year 2016 and 2017 for Adama appendix B.

In this scenario, solar panels are the only source of energy for the air conditioner and do not receive additional energy from exhaust heat. First, the types of panel must be selected, mono crystalline, polycrystalline, or thin film. The efficiencies of each vary so one value was assumed to be constant for each. Mono crystalline was 20%, polycrystalline was 15% and thin film was 12.5%. Taking additional consideration on this mono crystalline type solar panel had been selected because it has good efficiency than the other types (Charles, 2012).

5.1.2.2. Energy calculation of the heat resistance wire

The average solar irradiance in Adama during these four months is 224.4 W/m^2. Combining this value with the efficiencies stated previously, mono crystalline solar panels are able to produce 44.88 W/m^2. Next, these specific values will be combined with the roof area of the mid bus $13.23\ m^2$ to determine how much power can be generated from the available areas. The average amount of daily sunlight in Adama for four mouths is slightly over 8.7 hours. Therefore, the total electrical energy generated by solar panel through a day is the power generated per hour multiplied by daily sunlight hour, so we get $5.165\ kW$.

For four batteries $4 \times 10\ kWh = 40\ kWh$ power can be stored so, the time it takes to charge the batteries became

$$t = \frac{40\ kWh}{5.165\ kW} = 7.74\ h$$

Therefore the time it needs to charge the four batteries per day is 7.74 h which is good because less than average daily sunlight hour.

The heating resistance wire gives heat energy for the generator can be calculated, first the current from the batteries to the wire of $120\ V$ is

$$I = \frac{P_{battery}}{V} \tag{5. 1}$$

$$= 333.33\ A$$

This electric energy converts to heat energy by heating resistance wire which has resistance of $0.093\ \Omega$ became,

$$P = I^2 R \tag{5. 2}$$

$$p = 10.33\ kW$$

5.1.3. Performance simulation using solar PVC energy

Therefore, EES is used to simulate the performance of photo-voltaic cell powered aqua ammonia absorption system. The same parameters and assumptions were used in the simulation.

The input data required for simulating the system consists of the following: generator temperature, absorber temperature, generator and condenser pressure, evaporator and absorber pressure, pump output pressure, mass flow rate entering generator, ammonia solution concentration entering the generator and fixed saturated liquid state from heat exchanger to generator. The main input data is solar energy for the generator.

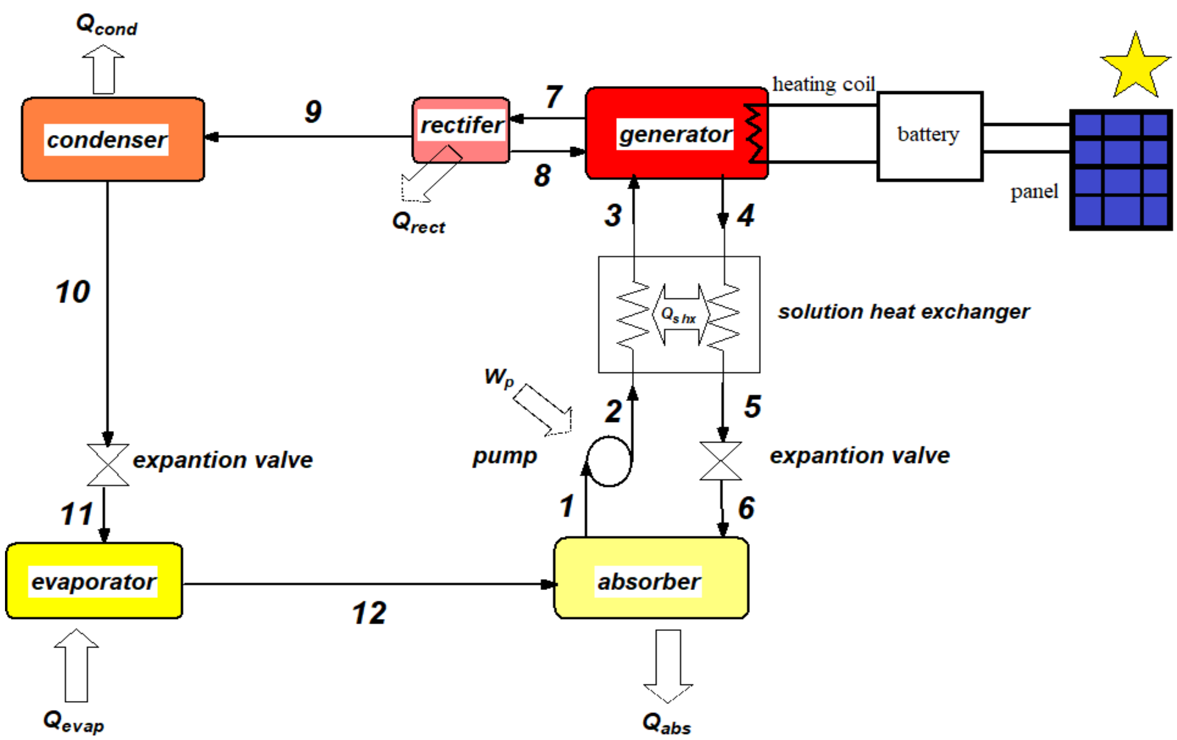

Figure 5.3 Photo-voltaic cell powered absorption air conditioning system.

The energy adaptation has caused the following Figure 5.4 change as illustrated in the to be fed to the software.

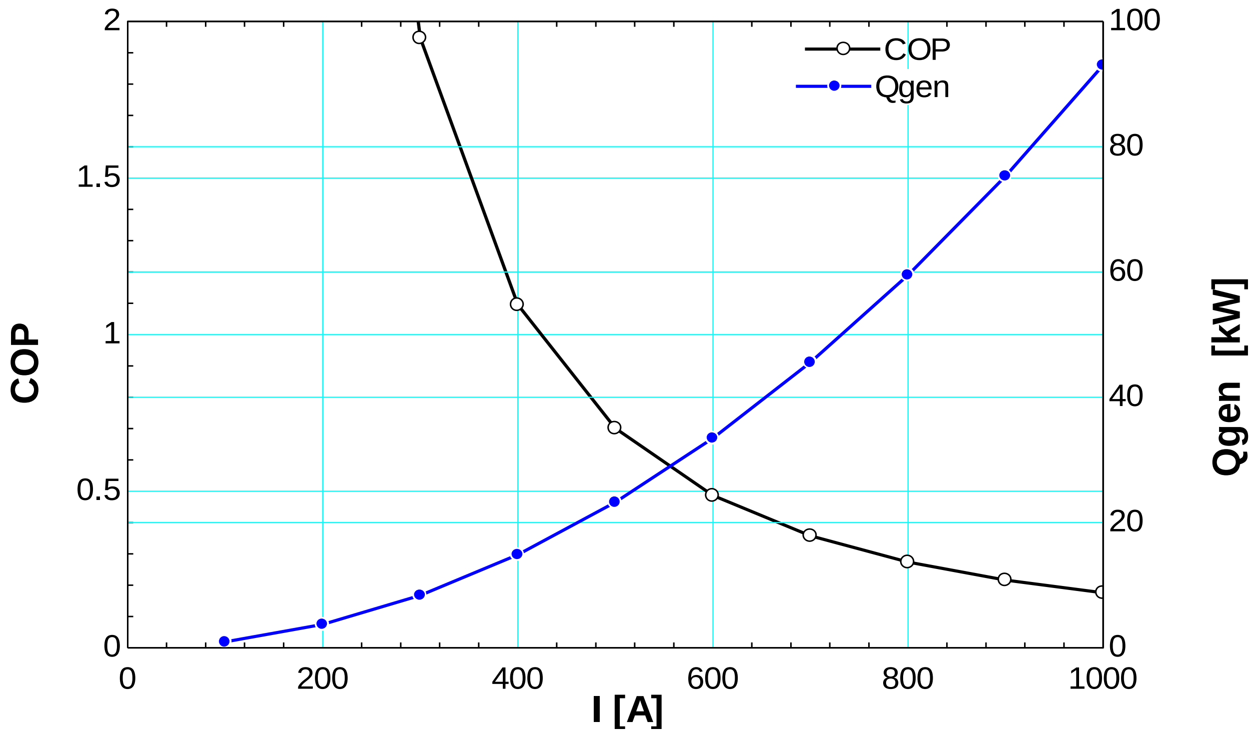

Figure 5.4 COP and PV energy versus current from batteries

From Figure 5.4 the performance is decrease as the current used from the batteries increase and also increases generator heat gain.

Even though it is possible for this case to work, it is un likely on an average day that the panels would be exposed to the necessary amount of sunlight because of clouds or shade.

Therefore, additional source of energy is likely to be required, or else the vehicle occupants may suddenly find themselves without air conditioning on a warm day.

5.2. Exhaust heat on vapor absorption cycle

5.2.1. Exhaust heat introduction

Vehicle manufacturers has faced a huge problem on removing exhaust heat so that the vehicle travel off land without concern of ignition and fire rise on the ground grass and trees around. The concerns about exhaust-system geometry (including exhaust coolers) trapping and accumulating debris are valid. These vehicles can travel off road, collect debris (grasses), and ignite the debris during the regeneration cycle. Baxter (2004) reports ignition of fine fuel accumulations of sphagnum moss (muskeg) and grass after exposure to an all-terrain vehicle (ATV) exhaust system. Baxter reports that the sequence of events from sinking the ATV in the muskeg to smoldering embers from the exhaust system took 15 minutes. Heat shields provide a significant reduction in temperatures; however, the shield provides pockets where debris can accumulate.

Therefore absorption refrigeration system is able to take advantage of the exhaust gas power availability and thus provides the cooling by running the cycle. Heat is applied to the generator, which contains a solution of ammonia water, rich in ammonia. The heat causes high pressure ammonia vapor to desorb the solution. The high pressure ammonia vapor flows to a condenser, typically cooled by outdoor air.

5.2.2. Energy estimation

To estimate the energy there is no available direct method of measuring the energy so it is good use math. The basic idea of the experiment is to measure exhaust manifold temperature which is to be used later in the cycle cooling load calculation and since the part is thermally sensitive it is attached on the external body of the manifold.

5.2.2.1. Experimental setup on Mid Bus engine exhaust gas temperature measurement

A Four cylinder diesel engine Mid Bus in the Mechanical Engineering Department work shop (Garage) at the Faculty of Engineering/ Adama University was used for the experiment. An experimental instrument is temperature recorder k-type thermocouple. According to experimental measuring point, the temperature recorder was fixed to prevent the external force to make it fall off. Prior to installing the components in the car, k-type thermocouple was calibrated to provide an accuracy of $\pm 0.3℃$ for the temperature range of $0/400℃$ and the after calibration the vehicle part was opened to be connected with the thermocouple. After some start up and heating of the vehicle, the real measures were taken. In order to ensure the correctness of data acquisition, the meter was set to record data each 5 minutes. Experimental instruments and car engine are shown in Figure 5.5.

Figure 5.5 Engine experimental setup of calibration and temperature measurement.

5.2.2.2. *Mathematical estimation and energy conversion*

After the experiment, the paper provides mathematical estimates of the internal energy from the following experiment result Table 5.2. The main objective of this work is to investigate the feasibility to utilize the waste heat from the diesel engine from the exhaust for automobile air conditioning system and to explore the advantages of this system over conventional air-conditioning system (Cengel and Boles, 2007).

$$Q = 2\pi L \times K \times \frac{(T2-T1)}{\ln\frac{r2}{r1}} \qquad (5.\ 3)$$

Where, Q is the engine energy produced L is the length from the engine to measured point which is $0.25\ m$. r_2 *and* r_1 are the inner and outer radius of exhaust pipe which are $0.04\ m$ *and* $0.05\ m$ respectively and also $T_2 and\ T_1$ are inner and outer temperatures of exhaust pipe. K is thermal conductivity of stainless steel the value $24\ W/m\ K$.

Table 5.1 Mid Bus exhaust pipe measured outside and calculated inside temperature with engine speed.

Engine speed in rpm	$T(K)$ of outside	$T(K)$ of inside
2500	144	424.26
2000	140	420.26
1500	133	413.26
1000	130.5	410.76

5.2.2.3. *Availability of waste heat from I.C engine*

The quantity of waste heat contained in a exhaust gas is a function of both the temperature and the mass flow rate of the exhaust gas:

$$\dot{Q} = \dot{m} \times C_p \times \Delta T \tag{5. 4}$$

Where, $\dot{Q}$ is the heat loss (kJ/sec); $\dot{m}$ is the exhaust gas mass flow rate (kg/sec); C_p is the specific heat of exhaust gas (kJ/kgK); and ΔT is temperature gradient in K. In order to enable heat transfer and recovery, it is necessary that the waste heat source temperature is higher than the heat sink temperature. Moreover, the magnitude of the temperature difference between the heat source and sink is an important determinant of waste heat's utility or "quality". The source and sink temperature difference influences the rate at which heat is transferred per unit surface area of recovery system, and the maximum theoretical efficiency of converting thermal from the heat source to another form of energy (i.e., mechanical or electrical). Finally, the temperature range has important function for the selection of waste heat recovery system designs.

Table 5.2 Temperature range from diesel engine (Jadhao and Thombare, 2013).

Sr. No.	Engine	Temperature in ℃
1	Single cylinder four stroke diesel engine	456
2	Four cylinder four stroke diesel engine (Tata Indica)	448
3	Six cylinder four stroke diesel engine (TATA Truck)	336
4	Four cylinder four stroke diesel engine (Mahindra ariun 605 DI)	310
5	Genset (Kirloskar) at power 198 hp	383
6	Genset (cummims) at power 200 hp	396

Exhaustive survey was made for measurement of exhaust temperature from internal combustion engine of automotive vehicles and stationary engine it is shown in Table 5.3.

Heat loss through the Exhaust in Internal Combustion Engine

Engine specification is given in Table 5.4. Heat loss through the exhaust gas from internal combustion is calculated as follows. The assumptions used are

Volumetric efficiency (η_v) is 0.9

Density diesel fuel is 0.85 gm/cc

Density of air is 1.167 kg/m^3

Specific heat of exhaust gas is 1.1 kJ/kgK

Table 5.3 Specification of Mid Bus engine.

Manufacture	Weichai Power Co., Ltd.
Engine	Four-stroke, direct-injection, four-cylinder inline, water-cooling, inter-cooling and electronic-control diesel engines
Bore	108 mm
Stroke	130 mm
Comp. ratio	14.5
Capacity	4760 ml
Power	132 kW at 2300 rpm
Sp. fuel combustion	195 g/kW.hr
RPM	2300 rpm
BHP@ 2300 rpm	132 kW
Cooling system	Water cooling

Exhaust heat loss through diesel engine

Mass flow rate of air into the cylinder,

$$volume\ rate = swept\ volume \times speed \tag{5. 5}$$

$$volume\ rate\ (\dot{V}) = V_s \times N$$

$$\dot{V} = 5.371\, m^3/sec$$

Volumetric efficiency (η_v)

$$\eta_v = \frac{volume\ of\ air}{sweft\ volume} \tag{5. 6}$$

$$\eta_v = \frac{\dot{m}_a}{\rho_a \times n \times V_s}$$

$$\dot{m}_a = 0.0958\, kg/sec$$

Mass flow rate of fuel (on the basis of specific fuel consumption), $\dot{m}_f$ is

$$s.f.c = \frac{\dot{m}_f}{power} \tag{5. 7}$$

$$\dot{m}_f = s.f.c \times power$$

$$\dot{m}_f = 0.00715\, kg/sec$$

Mass flow rate exhaust gas ($\dot{m}_E$)

$$\dot{m}_E = \dot{m}_f + \dot{m}_a \tag{5. 8}$$

$$\dot{m}_E = 0.10295\, kg/sec$$

Heat loss in exhaust gas (Q_E)

$$Q_E = \dot{m}_E \times C_p \times \Delta T \tag{5. 9}$$

Where: - ΔT is the difference of exhaust gas temperature and ambient temperature.

$Q_E = 44.35\ kW$

In order to measure the exhaust waste energy to know the amount of heat that can be utilize by the generator (Q_{gen}) the basic experiment was to take the standard measurements from the Mid Bus company as listed on the Appendix D. The results of the experiment is put here in a form of table including the conversion to the inside measure. This experiment tells that the value may be not high to make a huge change on the temperature of the absorber but it can be assisted by a photovoltaic cell to manage the power.

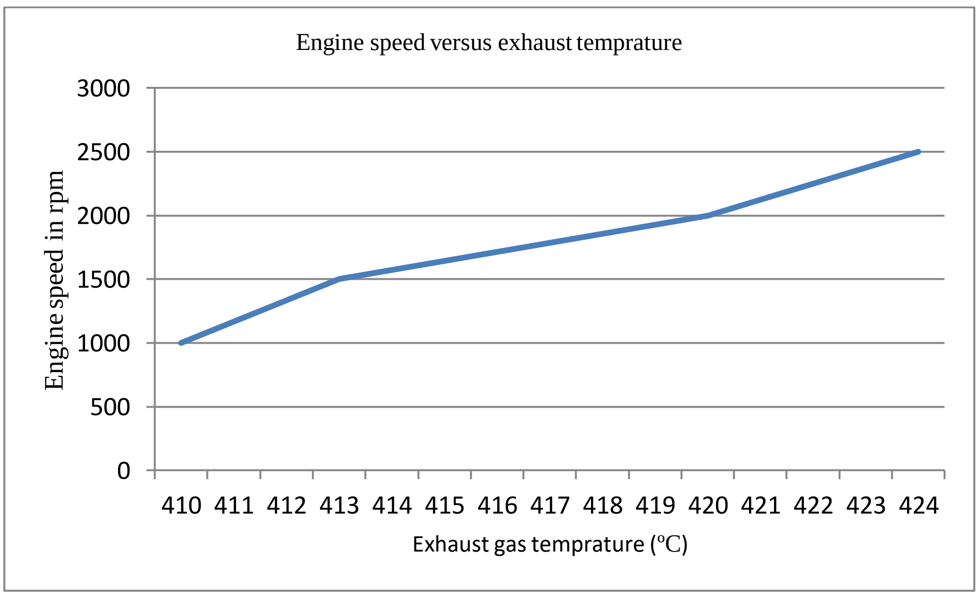

Figure 5.6 Engine speed and exhaust gas temperature variation. [Appendix B]

5.2.2.4. Data analysis

An automobile air conditioning load factors are constantly and rapidly changing as the automobile moves over highways at different speeds and through all kinds of surroundings (Beker et al., 2003). As the car moves faster there is greater amount of infiltration into the car and the heat transfer between the outdoor air and the car surface is increased. The physical sizing of the air conditioning system is critical, since space must be used efficiently to hold the design system.

Cooling capacity is the amount of heat that the air-conditioning system is able to remove from the Mid Bus. It is measured in kilowatts (kW). Previous studies and experiments were performed by researchers. The results obtained described the effect of each heat source inside the automobile (ASHRAE, 2009).Therefore, before making use out of the calculation from the paper it would be deductible to;

- Manufacture an adiabatic tube until the use of this heat on the absorption cycle./that has a length from the manifold tip to the usable place in the cycle.
- Calculate the temperature that can reach place of the tube in the common cycle.
- Calculate an optimum length of the tube which would be easy to install tube structure to the absorption cycle.

Accordingly to model the use of exhaust heat from the exhaust manifold the second one is easiest one to install on the original cycle but for better performance it would be necessary to consider the first one as has been discussed in the literature reviews.

5.2.3. Performance simulation using exhaust heat energy

Therefore, EES is used to simulate the performance of exhaust heat powered aqua ammonia absorption system. The same parameters and assumptions were used in the simulation.

The input data required for simulating the system consists of the following: generator temperature, absorber temperature, generator and condenser pressure, evaporator and absorber pressure, pump output pressure, mass flow rate entering generator, ammonia solution concentration entering the generator and fixed saturated liquid state from heat exchanger to generator. The main input is exhaust heat as a heat source for the generator.

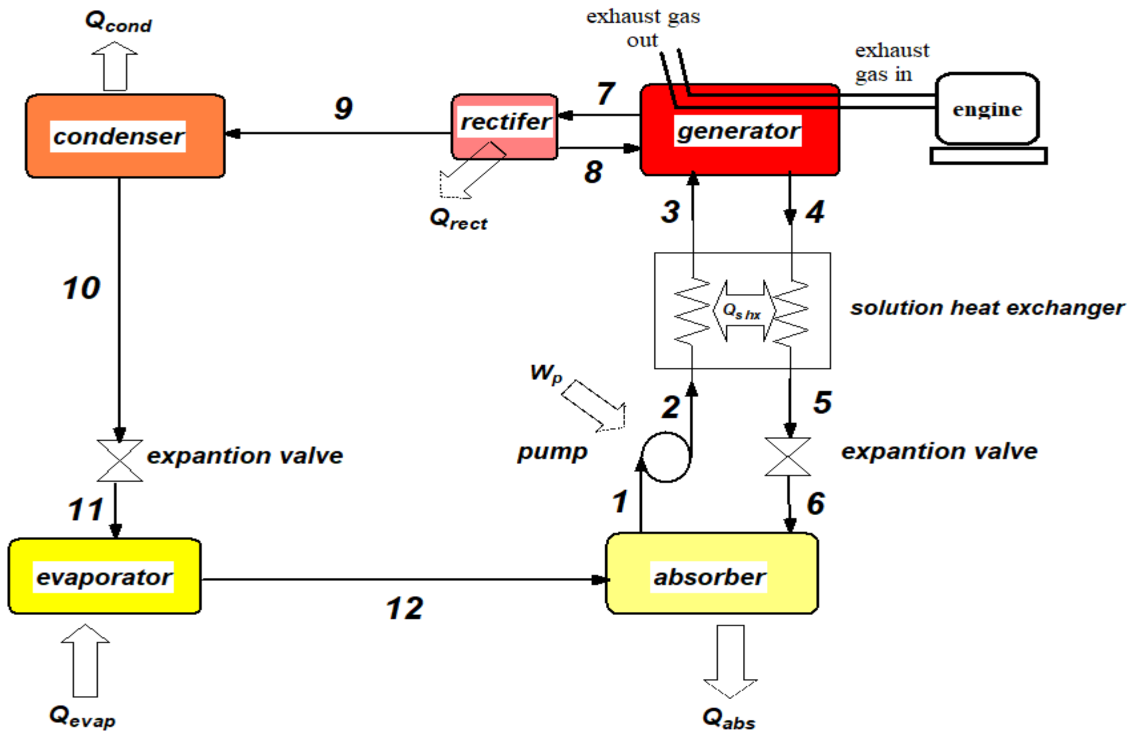

Figure 5.7 Exhaust heat powered absorption cooling system.

Heat exchanger is used to make a heat transfer from the exhaust heat to the generator. This is to make the heat of the generator constant at the best performing point of the cycle i.e. 0.656 according to the EES result. The exhaust heat that was measured from the thermocouple experiment has given the result of 44.03 kW and according to manufacturer's information same gathered has an error percent of 0.07% which is so little error to be made in making use of experiment. For the sake of understanding better way of this energy change which adapted experiment result from the experiment sub chapter. This energy adaptation has caused the following graph change as illustrated in the Table 5.5 list to be fed to the software.

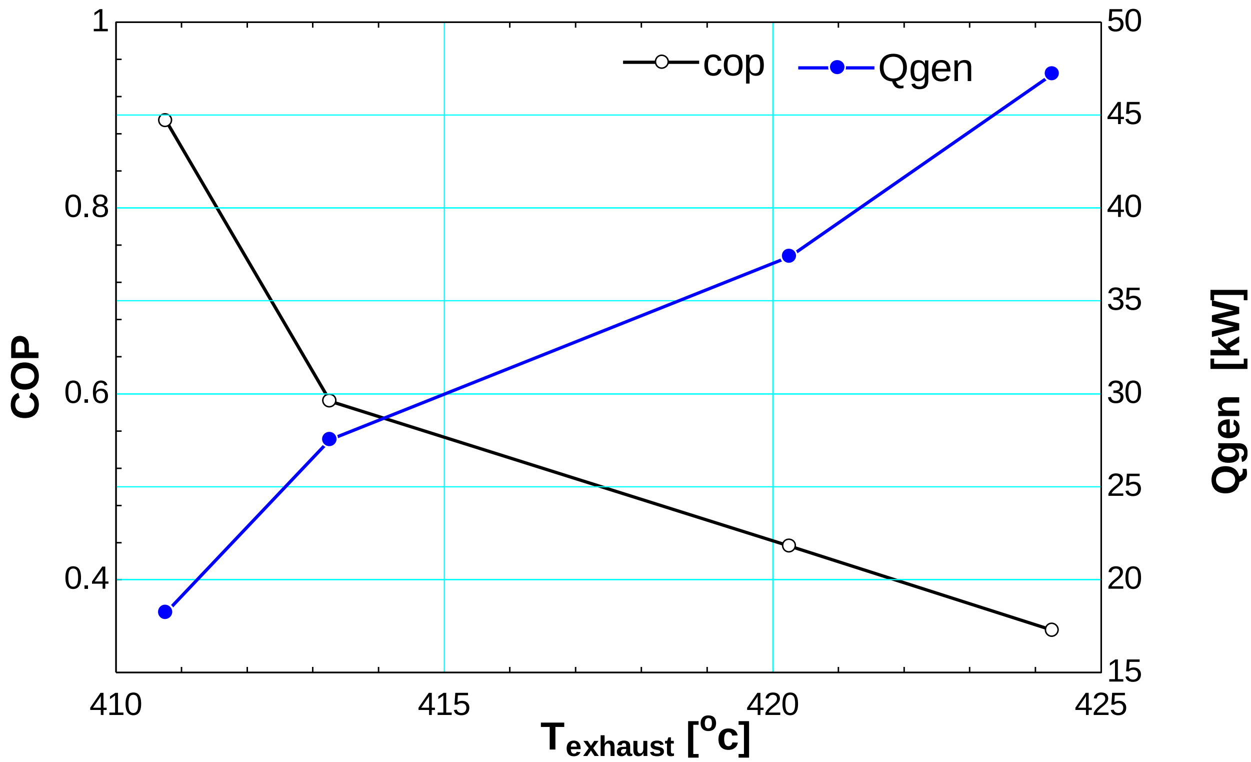

Figure 5.8 COP and exhaust heat with exhaust temperature.

This energy is available at the running time of the bus. Which should be install an other energy from to stabilize the use of the air conditioner while the car is stationary.

5.3. Hybrid consideration

The one reason that requires studying the hybrid is that when the bus is running if there is jam on the road or in slow speed the exhaust heat also decrease. This creates the generator inlet temperature decrease. This means the capacity to separate at needed time to air conditioning the bus.

Therefore, it need additional heat source so, now can be combine the two energy sources. This is studied alone at the previous section to complete the cycle and to increase COP of the system.

At the time of engine run with less speed now also electrical energy stored in the battery will start on to the heating coil to covert electrical energy into heat energy. This heat energy is used by adjusting with the exhaust heat until the exhaust heat is more sufficient to power the absorption. If the exhaust heat is achieved to power the system it doesn't need solar energy to power the system. To study more let us see the software result,

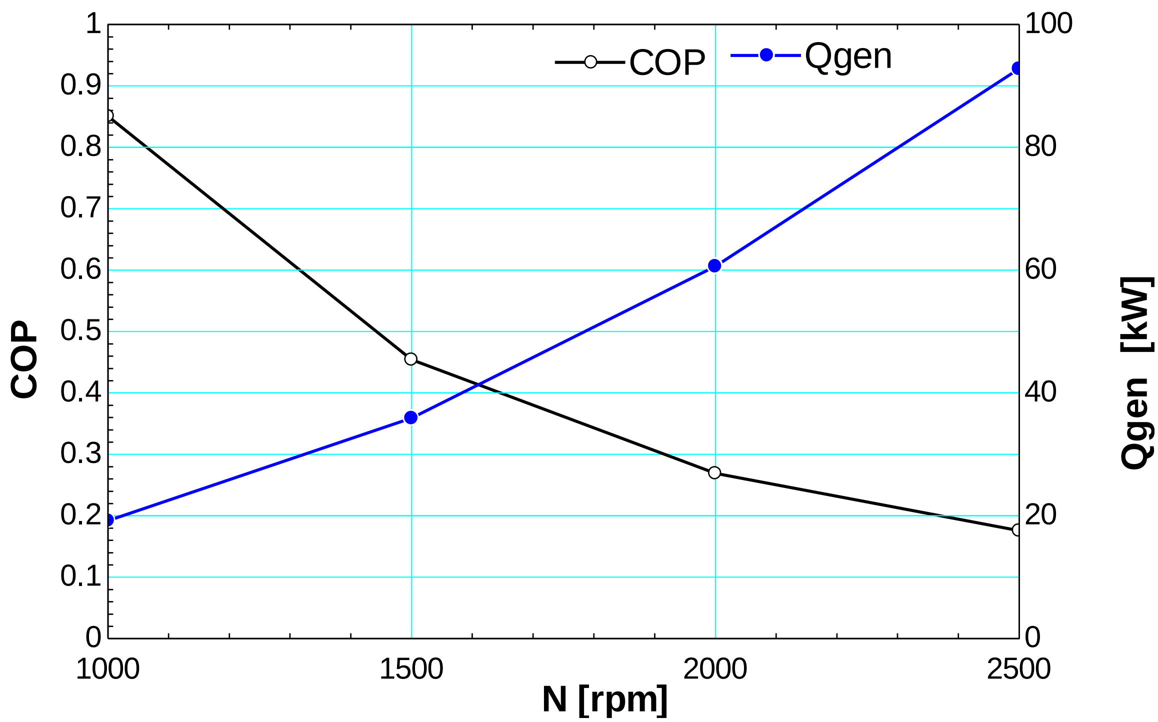

Figure 5.9 COP and hybrid energy with the speed of the bus

That variation of engine speed and the solar irradiation crates the coefficient of performance of the system. It can be seen from the graph the coefficient of performance decrease and generator heat energy gain increase. Now let see the other graphs and tables,

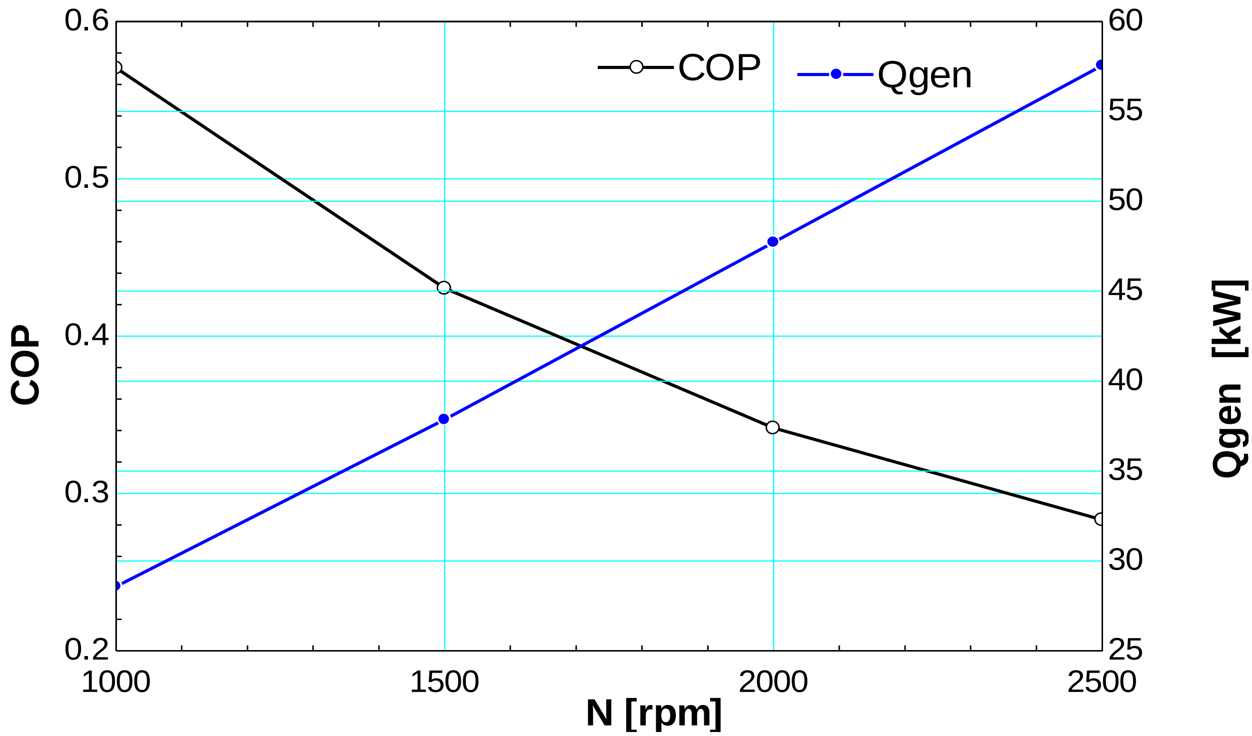

Figure 5.10 COP and hybrid energy at constant solar energy with engine speed of bus.

The coefficient of performance is decrease from 0.5705 to 0.2832 when the engine speed increases from 1000 rpm to 2500 rpm with constant current input from battery. And the energy generates to the generator also increase 28.57 kW to 57.55 kW.

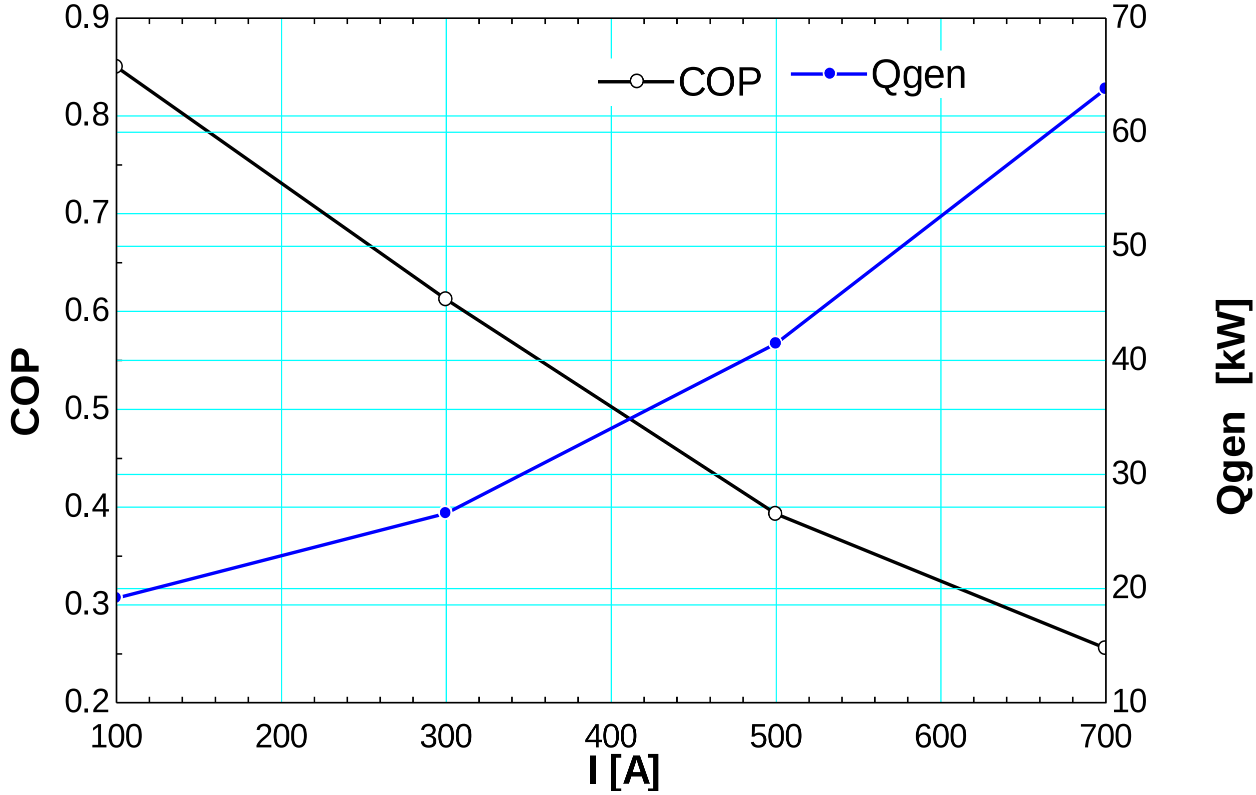

Figure 5.11 COP and hybrid energy at constant engine speed with the current

The above graph is the result for constant speed of the engine at 1000rpm and varying solar irradiation. Why does it selected the small engine speed was to see the performance simulations of hybrid which is power supported by solar energy. The variation of current from $100\ A$ to $700\ A$ results coefficient of performance dropped from 0.8503 to 0.2554 and the generated energy also increased from $19.27\ kW$ to $63.81\ kW$.

CHAPTER SIX

6. COMPONENTS SIZING

6.1. Introduction

The components were designed and sized to accommodate the relative mass and heat rates. These components are:

- Evaporator
- Condenser
- Generator
- Absorber
- Solution heat exchanger
- Expansion valve (capillary tube)
- Pump

The plant was designed for an average refrigeration capacity of $16.3\ kW$ at $5℃$ temperature. From the simulation program as demonstrated in chapter 4 using the above requirements, predicted working conditions which were used to design the components.

In this chapter the main results of the calculations as well as the detailed procedure for the design of the components are presented. The equations and calculations used for the sizing of each component are briefly stated below and for all these calculation computer codes were developed. Before that let as discus each component:

6.1.1. Condenser

In a condenser, refrigerant flows on one fluid side, and the ambient air from the vehicle front grille flows on the other fluid side. The refrigerant is de superheated, condensed and sub cooled in the condenser with cooler ambient air on the other side. The refrigerant coming to condenser gains heat as follows: heat transfer in the evaporator from air to refrigerant, compressor power input and heat gains in the refrigerant lines in the engine compartment. The condenser is kept fully immersed in the barrel fully filled with water. Water is used as a coolant in the condenser barrel here because water has the best heat transfer properties than air. Any leakages can also be detected easily because of the bubbles formed in the water. The leakage of NH_3 can also be absorbed by water. so, the leakage of the refrigerant is not harmful to the material.

6.1.2. Evaporator

The function of the evaporator is to dehumidify and cool the ambient air going to the passenger compartment, thus reducing the sensible and latent heat from the incoming air to the evaporator. The evaporator is located in the HVAC module before the heater core at some angle greater than about 45° with the heater core. Equal or lower amount of airflow (than that going through the evaporator) can go through the heater. HVAC module design allows conditioned air to the passengers cabin in the following modes: cooling, heating, bi-level (foot/face) foot/defrost modes, and defrost/demist; depending on the design requirements, either fresh or re circulated air is used in some or all above modes. An evaporator is a device used to turn the liquid form of a chemical into its gaseous form. The liquid is evaporated, or vaporized, into a gas. It is made up of thin metal sheet having internal tubes for circulating the refrigerant. It has two ports namely inlet & outlet port. Inlet port is connected to receiver and outlet port is connected to the absorber.

6.1.3. Absorber

Absorber is a chamber where the absorbent and the refrigerant vapor are mixed together. It is equipped with a heat rejection system, i.e. bundles of tubes as is in the condenser of VCRS, and operates under a low pressure level which corresponds to the evaporator temperature. The absorption process can only occur if the absorber is at a sensible low temperature level, hence the heat rejection system needs to be attached. The mixing process of the absorbent and the refrigerant vapor generate latent heat of condensation and raise the solution temperature. Simultaneous with the developmental processing of latent heat, heat transfer with cooling water will then lower the absorber temperature and, together with the solution temperature, creates a well-blended solution that will be ready for the next cycle. A lower absorber temperature means more refrigerating capacity due to a higher refrigerant's flow rate from the evaporator.

6.1.4. Generator

The generator is the device through which heat is supplied to the solution in order to release the refrigerant from its absorbing medium. Its action is more complicated than just heating a liquid from one temperature to another. The generator's process can be divided into a series of step processes:

1. Breaks up the bond of association between the refrigerant and the absorbent.
2. Changes the temperature of the resulting liquid refrigerant to its saturation temperature.
3. Vaporizes the liquid refrigerant.
4. Changes the temperature of the incoming strong solution to the generator's temperature.
5. If the absorbent is volatile, it evaporates a certain amount of absorbent and raises its temperature to the temperature of the generator.

In the generator exhaust heat will come through the exhaust recovery system where ammonia liquid vaporizes and temperature and pressure increases. Generator is made up of stainless steel. It is drilled with the help of vertical drilling machine to fit with the electric heater. A heater is sealed to prevent the leakage of water ammonia mixture from generator. Another hole is made to upper part of generator for admitting the mixture of ammonia and water from the pump placed in absorber. Third opening is made at the bottom for drain out the mixture from generator to the absorber.

6.1.5. Pump

A solution pump will mainly circulate and lift the solution from the lower pressure level side to the higher pressure level side of the system. To maintain this pressure difference, the centrifugal type pump is preferable (Assuming the solution is incompressible liquid). In short it is accountable of pumping the rich solution raising its pressure to the condenser pressure.

6.1.6. Expansion valve

An expansion valve is a component that reduces the pressure and splits the two different pressure levels. In a simple model of a single effect absorption refrigeration system, the pressure change is assumed only to occur at expansion valve and the solution pump. There is no heat added or removed from the working fluid at the expansion valve. The enthalpy of the working fluid remains the same on both sides. The pressure change process between the two end points of the expansion valve, while there is no mass flow change and the process is assumed as an adiabatic process, can change the volume if the fluid generates a small amount of steam phase via flashing.

An expansion device is essentially a restriction offering resistance to flow so that the pressure drops, resulting in a throttling process. Basically there are two types of expansion devices. These are:

i. Variable-restriction type
ii. Constant-restriction type

In the variable-restriction type, the extent of opening or area of flow keeps on changing depending on the type of control. There are two common types of such control devices, viz., the automatic expansion valve and the thermostatic expansion valve.

In addition, there are the float-valves which are also variable restriction type devices. The float valves again are two types: the high-side float and the low- side float.

The high-side float maintains the liquid at a constant level in the condenser and the low-side float maintains the liquid at a constant level in the evaporator.

The constant-restriction type device is the capillary tube which is merely a long tube with a narrow diameter bore. The pressure drop through the capillary tube is due to the following factors:

i. Friction, due to fluid viscosity, resulting in frictional pressure drop.
ii. Acceleration, due to the flashing of the liquid refrigerant into vapor, resulting in momentum pressure drop.

6.2. Components designing

The first law results of VAS provides basis for further design of each component of vapor absorption system. The detailed procedure for the design of a 16.3 kW capacity VAS has been presented.

6.2.1. Evaporator design

Evaporator of the absorption heat transformer system operates at low pressure as compare to generator. The evaporator is a shell-tube heat exchanger. In the tube side external hot water is flowing and the outside of the tube we have pure refrigerant. The main function of evaporator is to vaporize the pure refrigerant by heat addition at the intermediate temperature of the system.

Choice is made between the length and the number of water tubes as wall as tube diameters from the standard size materials for the sizing of evaporator. For a specified tube diameter iteration procedures evaluate the length of the tube. The water enters the tubes through four passes. The evaporator has the following characteristics:

Table 6.1 Characteristics of evaporator

Parameters	Type/ value
Heat exchanger type	Single pass horizontal tube, outside diameter $D_o = 17.04\ mm$ and inside diameter $D_i = 13.79\ mm$
Hot water inlet temperature	10℃
Hot water outlet temperature	7℃
Numbers of tubes	30
Mass flow rate of refrigerant	$0.016498\ kg/s$
Evaporator capacity, Q_{evap}	$16.3\ kW$

Evaporator pressure	$516\ kPa$

Heat transfer correlations, suggested by Klimenko (Mills, 1992), establish that the boiling is within the nucleate region and then calculate the refrigerant-side heat transfer coefficient. Correlations suggested by Gnielinski (Mills, 1992) calculate the water-side heat transfer coefficient.

To find the water side heat transfer coefficient the following procedure are used.

Mean temperature of water is,

$$T_b = \frac{T_{w,i} + T_{w,o}}{2} \tag{6. 1}$$

The average film temperature of water is,

$$T_f = \frac{T_b + T_{wall}}{2} \tag{6. 2}$$

At this time assumption is made for average wall temperature of the tube, for the first approximation $T_{wall} = 5.5℃$.

Using thermo-physical properties of water at average film temperature the Reynolds number and Prandtl number are found.

Area of flow of water (30 tubes)

$$A = 30\frac{\pi}{4}(D_i)^2 \tag{6. 3}$$

Mass flow rate of water through the tubes is,

$$\dot{m}_w = \frac{Q_{evap}}{C_p \times \Delta T} \tag{6. 4}$$

So the mass velocity of water can be calculated using

$$G = \frac{\dot{m}_w}{A} \tag{6. 5}$$

Therefore, Reynolds number of water became

$$Re = \frac{G \times D_i}{\mu} \tag{6. 6}$$

Water side forced convection heat transfer coefficient inside tubes using Dittus-Boelter equation

$$Nu = 0.023(Re)^{0.8}(Pr)^{0.3} = \frac{h_i D_i}{k} \tag{6. 7}$$

At the Ammonia side calculating $h_o$value nucleate boiling correlation given by Rohsenow is used. The Rohsenow correlation for nucleate boiling is as under; (Arora, 2010)

$$q/A = h_o \Delta T = \mu_f h_{fg} \left[\frac{g(\rho_f - \rho_g)}{\sigma}\right]^{1/2} \left[\frac{C_f \Delta T}{C_{sf} h_{fg} Pr_f^{1.7}}\right]^3 \tag{6. 8}$$

The above said equation 6.8 is the first and most widely used equation for nucleate boiling. In this expression all the properties of liquid and vapor refrigerant are evaluated at saturation temperature of evaporator. All other parameters are displayed in the nomenclature. The coefficients C_{sf} depend on the solid fluid combination and represents experimentally determined value is taken as; $C_{sf} = 0.013$ in combination of water with polished copper tubes. The surface tension (σ) is for water in the above equation. Rohsenow correlation is valid only for clean surfaces (Rohsenow, 1952).

Calculating $h_i$and h_o values and putting these in equation 6.9 give the overall heat transfer coefficient.

$$\frac{1}{U_o} = \left(\frac{D_o}{D_i}\right)\left(\frac{1}{h_i}\right) + \left(\frac{1}{2k_w}\right) D_o \ln\left(\frac{D_o}{D_i}\right) + \left(\frac{1}{h_o}\right) \tag{6. 9}$$

Where, k_w = Tube thermal conductivity, $24\,W/m\,K$

The Logarithmic Mean Temperature Difference is given by:

$$\Delta T_{LMTD} = \frac{(T_{w,o} - T_{evap}) - (T_{w,i} - T_{evap})}{\ln\left(\frac{(T_{w,o} - T_{evap})}{(T_{w,i} - T_{evap})}\right)} \tag{6. 10}$$

Heat transfer area of the passes became

$$A_o = \frac{Q_{evap}}{U_o \times \Delta T_{LMTD}} \text{ and } A_i = A_o \times \frac{D_i}{D_o} \tag{6. 11}$$

Check for the assumed value of average wall temperature of the tube using

$$T_{wall} = T_b + \frac{Q_{evap}}{h_i A_i} \tag{6. 12}$$

The length of tube in the pass

$$A_o = N \times \pi D_o L \tag{6. 13}$$

From further iteration converges to the results of the calculations are presented in Table 6.2

Table 6.2 Specification for evaporator

Parameters	Type/ value
Length of tube for single pass	$0.8736\ m$
Overall heat transfer coefficient	$887.1\ W/m^2K$
Log mean temperature difference (LMTD)	3.274℃
Area required for singe pass	$1.403\ m^2$

6.2.2. Generator design

Generator of the absorption heat transformer system operates at high pressure. The generator is designed as a shell-tube heat exchanger. The strong solution enters the top header and passes through 16 tubes to the bottom header. The exhaust gas enters the shell and passes the outside of the tubes. The main function generator is to separate pure ammonia from the strong solution.

As the same as evaporator choice is made between the length and the number of water tubes as well as tube diameters from the standard size materials for the sizing of generator. For a specified tube diameter iteration procedures evaluate the length of the tube. The water enters the tubes through four passes. The generator has the following characteristics:

Table 6.3 Characteristics of generator

Parameters	Type/ value
Heat exchanger type	Single pass horizontal tube, outside diameter $d_o = 9.6\, mm$ and inside diameter $d_i = 12\, mm$ Shell inner diameter $D_i =\ 74$ mm
Hot exhaust gas inlet temperature	422.66℃
Hot exhaust gas outlet temperature	227.685℃
Hot exhaust gas mass flow rate	$0.10295\, kg/s$
Mass flow rate of refrigerant	$0.0187\, kg/s$
Mass flow rate of strong solution	$0.02373\, kg/s$
Generator capacity,Q_{gen}	$24.85\ kW$
Generator pressure	$2033\ kPa$

The following is the procedure to find the physical properties of the exhaust gas at $1atm$.

The exhaust gas can be thought as a mixture gas of $C0_{2,}$ H_20, CO, 0_2 and N_2 . A stoichiometric analysis of the diesel fuel combustion leads to the following:

$$C_{12}H_{24} + x(O_2 + 3.76N_2) \rightarrow aCO_2 + bH_2O + cCO + dO_2 + eN_2$$

The a, b, c, d and e are mol. Fractions of each individual gas in the exhaust gas.

Considering an air/fuel mass ratio of 13.4, the left side of the equation would give:

$$x \times (32 + 3.76 \times 28) = 13.4 \times (12 \times 12 + 24)$$

From which $x = 16.4$ this leads to

$$C_{12}H_{24} + 16.4(O_2 + 3.76N_2) \rightarrow 8CO_2 + 12H_2O + 4CO + 0.4O_2 + 61.66N_2$$

For the exhaust gas mixture, the properties $\emptyset_e$

$$\emptyset_e = \frac{a\emptyset_{CO_2} + b\emptyset_{H_2O} + c\emptyset_{CO} + d\emptyset_{O_2} + e\emptyset_{N_2}}{a + b + c + d + e}$$

Where: - $\emptyset$ is any physical property of gases at 1 atm and exhaust gas temperature

For the exhaust gas in the generator, the Reynolds number is

$$Re_e = \frac{d_o G_{max}}{\mu_e} \tag{6. 14}$$

Here G_{max} is the mass velocity of the exhaust gas

$$G_{max} = \rho_e \times v = \frac{\dot{m}_e}{A} \tag{6. 15}$$

$$A = \frac{\pi}{4}\left(D_i^2 - n_p d_o^2\right) \tag{6. 16}$$

Where n_p is number of pipes for the single pass

At the exhaust gas side

For finding outside heat transfer coefficient (h_o), for flow perpendicular to a cylinder of diameter D, the average heat transfer coefficient can be obtained from the correlation (Serth, 2007):

$$Nu = 0.3 + \frac{0.62Re^{0.5}Pr^{1/3}}{\left(1+(0.4/Pr)^{2/3}\right)^{1/4}}\left(1 + \left(\frac{Re}{282,000}\right)^{5/8}\right)^{4/5} \tag{6. 17}$$

$$Nu = \frac{h_o D}{k} \tag{6. 18}$$

The properties of the gas at the film temperature estimated as

$$T_f = \frac{T_b + T_{wall}}{2} \quad (6.\ 19)$$

Where: - T_b is the bulk fluid temperature for an exhaust gas average temperature,

$$T_b = \frac{T_{e,i} + T_{e,o}}{2} \quad (6.\ 20)$$

As a first approximation, assume $T_{wall} = 110°C$

For the heat transfer on the inside of tubes,

At the generator temperature the properties of strong solution are evaluated and Reynolds number can be found using the same step as outside of tubes. The area is found from inside tube diameter.

For flow in the transition region ($2100 < Re < 10^4$), the Hausen correlation is recommended (Serth, 2007):

$$Nu = 0.116\left(Re^{2/3} - 125\right)Pr^{1/3}(\mu/\mu_w)^{0.14}\left(1 + (D/L)^{2/3}\right) \quad (6.\ 21)$$

Where, the subscript w refers to the inside wall temperature.

D is inside diameter of the pipes

L is the tube length

As a second approximation a choice is made for the tube length $L = 0.3m$ therefore h_i can be calculated $Nu = \frac{h_i D}{k}$.

Then the overall heat transfer coefficient can be evaluated using equation 6.9. And also the logarithmic mean temperature difference for the generator evaluated using equation 6.10 replacing evaporator temperature with generator temperature.

Then the length of the tubes is calculated using equation 6.13 and the temperature of wall of pipes can be checked by using equation 6.12.

These wall temperature and length of the pipes are iteratively calculated from equation 6.19 and 6.21 until convergence. The end results are

Table 6.4 Specification for generator

Parameters	Type/ value
Length of tube	$0.4757\ m$
Overall heat transfer coefficient	$105.6\,W/m^2K$
Log mean temperature difference (LMTD)	204.9℃
Area required	$1.148\ m^2$

6.2.3. Condenser design

The condenser is of the shell and tube type in which the refrigerant vapor is condensing over a bank of water tubes. The heat of the deflegmator is removed in the condenser.

Choice is made between the length and the number of water tubes as well as tube diameters from standard size materials.

Table 6.5 Characteristic of condenser

Parameters	
Heat exchanger type	Single pass horizontal tube, outside diameter $D_o = 15.9\ mm$ and inside diameter $D_i = 13.7\ mm$
Cold water inlet temperature	30 ℃
Cold water outlet temperature	34.8 ℃
Cold water mass flow rate	$0.3502\,kg/s$
Mass flow rate refrigerant	$0.016498\,kg/s$

Condenser capacity, Q_c	$16.63\ kW$
Condenser pressure	$2033\ kPa$

From thermodynamic properties of water the values of the specific heat Cp_w, the density ρ_w, the conductivity K_w, the Prandtl number Pr_w, and the viscosity μ_w for an average temperature between the inlet and outlet cooling water temperatures:

$$T_w = \frac{T_{w,i}+T_{w,o}}{2} \quad (6.\ 22)$$

As the first approximation, $T_w = 30°C$, for this average temperature the mass rate of the cooling water is

$$\dot{m}_w = n_t \rho_w V_w \frac{\pi}{4} d_i^2 \quad (6.\ 23)$$

Then the outlet temperature of the cooling water is

$$T_{w,o} = \frac{\dot{Q}_{cond}}{\dot{m}_w Cp_w} + T_{w,i} \quad (6.\ 24)$$

The iteration calculation from equation 6.22 converge the outlet water temperature.

The Reynolds number is calculated the same as before so, for finding Nuselt number an alternative equation for the transition and turbulent regimes has been proposed by Gnielinski (Serth, 2007):

$$Nu = \frac{(f/8)(Re-1{,}000)Pr}{1+12.7\sqrt{(f/8)}(Pr^{2/3}-1)}\left(1+\left({}^{D}/_{L}\right)^{2/3}\right) \quad (6.\ 25)$$

Here, f is the Darcy friction factor, which can be computed from the following explicit approximation of the Colebrook equation (Serth, 2007):

$$f = (0.782 \ln Re - 1.51)^{-2} \quad (6.\ 26)$$

Equation 6.25 is valid for $2100 < Re < 10^6$ and $0.6 < Pr < 2000$. The heat transfer coefficient at the inside and outside of tube (h_i, h_o) calculated. The procedure for the calculation of h_i is same as defined under section 6.2.2 using the above Nuselt number.

For a condensing refrigerant on the outside surfaces of tubes, the heat transfer coefficient is given by

$$h_o = 0.725\left(\frac{g(\rho_l - \rho_v)h^*_{fg}K_l^3}{n_t\mu_l d_o(T_{sat} - T_{wall})}\right)^{1/4} \tag{6. 27}$$

Where $n_t = 36$ is the number of passes of tubes within the shell and

$$h^*_{fg} = h_{fg} + \left(0.683 - \frac{0.228}{Pr_l}\right)Cp_l(T_{sat} - T_{wall}) \tag{6. 28}$$

Is the latent heat correction, according to Sadasivan and Lienhard (Mills, 1992)

The properties of the saturated condensate of ammonia at temperature $T_{sat} = 50$°C, are used. Assuming a wall temperature $T_{wall} = \frac{T_{w,i}+T_{w,o}}{2} + 0.5$ as a first approximation and substituting the above value into equation 6.28 and equation 6.27 to get h^*_{fg} and h_o.

Condenser should always be designed considering the formation of scales, i.e., fouling inside the tube (Arora, 2010). The resistances due to fouling are by the refrigerant $R_{ref} = 0.00025$ and by the water $R_{FF} = 0.0001$ the wall conductance $K_w = 24\ W/m$.

The overall heat transfer coefficient is given by the relation

$$\frac{1}{U} = \left(\frac{d_o}{d_i}\right)\frac{1}{h_i} + \frac{d_o \ln\left(\frac{d_o}{d_i}\right)}{2K_w} + \frac{1}{h_o} + R_{ref} + R_{FF} \tag{6. 29}$$

Logarithmic mean temperature difference for the condenser evaluated using equation 6.10 replacing evaporator temperature with condenser temperature. Then the length of the tubes is calculated using equation 6.31.

$$A = \frac{Q_{cond}}{U\ \Delta T_{LMTD}} \tag{6. 30}$$

$$L = \frac{A}{n_t \pi d_o} \tag{6. 31}$$

The temperature of wall of pipes is given by

$$T_{wall} = T_{sat} - \frac{Q_{cond}}{A \times h_o} \tag{6. 32}$$

This wall temperature is iteratively calculated from equation 6.27 until convergence.

The results in terms of overall heat transfer coefficient, area required and length of tube required are displayed in Table 6.6.

Table 6.6 Specification for condenser

Parameters	Type/ value
Length of tube	1.702 m
Overall heat transfer coefficient	309 W/m^2K
Log mean temperature difference (LMTD)	17.49℃
Area required	3.06 m^2

6.2.4. Absorber design

Absorber is the main part of any absorption system, required more attention. Since the proper absorption of the refrigerant is required in the absorber for achieving the desired performance of the system. For the proper absorption of the refrigerant the continuous heat is required to be emitted by the system, this require the effective design of the absorber heat exchanger.

For the effective design of these components the standard values of the diameter of tubes are adopted to find the length of the tube. In this analysis vertical tube are assumed for the absorber system and hot water is flowing inside the tube which is gaining heat from the absorber, also the $NH_3 - H_2O$ solution is present at the outside of the tube.

Table 6.7 Characteristics of absorber

Parameters	Type/ value
Heat exchanger type	Single pass horizontal tube, outside diameter $d_o = 20\ mm$ and inside diameter $d_i = 17\ mm$ The shell inside diameter $D_i = 69\ mm$
Hot water inlet temperature	18°C
saturation temperature of the strong solution	10°C
Weak solution mass flow rate	$0.02373\ kg/s$
Mass flow rate of refrigerant	$0.01649\ kg/s$
cooling water velocity	$0.4\ m/s$
concentration of ammonia vapor	1
concentration of weak solution	0.4436
concentration of strong solution	0.8304
Absorber capacity, Q_{abs}	$18.34\ kW$
Number of core tubes	7

The procedure for the design of absorber heat exchanger is as follows.

For an average temperature between inlet and outlet using equation 6.22 as the first approximation $T_w = 18°C$ and using water properties the mass flow rate of cooling water is

$$m_w = V_w \rho_w \frac{\pi}{4} (D_i^2 - n_t d_o^2) \quad (6.\ 33)$$

The outlet water temperature is given by

$$T_{w,o} = T_{w,i} + \frac{Q_{abs}}{Cp_w m_w} \tag{6. 34}$$

Iterative calculation from equation 6.22 gives the outlet water temperature $T_{w,o}$.

The hydraulic diameter and Reynolds number are

$$D_H = \frac{D_i^2 - n_t d_o^2}{D_i + n_t d_o} \tag{6. 35}$$

$$Re = \frac{\rho_w V_w D_H}{\mu_w} \tag{6. 36}$$

From (Welty et al., 1976) the friction factor and water side heat transfer coefficient are evaluated for Re > 2300 with equation 6.36.

$$f = (0.79 \ln(Re) - 1.64)^{-2}$$

$$h_o = 0.86 \left(\frac{K_w}{D_H}\right) \left(\frac{D_i}{d_o}\right)^{0.16} \frac{\left(\frac{f}{8}\right) Pr_w (Re - 1000)}{1 + 12.7 \left((Pr_w)^{\frac{2}{3}} - 1\right) \left(\frac{f}{8}\right)^{0.5}} \tag{6. 37}$$

At the solution side partial heat transfer coefficient can be calculated as the following procedure. The partial heat transfer coefficient is calculated according to (Horn, 1970), for a two phase flow of the solution in the inner tubes.

$$h_i = \varepsilon . h_{LF} + (1 - \varepsilon) . h_{LP} \tag{6. 38}$$

According to Hubbard (Scott, 1964), the thickness of the falling film on the inside surface of a tube is approximately given by: $\delta = 0.05 d_i$ as first approximation

The velocity of the vapor can be found by

$$u_G = \frac{m_{ref}}{n_t \rho \frac{\pi}{4} d_i^2} \tag{6. 39}$$

(Moissis, 1963) has expressed the absolute liquid film velocity of descending liquid of thickness δ as:

$$V_f = \frac{1}{4\delta(D-\delta)}\left(\left(1.2\frac{Q_G+Q_L}{A} + C\sqrt{gD}\right)(D-2\delta)^2 - D^2\frac{Q_G+Q_L}{A}\right) \quad (6.40)$$

Where, $c = 0.35$

If the liquid film is assumed to fill the gap between the wall and the rising slug, the characteristic length for the Reynolds number Re_{LF} is 2δ. Thus the Reynolds number Re_{LF} is:

$$Re_{LF} = \frac{4\delta.\rho_f.V_f\left(1-\frac{\delta}{D}\right)}{\mu_f} \quad (6.41)$$

For $Re_{LF} > 400$ the film thickness is recalculated by the equation 6.42 (Brauer, 1958):

$$\delta = 0.302(Re_{LF})^{\frac{8}{15}}\left(\frac{3\left(\frac{\mu}{\rho}\right)^2}{g}\right)^{\frac{1}{3}} \quad (6.42)$$

Iteration calculations from equation 6.40 until it convergence give the film thickness result. So for $Re_{LF} > 800$, the Nusselt number is given by:

$$Nu_{LF} = 0.00621(Re_{LF})^{\frac{14}{15}}Pr^{0.344} \quad (6.43)$$

And the heat transfer coefficient for the liquid film is:

$$h_{LF} = Nu_{LF}\frac{K_{sol}}{d_i} \quad (6.44)$$

The velocity of liquid slug in the tubes is dependent on the mass flow rate of weak solution. Thus,

$$m_{LP} = \frac{m_G}{n_t}.\left(\frac{x_{ref}-x_{ST}}{x_{ST}-x_{WE}}\right) \quad (6.45)$$

$$u_{LP} = \frac{m_{LP}}{\rho_L}.\frac{\pi}{4}d_i^2 \text{ And } Re_{LP} = \frac{u_{LP}.d_i.\rho_L}{\mu_L} \quad (6.46)$$

For a vapor concentration in ammonia $x_{ref} = 1$, its saturated solution has concentration x^*=0.72. The driving potential for mass transfer is:

$$dx = x^* - x_{WE} \quad (6.47)$$

Where: - dx = % concentration difference

Assuming a volumetric mass transfer coefficient $K_L\alpha = 18$ as a first approximation, the height "z" of the tubes necessary to absorb all the incoming vapor is given by (Keizer, 1982):

$$z = \frac{m_{ref}}{n_t.dx.K_L\alpha.\frac{\pi}{4}d_i^2} \tag{6. 48}$$

For $Re_{LP} < 2300$, according to Edwards, Denny and Mills (Mills, 1992), the Nusselt number is

$$Nu_{LP} = 3.66 + \frac{0.065\ Re_{LP}Pr\left(\frac{d_i}{z(1-\varepsilon)}\right)}{1+0.04\left(\ Re_{LP}Pr\left(\frac{d_i}{z(1-\varepsilon)}\right)\right)^{\frac{2}{3}}} \tag{6. 49}$$

And the liquid phase heat transfer coefficient is:

$$h_{LP} = Nu_{LP}\frac{K_{sol}}{d_i} \tag{6. 50}$$

The void fraction "ε" is defined as:

$$\varepsilon = \frac{(d_i-2\delta)^2}{d_i^2} \tag{6. 51}$$

Substituting these values into equation 6.38, the partial heat transfer coefficient is calculated. The overall heat transfer is given by equation 6.9 and the Logarithmic Mean Temperature Difference the same as equation 6.10. The height of the tube for heat transfer is given by:

$$z = \frac{Q_{abs}}{n_t.U\Delta T_{LMTD}\pi d_i} \tag{6. 52}$$

Iterative calculations from equation 6.48 converge in evaluating the volumetric overall mass transfer coefficient $K_L\alpha$ and the height of the core tubes. Results for the above analysis are displayed in Table 6.8.

Table 6.8 Specification for absorber

Parameters	Type/ value
Length of tube	$17.03\ m$
Overall heat transfer coefficient	$257.4\ W/m^2K$
Log mean temperature difference (LMTD)	11.19℃
Area required	$6.368\ m^2$

6.2.5. Solution heat exchanger design

For improving the performance of the VAC system solution heat exchanger is incorporated between the low pressure absorber and high pressure generator. The heat exchanger is of a double tube, counter flow design. The inner tube contains the hot weak solution and the annular gas contains the cold strong solution.

Table 6.9 Characteristics of solution heat exchanger

Parameters	Type/ value
Heat exchanger type	Single pass annulus, shell tube outside diameter $D_o = 10\ mm$ and inside tube outside diameter $d_o = 6\ mm$ with 1 mm wall thickness
Weak solution inlet temperature	105℃
Strong solution inlet temperature	10.631℃
Strong solution outlet temperature	55.245℃
strong solution concentration	0.8304

weak solution concentration	0.4436
Strong solution mass flow rate	$0.02373\ kg/s$
Weak solution mass flow rate	$0.00723\ kg/s$
Heat transfer, Q_{SHX}	$4.653\ kW$

In the present analysis a simple annulus heat exchanger is considered for the designing of solution heat exchanger. Also, the laminar flow of $NH_3 - H_2O$ solution is observed in the inner and outer tube. In the inner tube high temperature weak solution of $NH_3 - H_2O$ is flowing and in outer tube we have strong solution going in the absorber. Transfer of the heat takes place between the weak and strong solution.

The procedure of the design is as follows

For an average temperature of weak solution

$$T_{WE} = \frac{T_{w,i}+T_{w,o}}{2} \tag{6. 53}$$

$T_{WE} = 105°C$ as first approximation the specific heat Cp_{WE} is used. A heat balance across the heat exchanger gives:

$$Q_{ehx} = m_{ST}Cp_{ST}\left(T_{s,o} - T_{s,i}\right) = m_{WE}Cp_{WE}\left(T_{w,i} - T_{w,o}\right) \tag{6. 54}$$

Iterative calculation for weak solution outlet temperature is done using equation 6.53. For calculating LMTD (Log mean temperature difference) equation 6.10 is used.

For the average temperature of weak solution and average temperature of strong solution thermodynamic properties are used to get Reynolds number for both solutions. And also for a hydraulic diameter D_H is determined using equation 6.35. The fluid velocities are calculated by:

$$V_{WE} = \frac{m_{WE}}{\rho_{WE}} \cdot \frac{1}{\frac{\pi}{4} d_i^2} \tag{6. 55}$$

$$V_{ST} = \frac{m_{ST}}{\rho_{ST}} \cdot \frac{1}{\frac{\pi}{4}(d_o^2 - d_i^2)} \tag{6. 56}$$

The Reynolds numbers for the flows are:

$$Re_{ST} = \frac{D_H \cdot \rho_{ST} \cdot V_{ST}}{\mu_{ST}} \tag{6. 57}$$

$$Re_{WE} = \frac{D_H \cdot \rho_{WE} \cdot V_{WE}}{\mu_{WE}} \tag{6. 58}$$

The individual stream heat transfer coefficients are calculated by equations corresponding to inner and annular flows. Thus for turbulent flow, Gnielinski's formula gives:

$$f = (0.79 \ln(Re_{WE}) - 1.64)^{-2}$$

If $Re_{WE} > 2300$ equation 6.37 is used for $Re_{ST} < 2300$ equation 6.59 is used. For a first estimation of the tube length $L = 7\ m$ the heat transfer coefficient for the strong solution.

$$h_o = 0.86 \left(\frac{d_i}{d_o}\right)^{0.16} \left(\frac{K_{ST}}{D_H}\right) \left(3.66 + \frac{0.065\left(\frac{D_H}{L}\right) Re_{ST} Pr_{ST}}{1 + 0.04\left(\left(\frac{D_H}{L}\right) Re_{ST} Pr_{ST}\right)^{\frac{2}{3}}}\right) \tag{6. 59}$$

After, calculating h_i and h_o values and putting them in equation 6.9 gives the overall heat transfer coefficient (U). Putting U value with the LMTD in equation 6.10 results in the heat exchanger area required. From this area length of tube required can be calculated by equation 6.7. Iterative calculations using equation 6.59 give the following results:

Table 6.10 Specification for heat exchanger

Parameters	Type/ value
Length of tube	$8.591\ m$
Overall heat transfer coefficient	$515.9\ W/m^2K$
Log mean temperature difference (LMTD)	55.69℃
Area required	$0.1619\ m^2$

6.2.6. Capillary tube design

6.2.6.1. Capillary tube-1

The cumulative pressure drop must be equal to the difference in pressure at the two end of the tube. The mass flow through the capillary tube will, therefore, adjust so that the pressure drop through the tube just equals the difference in pressure between the condenser and the evaporator. For a given state of the refrigerant, the pressure drop is directly proportional to the length and inversely proportional to the bore diameter of tube.

The sizing of capillary tube implies the selection of bore and length to provide the desired flow for the design condenser and evaporator pressures. The method employed by manufacturer is usually that of cut and try. The principle of design based on methods proposed by Stocker, Hopkins and Cooper et al. is presented here.

A capillary of a particular bore diameter and cross-sectional flow area is first selected. Step decrements in pressure are then assumed and the corresponding required increments of length calculated. These increments can be totaled to give the complete length of the tubing for a given pressure drop.

Table 6.11 Characteristics of capillary tube

Parameters	Values
Capillary tube	Bore diameter of 2.3 mm
Mass flow rate refrigerant	$0.016498\ kg/s$
inlet temperature of a capillary tube	50℃
Outlet temperature of a capillary tube	5℃
Inlet pressure of capillary tube	$2033\ kPa$
outlet pressure of capillary tube	$516\ kPa$

Divide this temperature drop into a number of parts. Assume intermediate sections at 40, 30, 20 and 10℃ . Now there are two approaches to design these are isenthalpic expansion and adiabatic or Fanno-line expansion. The steps of calculations to be followed in both cases are the same and are as follows for the first element.

Determine the quality at the end of decrement assuming isenthalpic flow. Then at first point at pressure p_1

$$x_1 = \frac{h_k - h_1}{h_{fg_1}} \tag{6. 60}$$

Determine the specific volume

$$v_1 = v_{f_1} + x_1\left(v_{g_1} - v_{f_1}\right) \tag{6. 61}$$

Calculate the velocities from the continuity equation at both the ends of the element

$$u_k = \frac{\dot{m}v_k}{A}\ and\ u_1 = \frac{\dot{m}v_1}{A}$$

Or $\frac{u}{v} = \frac{\dot{m}}{A} = G =$ constant (6. 62)

Where: - G is mass velocity.

For Fanno-lone flow, an iteration procedure is necessary. This is done by applying the correction to enthalpy since $h_1 \neq h_k$. Thus

$$h_1 = h_k - \Delta h \tag{6. 63}$$

The calculations for quality, specific volume, velocity and enthalpy may be repeated until the final value of h_1, which is equal to its value in the preceding iteration.

Determine the pressure drop due to the acceleration, ΔP_A, from the momentum equation

$$\Delta P_A = G(u_k - u_1) \tag{6. 64}$$

Determine the pressure drop due to the friction, ΔP_F, from

$$\Delta P_F = \Delta P - \Delta P_A \tag{6. 65}$$

Determine the length ΔL from

$$\Delta P_F = \frac{G}{2D} fu \, \Delta L = Y \, fu \, \Delta L \tag{6. 66}$$

Where $Y = \frac{G}{2D}$ (6. 67)

From which the length ΔL may be calculated. For this purpose, the mean values of u and f for the liquid and vapor phases present may be taken for the section. The friction factor is a function of Reynolds number which in turn is expressed as

$$Re = \frac{Z}{\mu} \tag{6. 68}$$

Where $Z = DG$ (6. 69)

Niaz and Davis have proposed the following correlation for evaluating the friction factor (Arora, 2010):

$$f = \frac{0.32}{Re^{0.25}} \tag{6. 70}$$

Therefore repeat those equations for other element then capillary tube length is calculated the result is displayed in Table 6.12.

Table 6.12 Specification of capillary tube

Sections	$\Delta P\ (kPa)$	$\Delta P_A\ (kPa)$	$\Delta P_F\ (kPa)$	$\Delta L\ (m)$
k-1	479	58.02	420.99	1.82
1-2	388.4	87.81	300.59	0.56
2-3	309.81	135.55	174.26	0.17
3-4	242.54	204.79	37.75	0.02
4-5	99.38	138.21	-38.83	-0.02
Total length required $= \sum \Delta L = 2.553\ m$				

6.2.6.2. Capillary tube-2

This capillary tube is placed between the heat exchanger and absorber which is used to drop the pressure of weak solution. For a given state of the weak solution, the pressure drop is directly proportional to the length and inversely proportional to the bore diameter of tube.

The sizing of capillary tube implies the selection of bore and length to provide the desired flow is the same as before for the design condenser and evaporator pressures. A capillary of a particular bore diameter and cross-sectional flow area is first selected. Step decrements in pressure are then assumed and the corresponding required increments of length calculated. These increments can be totaled to give the complete length of the tubing for a given pressure drop.

Table 6.13 Characteristics of capillary tube-2

Parameters	Values
Capillary tube-2	Bore diameter of 3 mm
Mass flow rate refrigerant	$0.00723\ kg/s$
Concentration of ammonia in a weak solution	0.4436
inlet temperature of a capillary tube-2	72.72℃
Outlet temperature of a capillary tube-2	10℃
Inlet pressure of capillary tube-2	$2033\ kPa$
outlet pressure of capillary tube-2	$516\ kPa$

Divide this temperature drop into a number of parts. Assume intermediate sections at 60, 50, 40, 30 and 20℃ . Now there are two approaches to design these are isenthalpic expansion and adiabatic or Fanno-line expansion. The same procedure is used for the calculation as defined under section 6.2.6.1.

Therefore repeat those equations which are stated under section 6.2.6.1 for other element then capillary tube length is calculated the result is displayed in Table 6.14.

Table 6.14 Specification of capillary tube-2

Sections	$\Delta P\ (kPa)$	$\Delta P_A\ (kPa)$	$\Delta P_F\ (kPa)$	$\Delta L\ (m)$
k-1	411.7	44.04	367.7	0.04845
1-2	262	29.54	232.4	0.03025
2-3	214.9	26.07	188.8	0.02405
3-4	173.8	23.2	150.6	0.01866
4-5	138.4	20.72	117.7	0.01407
5-6	108.2	18.46	89.71	0.01026
Total length required $= \sum \Delta L = 145.74 \times 10^{-3}\ m$				

6.2.7. Pump selection

Table 6.15 Specification of solution pump

Parameters	Values
Mass flow rate of strong solution in the pump	$0.0088\ kg/s$
Specific volume of strong solution	$14.22 \times 10^{-6}\ m^3/kg$
Change in pressure in the pump	$1517\ kPa$
Efficiency of the pump	0.5
Work done by the pump	$1.06\ W$

Using this specification solution pump has to be selected.

Therefore the design components of VAC are generalized in the Table 6.16.

Table 6.16 Configuration of various component of VAC

Sr. No.	Component	Shell Material / Tube	Tube Material	Type	Shell side Fluid	Tube side Fluid	HT area, m^2
1.	Evaporator	Stainless steel	Stainless steel	Shell and Tube	NH_3	Hot water	1.403
2.	Generator	Stainless steel	Stainless steel	Shell and Tube	$NH_3 + water$	Hot water	1.148
3.	Condenser	Stainless steel	Stainless steel	Shell and Tube	NH_3	Cold water	3.06
4.	Absorber	Stainless steel	Stainless steel	Shell and Tube	$NH_3 + water$	Cold water	6.368
5.	Heat Exchanger	Stainless steel	Stainless steel	Tube in Tube	Inner tube hot fluid	Outer tube cold fluid	0.1619
6.	Expansion valve			Capillary tube-1			$L = 2.553\ m$
				Capillary tube-2			$L = 0.1457\ m$

Therefore, from the above design of each component the necessary calculations has done using understand able equations and correlations. The results indicate that each components dimension can fit the available space of Mid Bus. Evaporator, condenser and capillary tube-1 are placed on roof top area of the Mid Bus. Generator, pump, capillary tube-2, solution heat exchanger and absorber are placed around the engine before that the two compressors of the previous air conditioner must out, and then the space can be used. See the Figure 9.6 in Appendix E for visualization.

CHAPTER SEVEN

7. CONCLUSIONS AND RECOMMENDATION

7.1. Conclusions

In this thesis modeling and sizing Mid Bus air conditioning system using engine waste heat and dissipating solar energy based on vapor absorption refrigeration system was carried out by using ammonia and water as a refrigerant and absorbent combination. It saves the power of engine as it replaces the compressor by the four components i.e. absorber, pump, generator and pressure reducing valve out of which only the pump consumes some power that is very weak as compared to that of the compressor, and thus helps in saving of fuel.

Simulation of hybrid vapor absorption system was conducted using heat form engine exhaust of Mid Bus and dissipated electric collected by the roof top area of Mid Bus PV cell.

The heat balance method (HBM) was applied to calculate the various heating and cooling loads transferred to bus via radiation, convection, or conduction. Mathematical models of heat transfer phenomena are used to calculate the different load categories. As per the calculations of cooling load obtained from the Mid Bus is 16.3 kW.

Each component is sized using the relevant equations. Shell and tube type heat exchangers are analyzed for various components of absorption AC system except solution heat exchanger, capillary tubes and pump. For solution heat exchanger simple annulus heat exchanger was considered. For evaporator and generator four passes vertical tube heat exchanger was employed. Both uses nucleate boiling correlation to find the heat transfer coefficients and the lengths of tubes were found that 0.873 m and 0.475 m respectively. For condenser and absorber single pass horizontal heat exchanger was considered. Using condensation correlations both lengths of the tubes are 1.702 m and 17.03 m respectively. The length of tube of solution heat exchanger was calculated 8.591 m. For the two capillary tubes the lengths of capillary tube calculated using two approaches. These are isenthalpic expansion and adiabatic or Fanno-line expansion methods. The lengths are 2.553 m and 0.145 m. the pump was selected using the work done by the pump was 1.06 W.

Form the results of simulation, it has been concluded that, for the cooling load 16.3 kW the COP of vapor absorption refrigeration system is 0.656. The simulation model predicts accurate properties of the working fluid and culminates in designing an absorption refrigeration plant on the Mid Bus.

The average exhaust heat that was calculated from the measured temperatures using thermocouple experiment has given the result of $44.03\ kW$ and according to manufacturer's information same gathered has an error percent of 0.07% which is so little error to be made in making use of experiment.

In Adama 2017 the average solar irradiance was 224.4 W/m^2 and average amount of daily sunlight was slightly over 8.7 hours. From the roof available area of the bus 13.23 m^2 using mono crystalline solar PV cell is 5.165 kW energy was collected. This energy stored in four batteries which have the capacity of 12V rated for 833Ah for each. To convert this energy in to heat energy the heating resistance wire were used which has resistance of 0.093 Ω.

Based on the performance evaluations completed of the three scenarios, the option that offers the greatest flexibility is the third, which locates solar panels on the roof and trunk of the vehicle, but also includes a conventional alternator as a backup supply. Rather than using neither engine exhaust heat nor solar energy alone, good performance can be get in hybrid system especially during less engine speed.

7.2. Recommendation

The following recommendations are made to make the implementation of the thesis:

- The temperature of exhaust gas was measured by k-type thermocouple outside surface of the tube material but rather than using this outside temperature directly measuring the inside temperature by using infrared thermometer is more preferable.
- Form the result seen before absorption AC system is more useful than compression AC system therefore this thesis indicate that the absorption AC system using exhaust heat and solar PV cell comfortable to use for the automotive companies to consider it.

- This work can be suitable for vehicles which are similar with Mid Bus size and engine type.

7.3. Future work

- Reduce the thermal cooling load from the sun on the Mid Bus by methods such as, improving body foam insulation, using low-E film for window insulation and coating of sun reflecting paint on body outer surface during manufacture.
- Other alternative energy source available in the Mid Bus like radiator can be studied on their effect on the air conditioner.
- The road test should be conducted in order to get the real performance of vapor absorption air conditioner for Mid Bus.

REFERENCES

[1] A. A.Manzela, S. M.Hanriot, L. C. Go´mez, and J. R.Sodre, “Using engine exhaust gas as energy source for an absorption refrigeration system”, Applied Energy, vol. 87, 2010.

[2] A.Mittal, D.Shukla, and K. Chauhan, “A refrigeration system for an automobile based on vapor absorption refrigeration cycle using waste heat energy from the engine”, International Journal of Engineering Science and Research Technology, vol. 4, no. 4, 2015.

[3] Ajinkya Shinde, Ankita Dale, Sanket Shrotri, Shubham Mulay and Prof. Sahadev Jadhav, “Experimental investigation of vapor absorption refrigeration cycle for automobile cabin cooling”, ICIIIME, Volume: 5, Issue: 6, 2017.

[4] Al-Aqeeli N and Gandhidasan P, “The use of an open cycle absorption system in automobile as an alternative to CFC”, The 6th Saudi Engineering Conference, KFUPM, Dhahran, December 2002; Vol. 5. P. 517-530.

[5] Alper Yılmaz, “Transcritical organic rankine vapor compression refrigeration system for intercity bus air-conditioning using engine exhaust heat”, Science Direct Energy, 82 1047-1056, 26 February 2015.

[6] Althouse A.O., “Modern electric and gas refrigeration”, The Goodheart-Willcox co., Inc. 1948.

[7] Arndt, M., and Sauer, M., “Spectroscopic carbon dioxide sensor for automotive applications” Sensors, Proceedings of IEEE 2004, 1:252-255, 2004.

[8] ASHRAE Handbook of Fundamental, “American society of heating, refrigerating, and air conditioning”, Atlanta, GA, 2009.

[9] B. Paul Vinofer and S.Rajakumar, “Cooling load calculation and design of air conditioning system in automobile”, IJRSSH, Vol. No. 6, Issue No. I, Jan-Mar 2016.

[10] Baker, J.A., M., L.P. Scherer, P. Kadle, W.R. Hill, S.O. Anderson, “R-152a refrigeration system for mobile air conditioning”, SAE Paper 2003-01-0731.

[11] Brauer H, “substance exchange during the freezing film”, Chern Ing Techn (1958), pp75-84.

[12] Charles A. Lindgren, “Feasibility study of utilizing solar panels to power a vehicle’s onboard air conditioner”, Rensselaer Polytechnic Institute Hartford, CT ,December 2012.

[13] Charles J. Cromer, “Test results of energy savings and humidity control devices”, Energy Engineering, 2003, 100(3), pp. 15-30.

[14] D.Chandrakar and N. K.Saikhedkar, “Design of ammonia water vapor absorption air conditioning system for a car by waste heat recovery from engine exhaust gas”, Advance Physics Letter, vol. 3, no. 2, 2016.

[15] David Bergeron, “Solar powered refrigeration for transport application – a feasibility study”, Sandia Report, sand2001-3753, December 2001.

[16] David MacPhaul, “The basics of HVAC systems in humid climates - what goes wrong and why”, Energy Engineering, 2003, 100(3), pp. 31-38.

[17] Fletcher B. and Saunders C., “Air change rates in stationary and moving motor vehicles”, Journal of Hazardous Materials, 38:243-256, 1994.

[18] G. Karthik, K. Usha Rani and Sayi Likhitha S S, “Development of air conditioning system based on vapor absorption refrigeration cycle for automobiles using exhaust gasses with R134a-Dmf”, International Journal of Mechanical Engineering and Technology (IJMET), pp. 42-50, Volume 5, Issue 7, July 2014.

[19] G.Vicatos J.Gryzagoridis S.Wang, “A car air-conditioning system based on an absorption refrigeration cycle using energy from exhaust gas of an internal combustion engine”, Journal of Energy in Southern Africa , Vol 19 No 4 , November 2008.

[20] Ghodbane, W.R. Hill, S.O. Anderson, “R-134a refrigeration system for mobile air conditioning”, SAE Paper 2003-01-0731.

[21] H. G. Ozcana, H. Gunerhanb, A. Hepbaslia, and H. Yaldirakc, “Environmental impact and performance comparison of refrigerants (R744 and R134a) in a mobile air conditioning system used for cooling buses”, IACSIT International Journal of Engineering and Technology, Vol. 7, No. 3, June 2015.

[22] Hongye Pan, Lingfei Qi, Xingtian Zhang, Zutao Zhang, Waleed Salman, Yanping Yuan and Chunbai Wang, “A portable renewable solar energy-powered cooling system based on wireless power transfer for a vehicle cabin”, Applied Energy, 195, 334–343, 2017.

[23] Horn R K, “measurements for warm and mass transfer in falling film”, Dissertation University Karlsruhe, 1970.

[24] I. Daut, M. Adzrie, M. Irwanto, P. Ibrahim, M. Fitra, “Solar powered air conditioning system”, Energy Procedia 36, 444 – 453, 2013.

[25] I. M. Pavoodath, “Absorption ac in vehicles using exhaust gas”, International Conference on Automation, Control and Robotics, 2012.

[26] Ingersoll, J. Kalman, T. Maxwell, and Niemiec, “Automobile passenger compartment thermal comfort model - part i: compartment cool-down/warm-up calculation”, SAE Technical Paper 920265, 1992.

[27] ISO Standard, “Ergonomics of the thermal environment - determination of metabolic heat production”, ISO Standard 8996, Rev. 2004.

[28] J. S. Jadhao, D. G. Thombare, “Review on exhaust gas heat recovery for I.C. engine”, International Journal of Engineering and Innovative Technology (IJEIT), volume 2, Issue 12, June 2013.

[29] Jain P C and Gable G K, “Equilibrium property data equations for aqua-ammonia mixtures”, ASHRAE Trans 1971, pp. 149-151.

[30] Jordan R.C., “Refrigeration and air-conditioning”, Prentice-Hall, Inc. 1956.

[31] K. Mohan Kumar, Mannava. Rajesh and Mr. N. Sita Ramaiah, 2017, "CFD simulation of a car air conditioning system based on an absorption refrigeration cycle using energy from exhaust gas of an internal combustion engine", International Journal Of Innovative Technology And Research, Volume No.5, Issue No.6, October - November 2017.

[32] K.Veera Raghavulu, U.Sudhakar and K.Nirmala, "Utilization of exhaust gases for cooling the truck cabin by using vapor absorption system", IJLTET, vol. 6, issue 2, November 2015.

[33] Keizer C, "Absorption refrigeration machines", PhD Thesis, Delft University of Technology, 1982.

[34] Keizer C, "Absorption refrigeration machines", PhD Thesis, Delft University of Technology, 1982.

[35] Khaled S. AlQdah, "Performance and evaluation of aqua ammonia auto air conditioner system using exhaust waste energy", Energy Procedia, vol. 6, 2011.

[36] Khayyam, H., Kouzani, A. Z., and Hu, E. J., "Reducing energy consumption of vehicle air conditioning system by an energy management system", IEEE the 4th International Green Energy Conference, China, 2009.

[37] Md Shahid Imam, Dr.M.Shameer Basha, Dr.Md.Azizuddin and Dr. K.Vijaya Kumar Reddy, "Design of air conditioning system in automobile", IJIRSET, Vol. 2, Issue 12, December 2013.

[38] Mills A F, "Heat transfer", International Student Edition, IRWIN, 1992.

[39] Mohammad Ali Fayazbakhsh and Majid Bahrami, "Comprehensive modeling of vehicle air conditioning loads using heat balance method", SAE International, 10.4271/2013-01-1507, 2013.

[40] Moissis R, "The transition from slug to homogeneous two-phase flows", Journal Of heat Transfer Tras of the ASME, Pp. 367-370, 1963.

[41] N.reddy and G. Maruthi Prasad Yadav , "Performance analysis of VARS using exhaust gas heat of CI engine", International Journal for Research in Applied Science Engineering Technology, vol.3, no. 1, 2015.

[42] Pravanjan Padhihari, "Design of solar powered air -conditioning system for car", IJESC, Vol.6, No. 7, 2016.

[43] R P Arora, "Refrigeration and air conditioning", TATA McGraw Hill, third edition.

[44] Rahul D. Jadhav, Yogesh S. Khaladkar, Lalit H. Dorik, Gaurav M. Mahajan, Anil V. Fajage, "Water cooling system using engine exhaust heat", IOSR Journal of Mechanical and Civil Engineering (IOSR-JMCE), Volume 12, Issue 2, PP 22-26, Mar - Apr. 2015.

[45] Ravinder Goyal, Kanwar J.S Gill, Kulvir Singh, Harinder Singh and Prince Rajpal, "Designing and development of solar air conditioner system for automobiles", IOSR-JMCE, e-ISSN: 2278-1684, p-ISSN: 2320–334.

[46] Robert W. Serth, "Process heat transfer principles and applications", Elsevier Ltd, 2007.

[47] Rohsenow W M, "A method of correlating heat transfer data for surface boiling of liquids", Trans. ASME, Vol. 74, 1952.

[49] Ruth D W., "Simulation modeling of automobile comfort cooling requirements", ASHRAE Journal, pp. 53-5, 1975.

[50] S. Abeygunasekara, S.K. Chandrasiri and E.I. A.Virantha, "Enhance the efficiency of automotive ac system by using exhaust heat", SAITM – RSEA, 2014.

[51] S.Lakshmi Sowjanya, "Thermal analysis of a car air conditioning system based on an absorption refrigeration cycle using energy from exhaust gas of an internal combustion engine", Advanced Engineering and Applied Sciences: An International Journal, 3(4), 47-53, 2013.

[52] S.S.Mathapati, Mudit Gupta and Sagar Dalimkar, "A study on automobile air-conditioning based on absorption refrigeration system using exhaust heat of a vehicle",

International Journal of Engineering Research and General Science, Volume 2, Issue 4, June-July, 2014.

[53] Schulz S C G, "Equations of state for the system ammonia-water for use with computers", Proceedings IIF Congress, Washington DC, Vol. 2, paper 2 06, pp. 431-436, 1971.

[54] Scott D S, "Properties of concurrent gas-liquid flow", Advances in Chemical Engineering, Pp.199-277, 1964.

[55] Singh, A. K., Singh, H., Singh, S. P., and Sawhney, R. L., "Numerical calculation of psychrometric properties on a calculator", Building and Environment, 37(4):415-419, 2002.

[56] Talbi, M., and Agnew, B., "Energy recovery from diesel engine exhaust gases for performance enhancement and air conditioning", Applied Thermal Engineering, 1(5): 5-10, 2002.

[57] Vicatos G. and Gryzagoridis J., "A graphical analysis for the optimization of absorption refrigeration", International Congress of Refrigeration FRIGAIR 94, Durban, South Africa, May 1994.

[58] Welty, Wicks, Wilson, "Fundamentals of momentum, heat and mass transfer", John Wtley, NY 1976.

[59] Y.A. çengel and M.A.Boles., "Thermodynamics an engineering approach", Atlanta, GA, 2007 5th edition.

APPENDIX

APPENDIX A

Formulas and equations from the EES software

```
"===========================================================================
==
THIS PROGRAM CALCULATES THE PERFORMANCE OF A SINGLE-STAGE
ABSORPTION SYSTEM FOR MID BUS POWERED BY EXHAUST HEAT AND SOLAR PV
===========================================================================
== "

{Press F2 to solve.}


"INPUT PARAMETERS"

"Efficiencies"
etap=0.50                    "isentropic efficiency of pump"
eshx=1                       "solution heat exchanger effectiveness"
f=(x[9]-x[4])/(x[3]-x[4])    "solution circulation ratio"

"Temperatures in oc"
T[12]=5                      " for state point, see diagram window"
T[10]=50
T[1]=10
T[7]=105
Qevap=16.3[kW]

"Quality"
Q[12]=0.998
Q[10]=0.00
Q[7]=1
Q[9]=1
Q[1]=0
Q[4]=0

"Pressure"
P1_sat=P_sat(Ammonia,T=T[10])
P2_sat=P_sat(Ammonia,T=T[12])
P[10]=P1_sat*0.01
P[12]=P2_sat*0.01
CALL NH3H2O(128,T[12]+273,P[12],Q[12]:T_[12],P_[12],x[12],h[12],s[12],u[12],v[12],Q_[12])
x[10]=x[12]
x[11]=x[12]
CALL NH3H2O(138,T[10]+273,x[10],Q[10]:T_[10],P_[10],x_[10],h[10],s[10],u[10],v[10],Q_[10])

“GOVERNING EQUATIONS”

"ABSORBER"
P[1]=P[12]
CALL NH3H2O(128,T[1]+273,P[1],Q[1]:T_[1],P_[1],x[1],h[1],s[1],u[1],v[1],Q_[1])
```

```
m[12]+m[6]=m[1]
m[12]*x[12]+m[6]*x[6]=m[1]*x[1]
m[12]*h[12]+m[6]*h[6]-(m[1]*h[1])=Qabs

"GENERATOR"
m[8]+m[3]=m[7]+m[4]
m[8]*x[8]+m[3]*x[3]=m[7]*x[7]+m[4]*x[4]
x[8]=(x[12]+x[4])/2                         "let as assume the value average of max and min "
CALL NH3H2O(238,P[8],x[8],0:T[8],P_[8],x_[8],h[8],s[8],u[8],v[8],Q_[8])
P[8]=P[10]
x[3]=x[1]
P[3]=p[10]
CALL NH3H2O(238,P[3],x[3],0:T[3],P_[3],x_[3],h[3],s[3],u[3],v[3],Q_[3])
P[7]=P[10]
CALL NH3H2O(128,T[7]+273,P[7],Q[7]:T_[7],P_[7],x[7],h[7],s[7],u[7],v[7],Q_[7])
m[3]*h[3]+m[8]*h[8]+Qgen=m[7]*h[7]+m[4]*h[4]

"RECTIFIER"
x[9]=x[12]
p[9]=p[10]
CALL NH3H2O(238,P[9],x[9],Q[9]:T[9],P_[9],x_[9],h[9],s[9],u[9],v[9],Q_[9])
m[9]=m[10]
m[10]=m[11]
m[11]=m[12]
m[7]*h[7]=m[9]*h[9]+m[8]*h[8]+Qrect

"PUMP"
P[2]=P[10]
swp=v[1]*(p[2]-p[1])/etap
h[2]=h[1]+swp
Wp=m[1]*swp

"EXPANSION VALVE_1"
P[6]=P[12]
h[5]=h[6]
x[6]=x[4]

"SHX"
m[1]=m[2]
m[2]=m[3]
Qshx=m[2]*(h[3]-h[2])        "For strong solution in heat exchanger"
T[4]=T[7]
P[4]=P[10]
m[6]=m[5]
m[5]=m[4]
CALL NH3H2O(128,T[4]+273,P[4],Q[4]:T_[4],P_[4],x[4],h[4],s[4],u[4],v[4],Q_[4])
h[5]=h[4]-(Qshx*eshx)/m[4]      "For weak solution in heat exchanger"
x[5]=x[4]

"CONDENSER"
Qcond=m[9]*(h[9]-h[10])

"EVAPORATOR"
Qevap=m[12]*(h[12]-h[11])

"EXPANSION VALVE_2"
```

```
h[10]=h[11]

"OVERALL"
COP=Qevap/(Wp+Qgen)

"========================================================================
 EXHAUST GAS AVALIABLE ENERGY
========================================================================"

"Given inputs"
P=132
Vs=0.00467
N=2300
pa=1.167
cp=1.1
nv=0.9
T_exhaust=422.6622      “this temperature is taken from measured data at 2300 rpm”
Vr=14.7

" equations "
V=Vs*N/(2*60)
ma=nv*pa*V
mf=ma/Vr
me=mf+ma
delta_T=T_exhaust-31
qe=me*cp*delta_T
Qgen_ex=qe

"=======================================================================
SOLAR PV AVALIABLE ENERGY
========================================================================"

“Given inputs”
I_s=224.4
A_roof=13.23
SH=8.7
epanel=0.2
P_battery = 40000
time=1
V_voltage=120
R_risistance=0.093

“equations”
Pgen_panel=I_s*epanel*A_roof*SH
time_tocharge=P_battery/Pgen_panel
I=(P_battery/time)/V_voltage
P_wire=(I^2)*R_risistance
Qgen_solar=P_wire*0.001

"======================================================================
FOR HYBRID SYSTEM
======================================================================="
Qgen=Qgen_ex+Qgen_solar
```

APPENDIX B

Adama weather condition

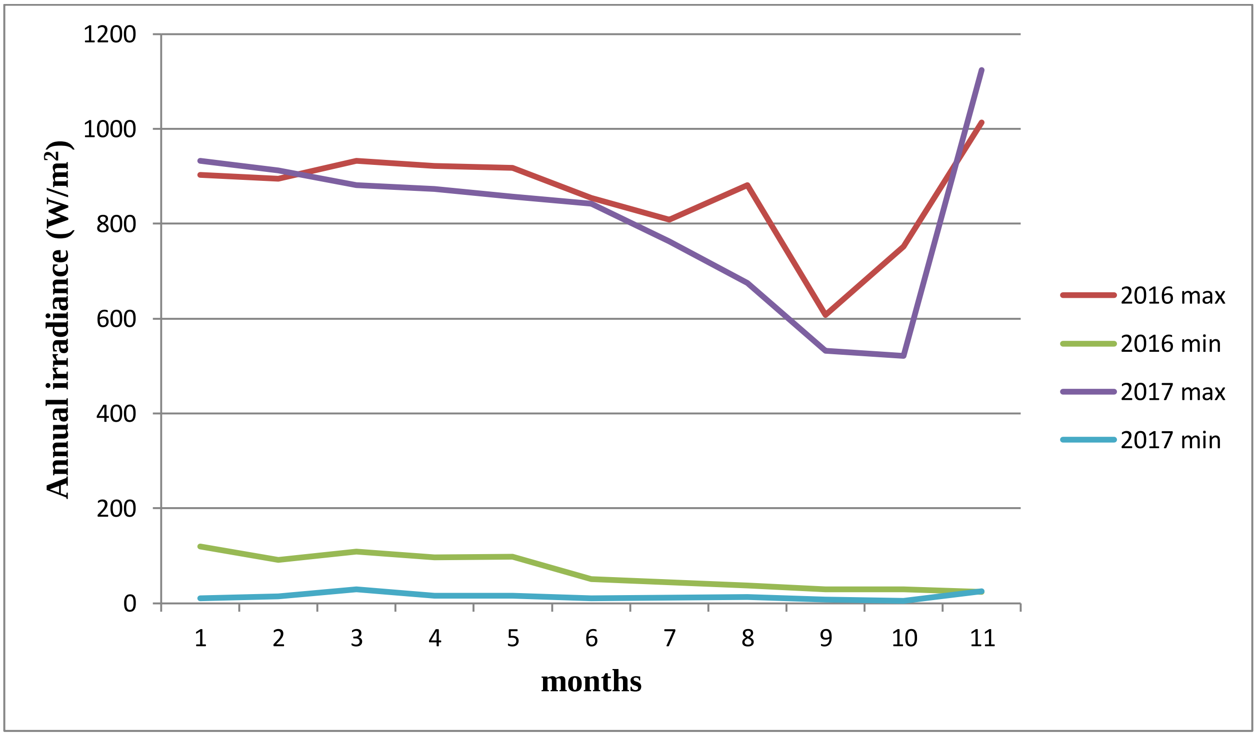

Figure 9.1 Annual irradiance 2016 and 2017.

Table 9.1 Annual irradiance 2016 and 2017.

year	2016	(W/m^2)	2017	(W/m^2)
months	max	min	max	Min
1	903.3	119.5	933.3	10.53
2	895	91.7	912.3	13.6
3	933	109.2	881	29
4	922.3	96.2	873	16.2
5	918.2	97.6	856.5	15.4
6	854.7	50.5	842.2	10.2
7	808.5	43.3	762.8	11.5
8	881.5	36.8	674.5	12.8
9	607.2	28.7	532.7	7.9
10	751.8	29.5	521.6	4.5
11	1013.2	23.6	1123.5	25.3

Figure 9.2 Annual average relative humidity of Adama in 2017.

Table 9.2 Annual average relative humidity of Adama in 2017

2017 annual average humidity		
	30 days average for maximum and minimum	
Months	minimum @18:00	max @ 6:00
1	12	43
2	23	54
3	29	91
4	26	63
5	38	91
6	32	82
7	57	74
8	54	91
9	69	99
10	69	91
11	32	57
12	25	70

Table 9.3 Adama's geographical location.

Adama geographical location
Adama Station-
Longitude = 8°33''23.8'N
Latitude=39°17''02.5''E
Altitude=1648m above sea level
Distance from Addis Ababa is 99km.
Dominating climate of the city is hot/arid climate type

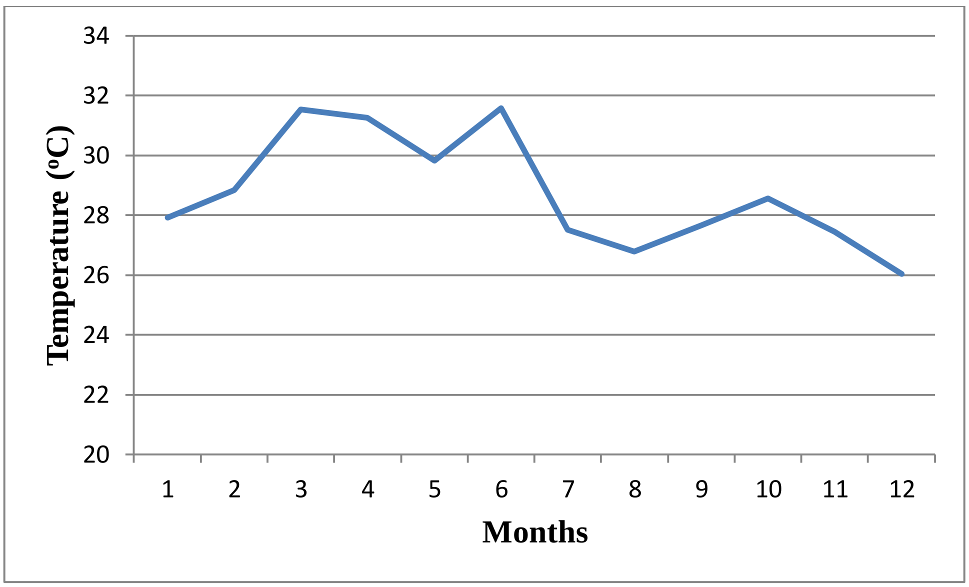

Figure 9.3 Adama's annual temperature variation versus months of 2017.

APPENDIX C

Characteristics table of Ammonia-Water solution

Saturated liquid

Table 9.4 Ammonia as a saturated liquid.

T in ℃	$\rho, kg/m^3$	$c_p, kJ/kg.℃$	$v, m^2/_s$	$k, ^W/_{m.℃}$	$\alpha, m^2/_s$	pr	β, k^{-1}
			AMMONIA.NH_3				
-50	703.69	4.46	$0.44*10^{-6}$	0.55	$1.74*10^{-7}$	2.60	
-40	691.68	4.47	0.41	0.55	1.78	2.28	
-30	679.34	4.48	0.39	0.55	1.8	2.15	
-20	666.69	4.51	0.38	0.55	1.82	2.09	
-10	653.55	4.56	0.38	0.54	1.83	2.07	$2.45*10^{-3}$
0	640.10	4.64	0.37	0.54	1.82	2.05	
10	626.16	4.71	0.37	0.53	1.8	2.04	
20	611.75	4.8	0.36	0.52	1.78	2.02	
30	596.37	4.9	0.35	0.51	1.74	2.01	
40	580.99	4.99	0.34	0.49	1.7	2.00	
50	564.33	5.12	0.33	0.48	1.65	1.99	

Table 9.4 Properties of Ammonia at atmospheric pressure (continued) values of μ, k, c_p, $and\ Pr$ are not strongly pressure dependant for H_2, O_2, and N_2 and may be used over a fairly wide range of pressure.

Table 9.5 Ammonia's as thermal properties.

T in ℃	$\rho, kg/m^3$	$c_p, kj/kg.0_c$	$v, m^2/_s$	$k, {}^W/_{m.0_c}$	$\alpha, m^2/_s$	pr
AMMONIA.NH_3						
273	0.79	2.18	$9.35*10^{-6}$	$1.18*10^{-5}$	0.02	$0.13*10^{-4}$
323	0.65	2.18	11.04	1.70	0.03	0.19
373	0.56	2.24	12.89	2.30	0.03	0.26
423	0.49	2.32	14.67	2.97	0.04	0.34
473	0.44	2.4	16.49	3.74	0.05	0.44

Ammonia-Water solution characteristics curve

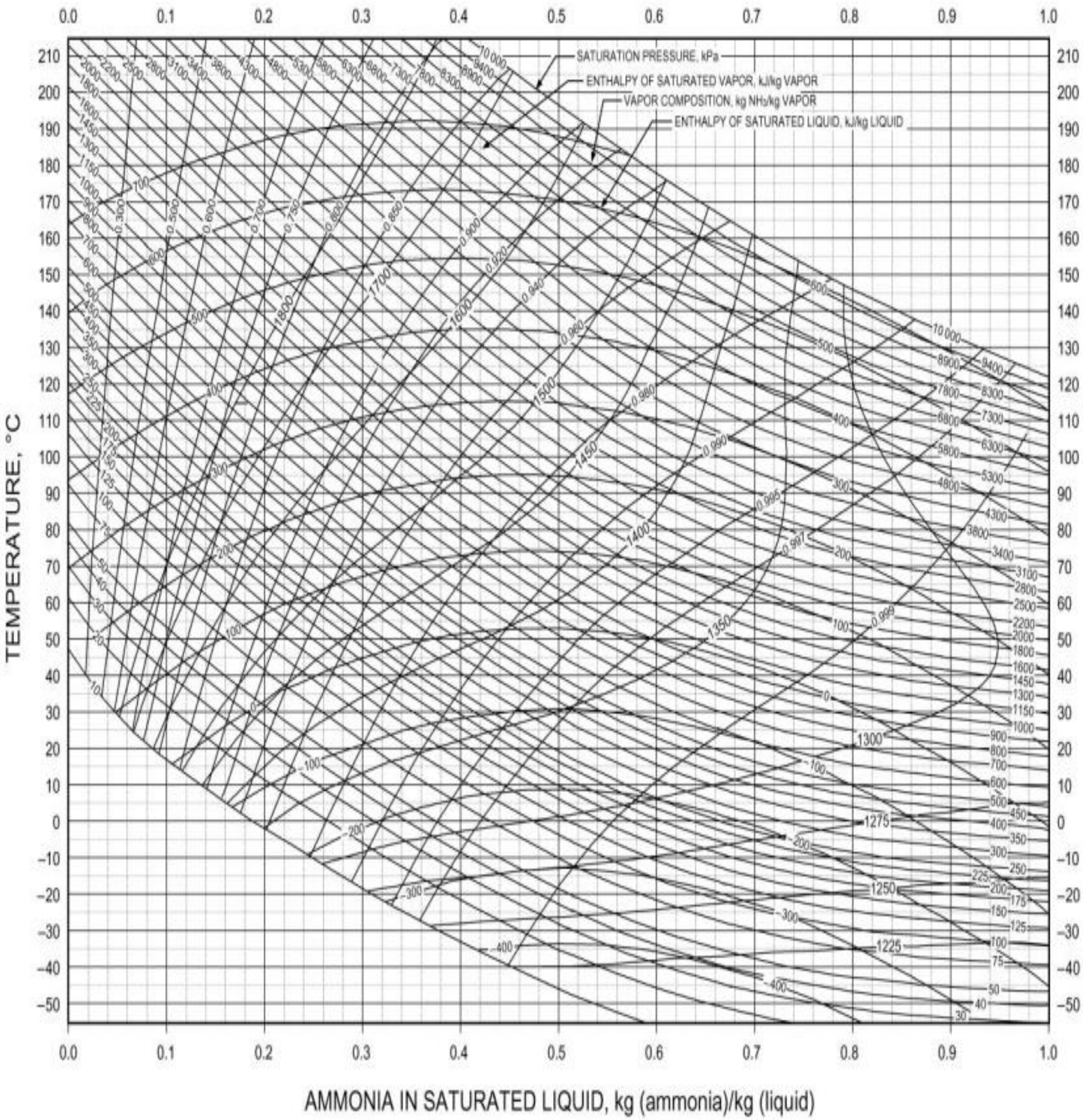

Figure 9.4 Enthalpy-concentration diagram for ammonia-water solutions [ASHRAE 2009 P.19.82].

APPENDIX D

WP5.180E3 TECHNICAL SPECIFICATION

Figure 9.5 WP5.180E3 technical specification. [Changzhou Huanghai Automotive Co., Ltd.]

Table 9.6 Overall dimensions of Mid Bus [Changzhou Huanghai Automotive Co., Ltd.].

Overall Dimensions	
Vehicle length	8540
Vehicle width	2455
Vehicle height	3350 (Air-conditioned)
Overhang length (front/rear) of the vehicle	1890/2550
Wheelbase	4100
Minimum ground clearance	210
Minimum turning diameter	≤19000
Chassis length	7962
Chassis width	2100
Chassis height	1811
Overhang length (front/rear) of the Chassis	1657/2205
Wheel track (front/rear)	1915/1800

Approach angle/departure angle	13°/10°
Maximum steering angl(inside/outside)	41°/33°
Chassis length	7962
Min. turning diameter (m)	20
Luggage compartment(m^3)	6
Engine	
Arrangement of Engine	Four-stroke, direct-injection, four-cylinder inline, water-cooling, inter-cooling and electronic-control diesel engines
Model	WP5.180E3
Displacement (cc)	4760 ml
Position	Front mounted
Max. Output (kw/rpm)	132 kW/2300 rpm
Max. Torque (N.m/rpm)	650 Nm/1200-1700 rpm
Type of Fuel	Diesel
Minimum rate of fuel oil consumption	≤195 g/kW·h
Emission Standard	Euro Ⅲ
Chassis	
Manufacturer	Zhengzhou Yutong Bus Co., Ltd
Model	ZK6760CD
Clutch	Hubei Tri-ring Clutch Ltd.
Gearbox	CA6-75 Manual, six forward gear.
Suspension system	Leaf spring suspension
Steering system	Integral power steering
Braking system	Dual-circuit air braking Air release parking WABCO ABS
Tire	11 R22.5
Electric system	24 V Single wire; Minus earth
Body	
Body structure	Semi-integral body

	Pre-stress stretched panel skin Full metal body
Inner trimming	Luggage rack, curtain
Door and door pump	Front pneumatic single door
Windows	Sliding windows
Seat	32+1 seats; all seats with belt
Air-conditioning system	Air-conditioning system (if installed for use) Type: KT20D5-2C-type non-independent overhead air conditioner Refrigerating capacity: .... Defrost system Model: .... Heating capacity ....
Audio and Visual system	MP3 PLAYER
Rear view system	Rabbit ear rear view mirror
Lamp	Integral head lamp Separate tail lamp
Maximum vehicle speed	≥105 km/h
Maximum gradeability	25% (at full load, on dry and hard roads, with the slope length not less than 15 m)
Maximum braking distance	≤ 9 m (at full load, on dry and flat asphalt or concrete pavement, with the vehicle speed being 30 km/h)
Parking braking performance	Under the same conditions as the maximum grade ability, the bus can be braked reliably and securely
100 km volumetric fuel consumption under limited conditions	22 L (at full load, at uniform speed of 50 km / h, on flat good roads)
Capacity of the fuel tank	200 L

APPENDIX E

3D Catia V5 drawing

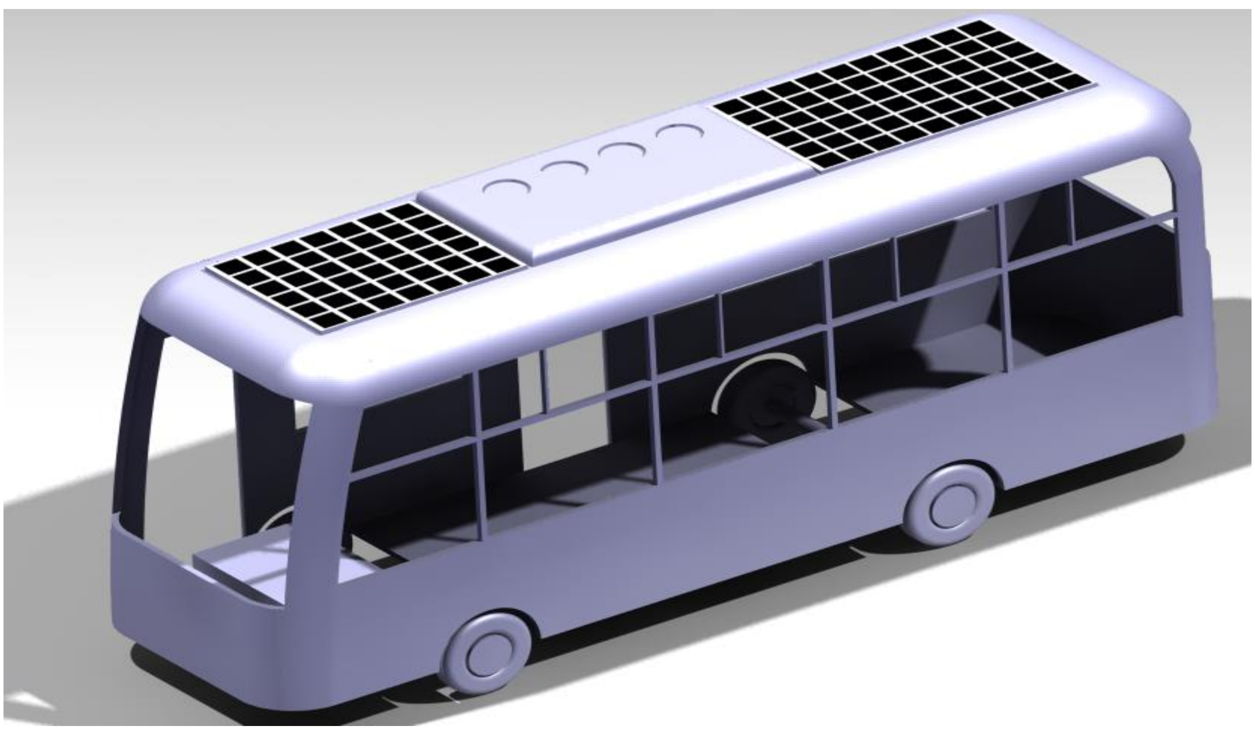

Figure 9.6 3D view of Mid Bus with installed new AC system